Chem Soc Rev

REVIEW ARTICLE

View Article Online
View Journal

Cite this: DOI: 10.1039/d6cs00145a

Functional group translocation: moving functionalities without changing molecular scaffolds

Eito Moriya and Junichiro Yamaguchi *

Functional group position plays a decisive role in molecular properties and function, with even subtle positional changes leading to pronounced differences in biological activity, material performance, and reactivity. Access to positional isomers is therefore central to drug discovery and materials chemistry, yet their synthesis has traditionally required independent and often inefficient synthetic routes. Recent advances have given rise to functional group translocation reactions, which enable the direct relocation of functional groups within a molecular framework without altering the underlying scaffold. In this review, we use the term functional group translocation in a narrow sense to describe transformations in which only the bonding position of a functional group changes while the molecular framework and functional group identity remain intact. Such processes offer a concise molecular editing strategy that enables direct access to positional isomers from a common precursor. Enabled by developments in transition metal catalysis and photoredox chemistry, functional group translocation has rapidly progressed beyond classical stoichiometric and substrate-specific processes. This review defines functional group translocation, distinguishes it from traditional rearrangement reactions and broader isomerization processes, and summarizes recent advances across aromatic and aliphatic systems. By organizing the field according to molecular scaffold, functional group identity, and migration distance, this review highlights current capabilities, remaining challenges, and future opportunities in synthesis, drug discovery, and materials chemistry.

Received 25th February 2026

DOI: 10.1039/d6cs00145a

rsc.li/chem-soc-rev

1. Introduction

1.1. Structural isomers

Structural isomers share an identical molecular formula but differ in the connectivity or positional arrangement of their

Department of Applied Chemistry, Waseda University, 513 Wasedatsurumakicho, Shinjuku, Tokyo 162-0041, Japan. E-mail: junyamaguchi@waseda.jp

Eito Moriya

Eito Moriya was born in Aichi in 1998. He enrolled at Waseda University, where he earned his bachelor's degree in 2021. He then continued to graduate studies at Waseda University, receiving his PhD degree in 2026 under the supervision of Prof. Junichiro Yamaguchi. He is currently a JSPS Postdoctoral Research Fellow at Kobe University.

Junichiro Yamaguchi

Junichiro Yamaguchi earned a BS in 2002 from Tokyo University of Science and then a PhD in 2007 under the direction of Prof. Yujiro Hayashi. Following postdoctoral studies with Prof. Phil S. Baran at The Scripps Research Institute, he began his career at Nagoya University in 2008 as an assistant professor working with Prof. Kenichiro Itami, and was promoted to associate professor in 2012. He moved to Waseda University in 2016 as a principal investigator and was promoted to full professor in 2018.

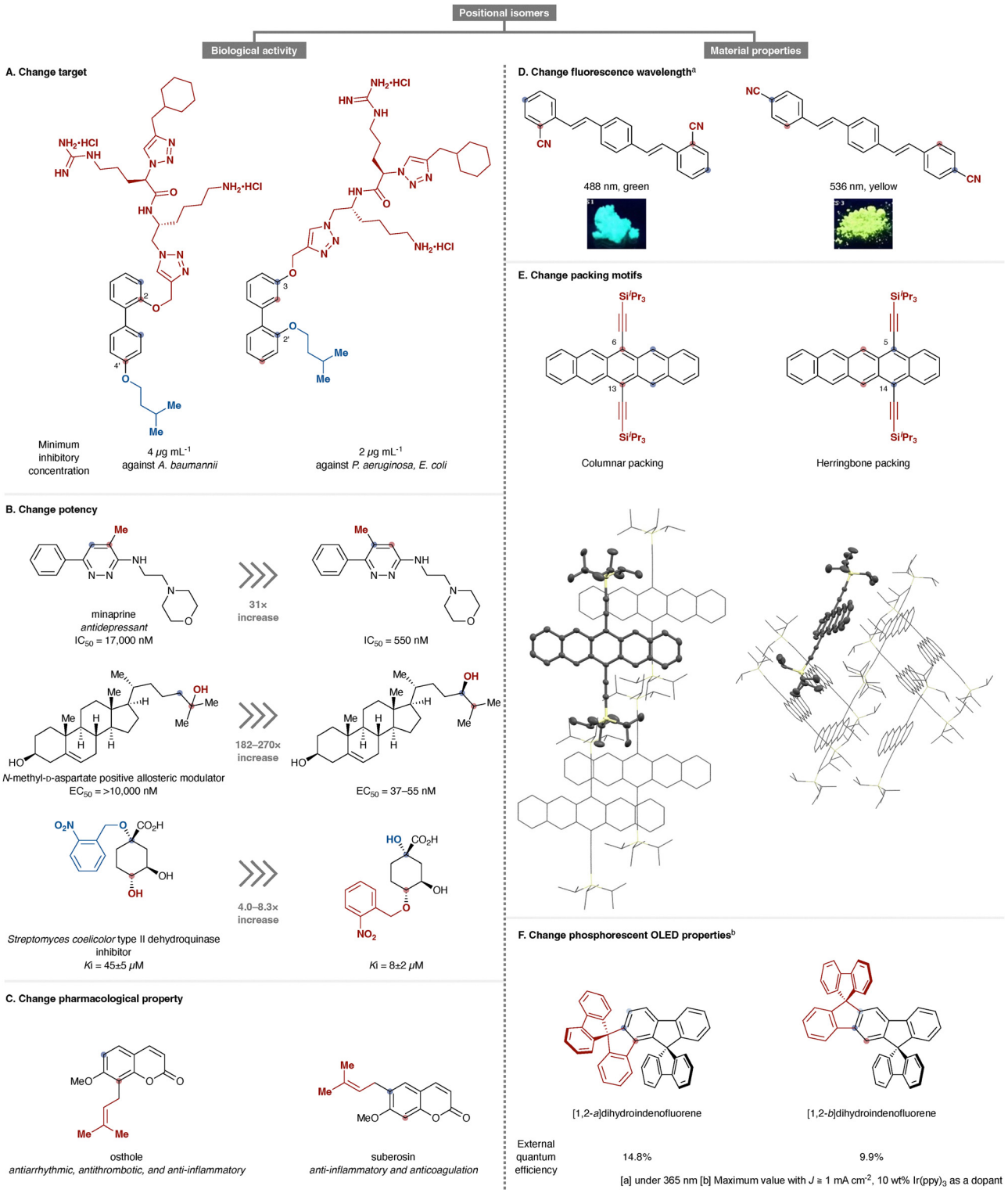

Fig. 1 Representative structural isomers showing how positional changes alter molecular properties. (A) Change target, (B) change potency, (C) change pharmacological property, (D) change fluorescence wavelength, (E) change packing motifs, (F) change phosphorescent OLED properties.

constituent atoms. Despite this formal similarity, even subtle changes in substituent position can profoundly alter physicochemical properties, reactivity, biological activity, and material performance. In medicinal chemistry, systematic evaluation of positional isomers remains central to structure–activity relationship studies,[1] while in materials science, minor positional variations can dramatically influence molecular packing, electronic structure, and macroscopic properties.[2] Selected examples are shown in Fig. 1.

Even small positional changes can produce dramatic differences in biological activity (Fig. 1A). In biphenyl-based antimicrobial peptide mimetics, compounds bearing an oxygen substituent at the C1 and C2' positions exhibit a fourfold increase in activity against *Acinetobacter baumannii* (MIC = 4 μg mL^{-1}).[3] In contrast, the structural isomer substituted at the C2 and C4' positions shows a 4–8-fold enhancement in potency against the Gram-negative pathogens *Pseudomonas aeruginosa* and *Escherichia coli* (MIC = 2 μg mL^{-1}). Thus, positional isomerism directly modulates antibacterial selectivity and potency.

Positional relocation can also markedly enhance intrinsic activity (Fig. 1B). In aminopiperazine muscarinic agonists, formal 1,2-migration of a methyl group improves activity from IC_{50} = 170 000 nM to 550 nM.[4] Similarly, in neuroactive steroids acting as positive allosteric modulators of NMDA receptors, conversion of a tertiary alcohol into a secondary alcohol *via* formal 1,2-relocation enhances GluN2A potency from EC_{50} >10 000 nM to 37 nM.[5] A related trend is observed for inhibitors of *Streptomyces coelicolor* type II dehydroquinase: one derivative displays K_i = 45 ± 5 μM, whereas its structural isomer, in which the alcohol and ether side chain are formally interchanged, exhibited K_i = 8 ± 2 μM, corresponding to an approximately sixfold increase in activity.

In some cases, positional isomerism alters not only potency but also pharmacological profiles (Fig. 1C). Osthole exhibits antiarrhythmic, antithrombotic, and anti-inflammatory activities, whereas its structural isomer suberosin displays anti-inflammatory and anticoagulant effects,[6] highlighting that positional variation can reshape biological functions rather than merely tune its magnitude.

The consequences of positional isomerism are equally pronounced in materials science. In cyanostilbene derivatives relocation of the cyano substituent from the *para* to the *ortho* position significantly changes solid-state packing and fluorescence behavior (Fig. 1D).[7] The *ortho* isomer emits green fluorescence at 488 nm, whereas the *para* isomer shows yellow emission at 536 nm in both powder and crystalline forms.

Structural isomerism also impacts crystal packing in triisopropylsilylethynyl-substituted pentacenes (Fig. 1E).[8] Substitution at the 6,13-positions affords an efficient two-dimensional π-stacking motif with enhanced intermolecular orbital overlap and superior charge-transport properties, whereas substitution at the 5,14-positions leads to a herringbone-like packing arrangement with limited π-overlap and inferior electronic characteristics. Device performance further reflects positional sensitivity (Fig. 1F).[9] In dihydroindeno[1,2-*b*]fluorene derivatives, the *para* isomer exhibits an external quantum efficiency (EQE) of 9.9%, whereas the *meta* isomer achieves a significantly higher EQE of 14.8%.

Collectively, these examples illustrate a fundamental principle: molecular function is highly sensitive to positional information. The deliberate control of substituent location therefore represents a powerful means of modulating molecular behavior. However, efficient and general synthetic access to positional isomers remains a longstanding challenge in organic synthesis.

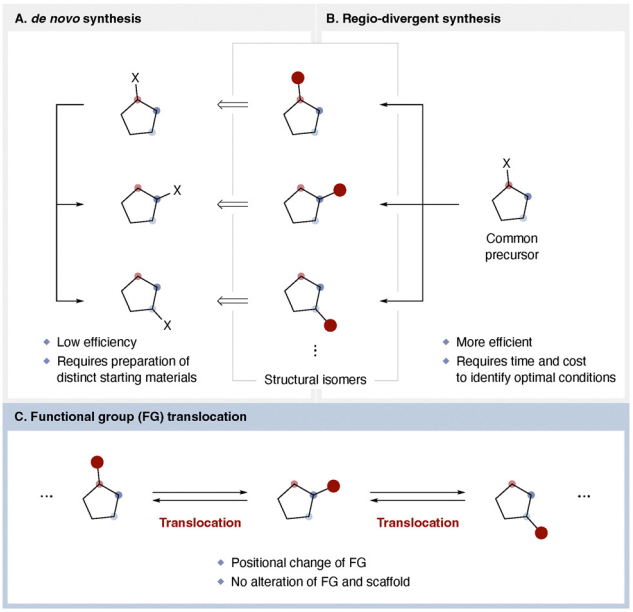

Fig. 2 Strategies for accessing structural isomers: (A) *de novo* synthesis; (B) regio-divergent synthesis; and (C) functional group translocation.

1.2. Efficient access to structural isomers

Traditionally, positional isomers are synthesized through *de novo* preparation of distinct starting materials corresponding to each target structure (Fig. 2A). Although this approach is reliable and broadly applicable, it is inherently linear and often inefficient, as each isomer requires an independent synthetic sequence. Such strategies can significantly slow the exploration of chemical space, particularly in medicinal chemistry and materials development, where rapid access to multiple positional variants is highly desirable.

Regio-divergent synthesis has emerged as a conceptually attractive alternative, enabling selective access to different positional isomers from a common precursor by modulating reaction conditions (Fig. 2B).[10] Advances in catalyst design, ligand development, and reaction engineering have made selective divergence increasingly feasible, allowing control over regioselectivity through subtle changes in reaction parameters.[11] Nevertheless, identifying suitable conditions typically demands extensive experimental screening and careful optimization, and regio-divergent strategies are often limited to specific substrate classes or reaction manifolds.

An alternative and conceptually distinct strategy is to relocate an already installed functional group within a molecular framework. If such relocation can be achieved without altering the molecular formula, the identity of the functional group, or the carbon scaffold, positional isomers could in principle be accessed directly from a single precursor. This approach transforms positional isomer synthesis from a problem of divergent construction into one of controlled molecular editing. The

development of such transformations underlies what we define here as functional group translocation (Fig. 2C).

1.3. Functional group translocation: challenges, classification, and recent chronology

In this review, we define functional group translocation in a narrow and operational sense as a transformation in which the molecular formula, the identity of the functional group, and the carbon framework remain unchanged, while only the bonding position of the functional group is altered (Fig. 3A). By explicitly requiring preservation of both scaffold and functionality, this definition distinguishes translocation from broader rearrangement or transposition reactions that involve skeletal reorganization or functional group interconversion. This conceptual clarification is essential for recognizing translocation as a distinct molecular editing strategy rather than a subset of classical rearrangement chemistry.

Despite its apparent simplicity, functional group translocation presents substantial synthetic challenges (Fig. 3B). First, the selective relocation of a functional group within a densely functionalized molecule requires precise control over both site and direction of migration. Thermodynamically, positional isomers often differ only marginally in stability, rendering selective and irreversible translocation difficult. From a kinetic standpoint, discrimination among multiple similar C–H or C–C bonds demands exceptional selectivity in bond activation. Furthermore, control over migration distance—whether 1,2-, 1,3-, 1,4-, or longer-range shifts—remains a central issue. Reversibility and product inhibition, arising from small energy differences between isomers, must also be addressed. Historically, most examples relied on harsh acidic or basic conditions, severely limiting functional group compatibility. The development of catalytic, mild, and highly selective processes therefore constitutes a formidable challenge in modern synthesis.

To rationalize recent advances, functional group translocation reactions can be classified along several orthogonal dimensions (Fig. 3C): (i) the molecular scaffold, including (hetero)aromatic systems, aliphatic frameworks involving sp^2–sp^3 exchange, and fully aliphatic sp^3–sp^3 systems; (ii) the identity of the migrating functional group, such as alkyl, aryl, ester, amide, acyl (ketone), cyano, amine, hydroxy, halogen, and silyl groups; and (iii) the migration distance, encompassing 1,2-, 1,3-, 1,4-, 1,*n*-, and double translocation processes. Mechanistically, these transformations proceed through diverse pathways, including strong acid or base activation, transition-metal catalysis, photoredox-induced radical processes, and related relay strategies.

Historically, functional group translocation emerged from classical stoichiometric processes operating under strongly acidic or basic conditions (Fig. 3D, left). Early examples established the feasibility of positional migration but were largely confined to robust substituents and limited substrate classes. Mechanistic studies in the mid-20th century clarified key intermediates and thermodynamic convergence principles, yet translocation chemistry remained fragmented and rarely conceptualized as a unified strategy. What was once a mechanistic curiosity has evolved into a powerful molecular editing strategy (Fig. 3D, right, details are described in Section 2).

A decisive shift occurred around 2020, when advances in transition-metal catalysis, photoredox activation, and radical relay design enabled catalytic and selective translocation under significantly milder conditions (details are shown in Sections 3–5). These developments dramatically broadened the range of migratable functional groups, accessible scaffolds, and controllable migration distances. As illustrated in Fig. 3D right, functional group translocation has evolved from isolated stoichiometric rearrangements into a coherent and rapidly expanding platform for molecular editing.

1.4. Scope and exclusions

To clarify the scope of the term ''translocation'' as used in this review, we present a flowchart that delineates related but distinct reaction classes. Because these transformations involve a change in substituent position, the term ''transposition'' can broadly describe many of them (Fig. 4). Likewise, there is substantial overlap with ''rearrangement'' chemistry. A key distinction, however, lies in whether the molecular formula changes. When the molecular formula changes, the process is more appropriately described as a ''transfer'' reaction, which is outside the scope of this review.[12,13] When the molecular formula remains unchanged, the transformation falls under the broader category of ''isomerization.'' Within isomerization, it is instructive to consider whether the bonding relationships between atoms are altered. If the bonding positions do not change, the process corresponds to stereochemical or conformational isomerization, such as *E*/*Z* isomerization, epimerization, or conformational interconversion, and is not considered here.[14,15] If bonding positions do change, but either the molecular scaffold or the functional group identity is altered, such reactions are classified as follows:

A. Rearrangement or scaffold alteration[16,17]

These are transposition-type processes in which the molecular skeleton changes between starting material and product. This represents the broadest sense of transposition. A recent example is the photochemical conversion of isoxazoles to oxazoles reported by Leonori and co-workers.[18]

B. Functional group alteration[19,20]

These are transposition-type processes in which the identity of the functional group changes during migration. A recent example includes transformations such as the conversion of aldehydes to thioethers reported by Yamada.[21]

C. Unsaturated bond isomerization[22,23]

These involve positional changes of alkenes or alkynes. Although formally a type of translocation, unsaturated bond isomerization has been thoroughly summarized in several recent and authoritative reviews.[24] In view of these comprehensive treatments, we do not discuss these processes further here, and instead concentrate on underexplored classes of functional group translocation. The breadth and maturity of this field, exemplified by recent isomerization studies from groups such as Kuniyil, Du, and Guo, place it outside the scope of this review.[25]

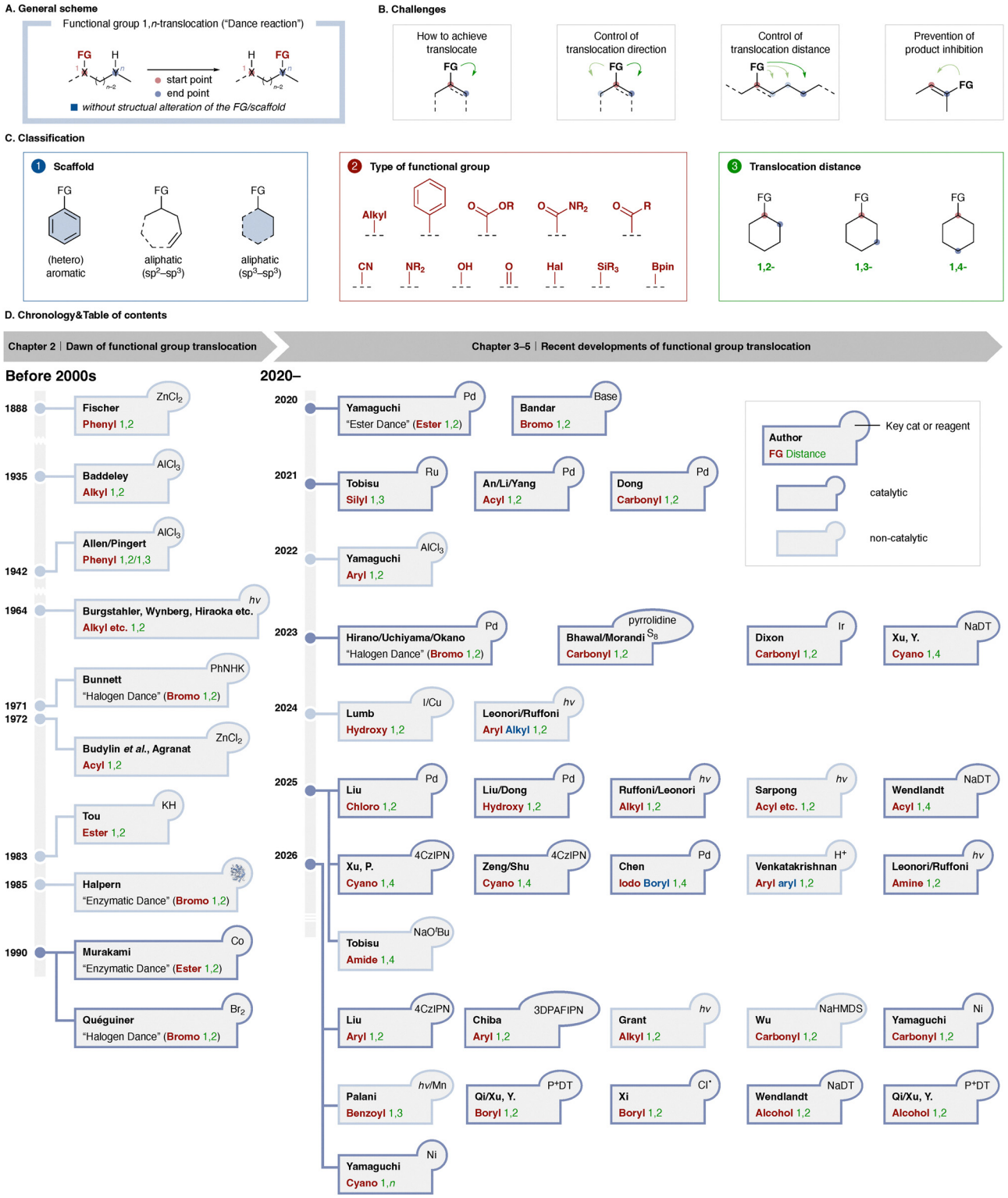

Fig. 3 Definition, challenges, classification, and chronology of development of functional group translocation. (A) General scheme, (B) challenges, (C) classification, (D) chronology & table of contents.

D. Metal-centered translocation[26]

These involve positional exchange or migration processes centered on metal–ligand frameworks. Representative examples include exchange processes on iridium complexes reported by Ihee, Kim, and Chang. Because this review focuses on carbon–functional group relationships, such metal-centered processes are excluded.[27]

E. Classical named rearrangements[28]

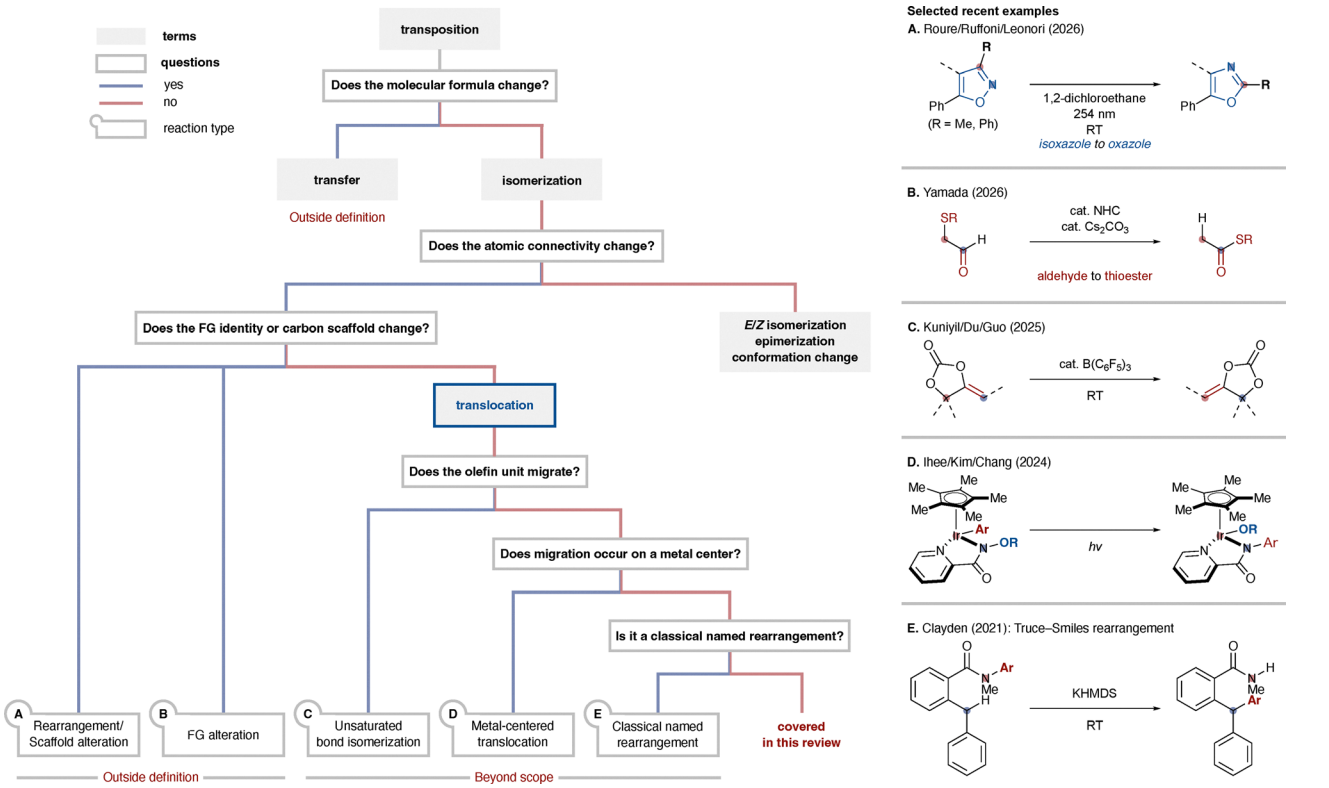

Fig. 4 Scope and exclusions distinguishing translocation from related reaction classes. (A) Rearrangement/Scaffold alteration, (B) FG alteration, (C) unsaturated bond isomerization, (D) metal-centered translocation, (E) classical named rearrangement.

Certain classical named reactions contain translocation elements, such as the Truce–Smiles rearrangement discussed by Clayden and others.[29] However, these are typically categorized as rearrangements and often involve bond reorganization beyond simple positional change. They are therefore not treated here.

Accordingly, transformations in which either the molecular scaffold or the identity of the functional group changes are classified as **A** or **B** and are not considered translocation in the context of this review. In contrast, reactions in which the molecular scaffold and functional group identity are preserved while only the position of the functional group changes fall under the broad definition of translocation. However, categories **C–E** have already been comprehensively covered in several excellent reviews and are therefore excluded from the present discussion. This review focuses exclusively on functional group translocation reactions outside those categories.

Operationally, the present review includes not only single-step translocation reactions but also concise one-pot or sequential multi-step processes when they achieve direct positional editing of a functional group without reconstruction of the molecular scaffold. Accordingly, transformations involving strategically linked activation, migration, and deprotection or hydrolysis steps are discussed when the overall process conceptually corresponds to functional group translocation. In contrast, lengthy synthetic sequences involving complete removal and reinstallment of a functional group are considered outside the scope of this review.

1.5. Organization of this review

To facilitate systematic comparison of recent advances, the reactions discussed in Sections 2–5 are presented in a standardized format (Fig. 5).

1. Identifies the corresponding author and year of publication;

2. Briefly summarizes characteristic reagents, catalysts, or reaction conditions associated with the transformation;

3. Classifies the transformation according to the migrating functional group, translocation distance, and the molecular scaffold;

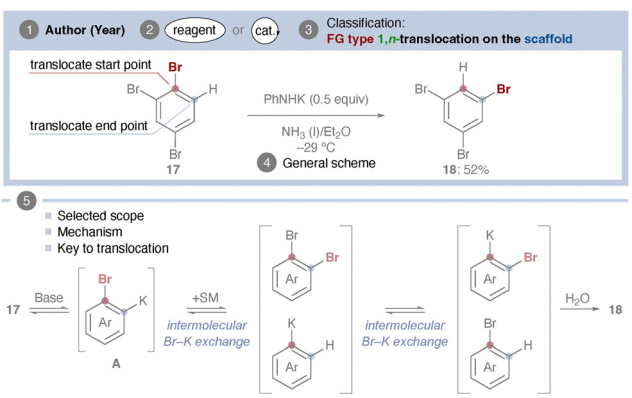

Fig. 5 Standardized summary format used for reactions discussed in this review.

4. Provides a generalized reaction scheme, highlighting in red the carbon bearing the functional group prior to translocation and in blue the new position after translocation, while catalyst structures are shown for catalytic reactions; and

5. Summarizes representative substrate scope, the proposed reaction mechanism, together with the key design feature that enable functional group translocation.

This unified presentation is intended to clarify mechanistic patterns, highlight conceptual relationships, and reveal emerging principle across diverse reaction classes.

1.6. This review

While several excellent reviews have examined particular aspects of functional group transposition chemistry,[30] a comprehensive synthesis focused specifically on functional group translocation as defined herein has not been reported. The present review aims to provide such an account by integrating classical and modern developments within a consistent conceptual framework.

This review begins by revisiting classical transformations that laid the conceptual foundations of functional group translocation (Section 2). We then examine major advances reported since 2020, organized according to molecular scaffold and the identity of the migrating functional group. Section 3 addresses translocation on aromatic and heteroaromatic frameworks, Section 4 focuses on sp^3 carbon systems, and Section 5 discusses emerging examples of double functional group translocation.

By framing recent developments within the unified concept of functional group translocation, this review seeks to provide a coherent overview of the field, delineate its current limitations, and outline future directions in synthetic methodology, drug discovery, and materials science.

2. Dawn of functional group translocation

Before discussing recent advances, we first revisit classical examples of functional group translocation on carbon frameworks. These early transformations typically required harsh conditions, including strong Brønsted or Lewis acids, strong bases, or elevated temperatures or irradiation with high-pressure mercury lamps rather than modern LED sources. As a result, the migrating groups were largely limited to robust substituents such as alkyl and aryl groups that could withstand such environments. We also highlight the halogen dance reaction, which has found important applications in natural product synthesis and remains one of the most well-established examples of positional functional group migration. In addition, enzymatic 1,2-migration reactions of amino and hydroxy groups are briefly described, as biologically evolved counterparts that operate under fundamentally different, mild conditions.

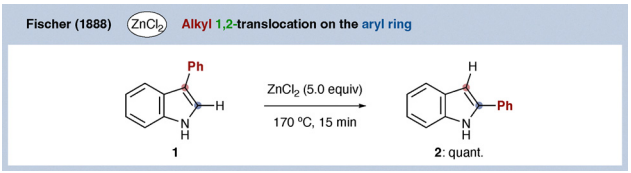

Scheme 1 $ZnCl_2$-promoted 1,2-aryl translocation of 3-phenylindole to 2-phenylindole.

2.1. Alkyl/aryl dance

The 1,*n*-translocation of alkyl groups on aromatic rings, commonly referred to as transalkylation, has long been recognized. In the petrochemical industry, such reactions are widely employed to convert low-value aromatic fractions into more valuable aromatic products, often using zeolite catalysts.[31] Historically, the phenomenon was first observed in 1877 as a by-product in the discovery of the Friedel–Crafts alkylation reaction.[32] Subsequently, in 1886, Anschütz clearly described this behavior in their paper entitled "On the action of aluminum chloride."[33] For example, when toluene is treated with aluminum chloride under appropriate conditions, not only is toluene recovered, but xylenes and trimethylbenzenes are also formed. This observation implies that methyl groups migrate between benzene rings. The authors emphasized that this process should not be regarded as simple elimination, but rather as a translocation reaction in which a methyl group transfers from one molecule to another.

With respect to 1,2-aryl translocation, one of the earliest documented examples involves indole derivatives. In 1888, Fischer and co-workers reported that 3-phenylindole (**1**), when heated with $ZnCl_2$ at 170 °C, underwent quantitative conversion to the corresponding 2-phenyl isomer **2** (Scheme 1).[34] This study represents one of the earliest observations of intramolecular aryl migration on a heteroaromatic framework.

With regard to positional isomerization within a single aromatic framework, a clear experimental demonstration was later provided by Baddeley and co-workers in 1935 (Scheme 2).[35] They reported that heating *p*-di-*n*-propylbenzene (**3**) in the presence of aluminum chloride resulted in formation of the corresponding *meta* isomer **4**, thus establishing intramolecular alkyl migration on the aromatic ring. For this reason, this type of alkyl 1,2-translocation is sometimes referred to as the Baddeley isomerization.[36]

Although related studies were subsequently reported, the reaction mechanism was not initially well understood.[37] During

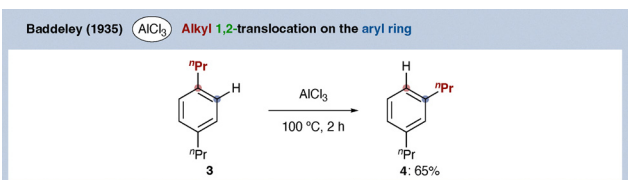

Scheme 2 $AlCl_3$-promoted intramolecular alkyl 1,2-translocation of *p*-diisopropylbenzene.

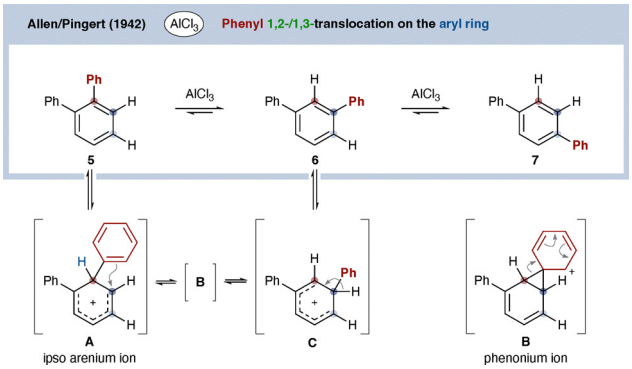

Scheme 3 Lewis acid-induced aryl 1,2-translocation in terphenyl systems *via* arenium-type intermediates.

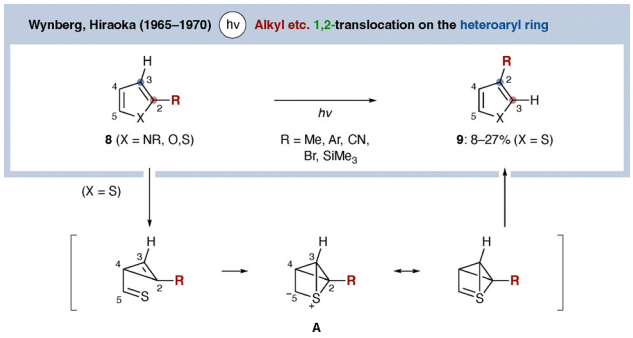

Scheme 4 Photochemical 1,2-aryl migration of heteroarenes.

the 1950s and 1960s, mechanistic investigations clarified the process, including the proposal of *ipso*-arenium intermediates.[38] Despite the harsh conditions required, this transformation has since been applied in synthetic contexts for the preparation of structurally reorganized aromatic compounds.[39]

In the 1950s, alkyl migration on indole frameworks was also reported under strongly acidic conditions[40] (For further details, see ref. 41). More recently, it was shown that heating a chiral 3-alkylindole bearing a stereogenic center at the benzylic 3-position with TRIFLIC ACID (TfOH) affords the corresponding chiral 2-alkylindole without erosion of enantioselectivity by Nakashima and co-workers.[42] This finding highlights that, under appropriately controlled conditions, even acid-promoted alkyl translocation on indoles can proceed with preservation of stereochemical information.

In contrast, 1,2-aryl translocation on simple aromatic systems (as opposed to heteroarenes) was reported somewhat later. In 1942, Allen and Pingert described such a transformation in the context of their studies on the synthesis of *ortho*-terphenyl (Scheme 3).[43] When the synthesized *ortho*-terphenyl (**5**) was treated with $AlCl_3$, formation of *meta*-terphenyl (**6**) was observed. Later mechanistic studies suggested that these transformations proceed through *ipso*-arenium ion intermediates under strongly Lewis acidic conditions.[44] In this mechanism, coordination of $AlCl_3$ generates an *ipso*-arenium ion intermediate A. Subsequent intramolecular attack of an adjacent benzene ring leads to formation of a phenonium ion (Wheland-type) intermediate B. Rearomatization produces a new *ipso*-arenium ion C, ultimately affording *meta*-terphenyl. Formation of *para*-terphenyl (**7**) could be rationalized through an analogous pathway.

These transformations are particularly valuable for the synthesis of polycyclic aromatic hydrocarbons that are otherwise difficult to access through conventional functionalization methods, and they continue to find applications in modern synthetic studies.[45,46]

In addition to thermally or acid-promoted processes, photochemical 1,2-aryl and alkyl migrations have also been reported (Scheme 4). A pioneering example was disclosed in 1965 by Wynberg and co-workers, who described the 1,2-aryl migration of phenylthiophene.[47] Irradiation of 2-phenylthiophene (**8**, X = S, R = Ph) with a high-pressure mercury lamp afforded the corresponding 3-phenylthiophene (**9**, X = S, R = Ph), albeit in yields generally below 30%. Between the late 1960s and 1970, Wynberg and Hiraoka expanded the scope of this transformation to various aryl substituents, alkyl groups, and related heteroaromatic systems such as furans and pyrroles.[48] Although conceptually intriguing and mechanistically insightful, these early photochemical studies were conducted under relatively harsh conditions using high-pressure mercury lamps, which offered limited wavelength selectivity. In addition, purification techniques at the time were less advanced than those available today. Consequently, most examples were obtained in low to modest yields.

The reaction mechanism is highly complex, and the authors discussed multiple possible pathways. One possibility involves photoinduced cleavage of the C2–S bond to generate a thioaldehyde intermediate through a ring opening–ring closure process. However, such a mechanism would be expected to produce multiple isomerization pathways and therefore does not readily account for the high selectivity observed for formation of 3-arylthiophene. Alternatively, the authors proposed that photoexcitation activates the thiophene ring to generate a three-center hypervalent sulfur intermediate A through interaction of the sulfur 3d orbital with the C2–C3 π-bond. Concerted rearrangement of A then leads to re-aromatization with exchange of the C2 and C3 positions, ultimately furnishing 3-arylthiophene. The authors considered this mechanism to best explain the observed positional selectivity and labeling experiments.

Later studies further demonstrated that similar photochemical translocations could occur on pyrrole or thiazole frameworks, and that migrating groups were not limited to aryl substituents but also included cyano, halogen, and silyl groups.[49,50]

Photochemical alkyl migration was also observed in benzene derivatives. In 1964, Burgstahler reported one of the earliest examples of light-induced 1,2- and 1,3-*tert*-butyl migration on aromatic systems (Scheme 5).[51,52] Historically, this work was inspired by the 1963 synthesis of Dewar benzene,[53] which stimulated intense interest in photochemical valence isomerization of aromatic compounds. Upon ultraviolet irradiation

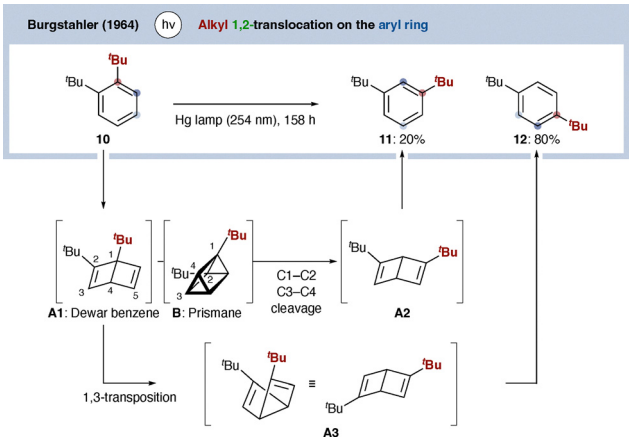

Scheme 5 Light-induced 1,2- and 1,3-*tert*-butyl migration in benzene derivatives.

(254 nm), substrate **10** first undergoes valence isomerization to generate Dewar benzene intermediate **A1**. Subsequent skeletal reorganization through prismane-type intermediate **B** ultimately furnishes products **11** and **12** *via* re-aromatization pathways involving intermediates **A2** and **A3**. Although the detailed bond reorganization process remains complex, these studies established an early conceptual foundation for photochemical positional translocation on aromatic systems.

Although the above studies mainly involved alkyl substituents, Pincock and co-workers later reported related photochemical positional isomerization reactions of benzonitrile derivatives. Under ultraviolet irradiation, methylbenzonitriles underwent reversible positional isomerization through excited-state rearrangement pathways involving highly strained intermediates. Together, these studies established important conceptual foundations for contemporary photochemical translocation chemistry.

Together, these early studies established key conceptual foundations for contemporary photochemical functional group translocation chemistry.

2.2. Acyl migration

Among highly reactive functional groups, 1,2-acyl migration on aromatic rings represents one of the early recognized examples of positional functional group translocation. Although the introduction of acyl groups onto aromatic systems *via* Friedel–Crafts acylation has long been established, the reversibility of this transformation was not initially appreciated.

As early as 1927, Hayashi reported that *ortho*-benzoylbenzoic acid undergoes acyl migration in concentrated sulfuric acid or in the presence of phosphorus pentoxide, a transformation that is still referred to as the Hayashi rearrangement.[54] At the time, however, such migrations were considered exceptional cases restricted to specific substrates. The broader concept of reversibility in Friedel–Crafts acylation was introduced in 1955 by Gore, who proposed that ''The Friedel–Crafts acylation reaction of reactive aromatic hydrocarbons is a reversible process''.[55] In contrast, Olah later stated in 1973 that ''acylation differs from

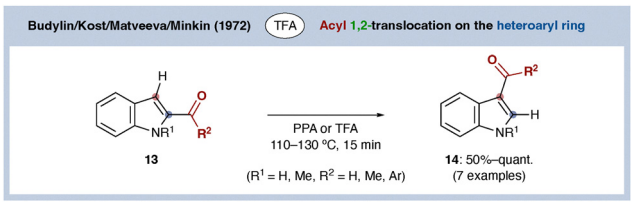

Scheme 6 1,2-acyl migration of 3-acylindoles to 2-acylindoles.

alkylation in being virtually irreversible,'' highlighting the lack of consensus at that time.[56]

Clear experimental evidence for reversible acyl migration first emerged clearly in heteroaromatic systems. In 1972, the groups of Budylin, Kost, and co-workers reported acid-promoted acyl migration reactions of indoles (Scheme 6).[57] Under strongly Brønsted acidic conditions, 2-acylindoles **13** underwent migration of the acyl group to the C3 position to afford 3-acylindoles **14**. These studies established that acyl groups on indole frameworks can undergo migration under acidic conditions. Shortly thereafter, in 1974, Agranat and co-workers demonstrated analogous behavior in simple aromatic systems (Scheme 7).[58] Heating 2-benzoylnaphthalene (**15**) in polyphosphoric acid (PPA) at 140 °C resulted in migration of the acyl group to the 3-position, affording isomer **16**. Subsequent studies reported additional examples of aromatic acyl migration.[59] However, these transformations generally required harsh acidic and thermal conditions. As a consequence, substrates bearing sensitive functional groups were generally incompatible, and the scope of such acyl translocations remained limited to relatively robust systems.

2.3. Halogen dance

The halogen dance reaction refers to a transformation in which an arylmetal species, as well as related arylsodium or arylpotassium species generated under basic conditions, exchanges positions with a bromine or iodine substituent on an aromatic ring.[60] Historically, this reaction has also been described as ''halogen scrambling'' or ''halogen isomerization''. Halogen migration itself had been observed earlier by Vaitiekunas and Nord, who described the synthesis of tetrabromothiophene from 2-bromothiophene.[61] However, the concept of a positional ''dance'' involving translocation of a single halogen atom was established later.[62] The first report explicitly using the term *halogen dance* was published in 1971 by Bunnett and co-workers (Scheme 8).[63]

Mechanistically, the arylpotassium species **A** formed *via* deprotonation is believed to undergo intermolecular halogen–

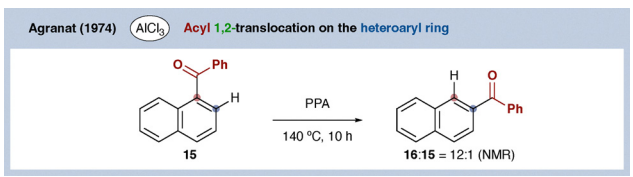

Scheme 7 1,2-acyl migration of 2-benzoylnaphthalene.

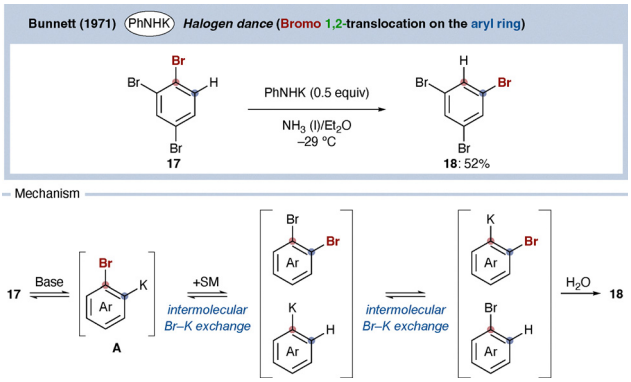

Scheme 8 Halogen dance reaction.

metal exchange twice, thermodynamically most stable arylmetal species. However, when simple benzene derivatives are employed, control over the product distribution is often difficult, leading to mixtures of regioisomers.

The halogen dance reaction is generally driven by formation of the thermodynamically more stable aryllithium species. For example, further lithiation of an aryl bromide already bearing an *ortho*-lithium substituent is disfavored. Consequently, generation of a more readily lithiated bromoarene under the reaction conditions can accelerate the halogen dance process through rapid halogen–metal exchange. This concept was demonstrated by Quéguiner and co-workers (Scheme 9).[64] By adding 3 mol% of bromine as a catalyst, they generated, within the reaction mixture, a more easily lithiated tribromopyridine species, which in turn acted as a catalyst to accelerate the halogen dance reaction. Under these conditions, dibromopyridine or bromochloropyridine **19** underwent efficient 1,2-halogen translocation to afford the corresponding dihalogenated product **20** in 75% yield (X = Cl) and 80% yield (X = Br).

2.4. Enzymatic dance

Enzymatic 1,2-functional group translocations have long been known.[65] In 1985, Halpern reported that coenzyme B_{12}, the biologically active form of vitamin B_{12}, functions as a cofactor in a variety of enzymatic reactions in which a substituent exchanges position with an adjacent hydrogen atom (Scheme 10).[66] Homolytic cleavage of the Co–C bond generates a carbon-centered radical, which abstracts a hydrogen atom (HAT) from the carbon adjacent to the functional group, forming radical intermediate **A**. A subsequent 1,2-shift of the functional group is proposed to proceed *via* transition state B or

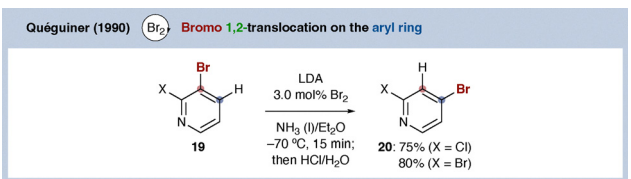

Scheme 9 Catalytic halogen dance promoted by *in situ* generation of a more readily lithiated bromoarene.

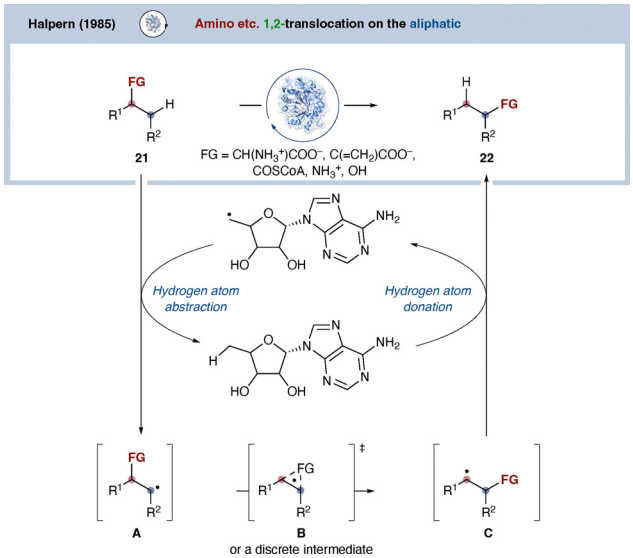

Scheme 10 Coenzyme B_{12}-mediated enzymatic 1,2-functional group translocation *via* radical intermediates.

through a discrete radical intermediate, ultimately to generate radical **C**. The hydrogen atom abstracted earlier is then returned by the coenzyme, which acts as a hydrogen atom donor and thereby completes the catalytic cycle. Such enzymatic transformations most commonly involve migrating groups such as amino or hydroxy substituents. Although radical-mediated 1,2-shift pathways have been proposed, the detailed rearrangement mechanism remains unclear for several substrate classes.

On the other hand, examples have also been reported in which the use of hydrophobic vitamin B_{12} enables 1,2-migration of carbon-based functional groups. In 1990, Murakami and co-workers prepared a hydrophobic vitamin B_{12} derivative, [Cob(II)7C_3ester]ClO_4, incorporated into an octopus cyclophane framework, and successfully applied it to promote 1,2-carbon skeletal migration reactions (Scheme 11).[67] Although the yields were modest, 1,2-migration of acyl (**24a**), ester (**24b**), and cyano (**24c**) groups was achieved.

The proposed mechanism follows a radical-based 1,2-shift pathway similar to that described above. Notably, rendering the vitamin B_{12} complex hydrophobic proved crucial for enabling these carbon-centered functional group migrations, presumably by allowing the reaction to proceed efficiently in nonpolar organic media and thereby promoting productive radical recombination within the solvent cage. These observations highlight the importance of the reaction environment in controlling reactivity.

2.5. 1,2-Ester translocation on sp^3 carbons

Examples of functional group translocation on sp^3 carbons without the involvement of enzymes are rare. However, in 1985, Tou and co-workers reported a 1,2-ester translocation (Scheme 12).[68] They found that treatment of ester **25** with KH in

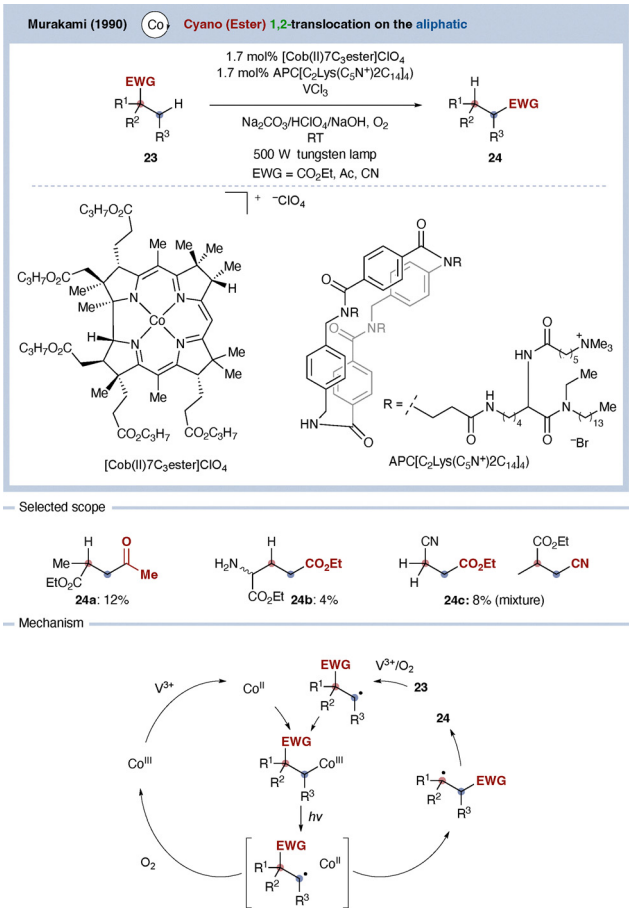

Scheme 11 Hydrophobic vitamin B_{12}-enabled radical 1,2-carbon functional group translocation.

1,2-dimethoxyethane (DME) afforded the corresponding product **26** in which the ester group had undergone 1,2-migration.

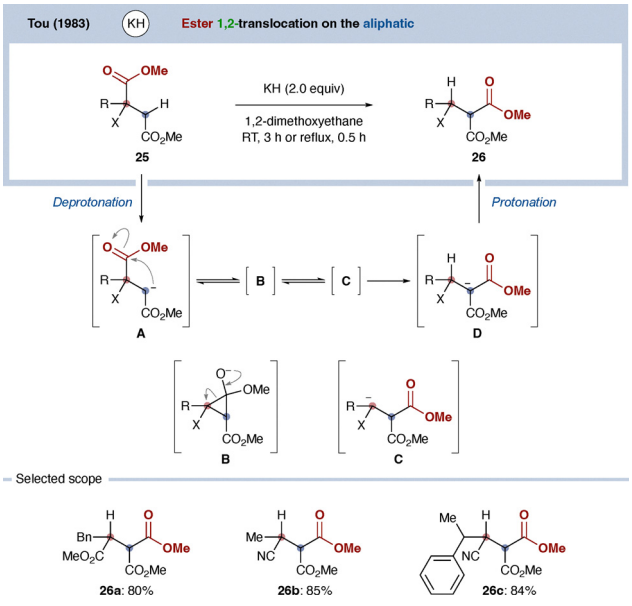

Scheme 12 Base-promoted 1,2-ester translocation on sp^3 carbons *via* cyclopropane intermediates.

The proposed mechanism begins with deprotonation at the α-position of the ester to generate intermediate **A**. A Dieckmann-type cyclization then forms cyclopropane intermediate **B**. Intermediates **A** and **B** are in equilibrium, and ring opening of the cyclopropane from the opposite side produces diester anion **C**. Subsequent proton transfer furnishes doubly stabilized anionic intermediate **D**, which is proposed to play a key role in rendering the process effectively irreversible and thereby driving the reaction forward. The existence of such an anionic intermediate was supported in the original study by trapping experiments with MeI. It was demonstrated that diesters undergo migration to give diester **26a**, and that cyano esters similarly furnish diesters **26b** and **26c**, indicating that ester translocation proceeds under these strongly basic conditions.

Collectively, these classical studies established key conceptual foundations for modern functional group translocation chemistry. Although most early examples required harsh acidic, basic, thermal, or photochemical conditions and were limited to relatively robust functional groups, they revealed important mechanistic principles, including thermodynamic positional exchange, radical-mediated rearrangement, photochemical skeletal reorganization, and organometallic-driven migration processes.

3. Translocation on the aryl ring

3.1. Halogen group (halogen dance)

As discussed in Section 2, halogen dance reactions constitute one of the most widely utilized classes of functional group translocation in organic synthesis.[69] Conventional protocols, however, typically rely on strong bases and cryogenic conditions, which limit functional group tolerance and practical applicability. The development of milder catalytic approaches to halogen translocation and isomerization would therefore significantly enhance the synthetic utility of these transformations.

In 2020, Bandar and co-workers reported an exploratory study toward catalytic halogen dance reactions (Scheme 13).[70] They proposed that non-nucleophilic superbases could promote reversible HX elimination, generating aryne intermediate that undergoes subsequent HX readdition at a different position, thereby enabling halogen isomerization. Consistent with this hypothesis, treatment of bromoarene **27** with the organic superbase P_4-^{t}Bu at 80 °C,[71] resulted in halogen translocation, albeit in modest yields, affording regioisomers **28** and **29**. For example, bromoarene **27a** furnished isomer **28a** in 20% yield, together with the further isomerized product **29a** in 10% yield. Similar reactivity was observed for other bromoarenes, including conversion of **27b** to **28b**, thiophene **27c** to **28c**, and pyridine **27d** to **28d**. Although the efficiencies were limited, these results demonstrated that halogen dance reactivity can be induced without stoichiometric lithium amide bases.

Importantly, regioselective trapping of the translocated isomers was achieved by exploiting intrinsic differences in

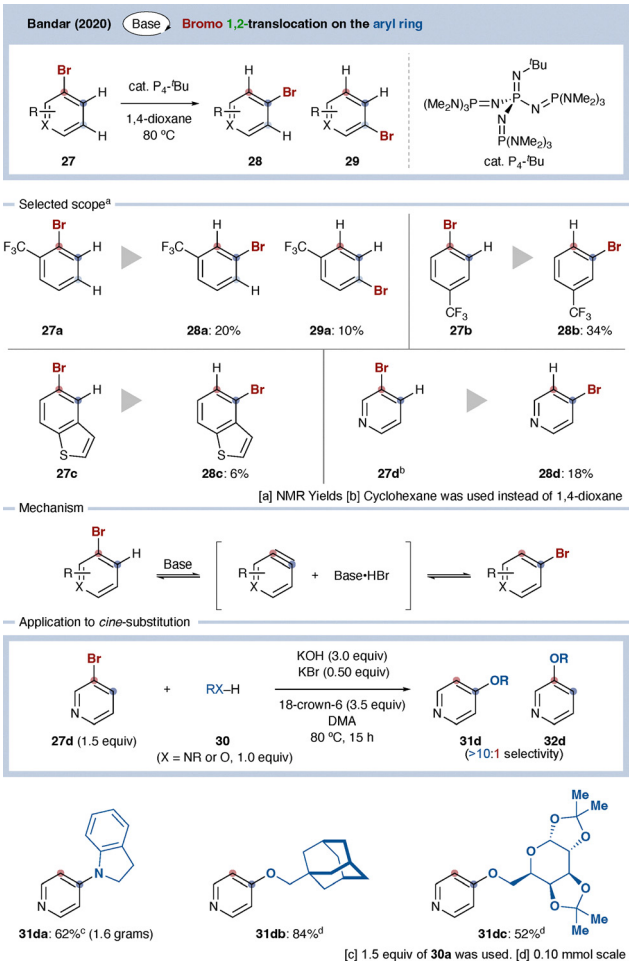

Scheme 13 Catalytic halogen dance reaction.

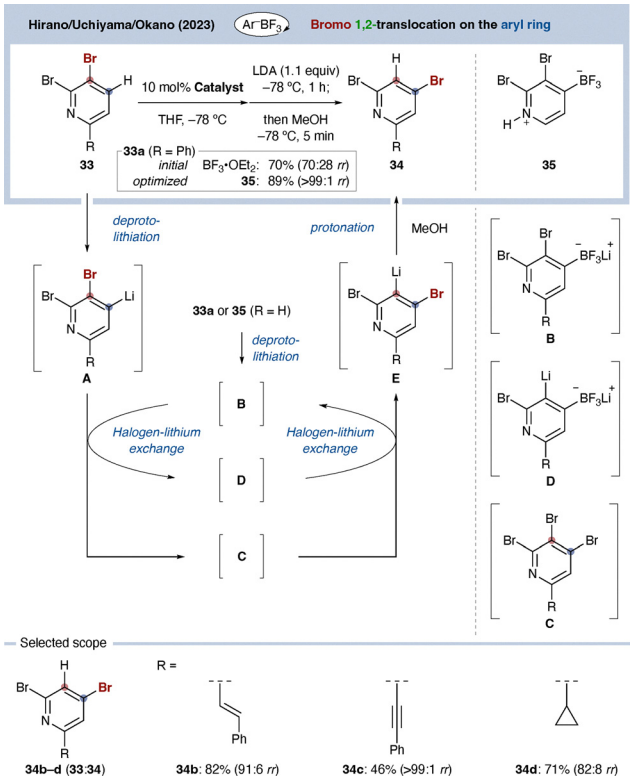

Scheme 14 Lithium aryltrifluoroborate acts as an organocatalyst for the halogen dance reaction.

nucleophilic aromatic substitution reactivity. For instance, treatment of 3-bromopyridine (**27d**) with KOH/KBr in the presence of 18-crown-6 selectively afforded C4-functionalized products **31da** (1.6 g scale), **31db**, and with more complex nucleophile **31dc** (*dr* = >10 : 1). This selectivity reflects the inherent preference for substitution at the C4 position of the pyridine ring. While not yet a fully developed catalytic halogen dance process, this study established a valuable proof of concept for halogen isomerization mediated by reversible HX elimination under comparatively mild conditions.

On the other hand, intriguing examples have emerged in which halogen dance reactivity is markedly accelerated by a specific catalyst, even though strong bases remain necessary. In 2023, the groups of Hirano, Uchiyama, and Okano reported a catalytic halogen dance reaction mediated by lithium aryltrifluoroborates (Scheme 14).[72] When dibromopyridine **33a** was treated with $BF_3{\cdot}OEt_2$, followed by a stoichiometric amount of LDA, migration of the bromo group from the C3 to the C4 position occurred, affording the dance product **34a** together with the starting material **33a** in 70 : 28 ratio. From these observations, the authors proposed that deprotonation of **33a**, followed by reaction with $BF_3{\cdot}OEt_2$, generates a lithium aryltrifluoroborate species **B** which serves as the active catalyst. To substantiate this hypothesis, independently prepared **35** was introduced in 10 mol%, resulting in exclusive formation of **34a** in 89% yield. The scope was further demonstrated by varying the substituent on the pyridine framework; styryl (**34b**), alkynyl (**34c**), and cyclopropyl (**34d**) derivatives all underwent efficient halogen translocation under the optimized conditions.

Mechanistically, deprotonation of dibromopyridine **33** generates a pyridyllithium intermediate **A**, which undergoes first lithium-halogen exchange with catalyst **B** to form tribromopyridine **C** and lithium aryltrifluoroborate **D**. A second lithium–halogen exchange between **C** and **D** then furnishes the thermodynamically favored pyridyllithium species **E** while regenerating catalyst **B**, and completing the catalytic cycle. In this scenario, the C–BF_3Li unit functions as a transient halogen shuttle, and stabilizing F–Li interactions are proposed to lower energy of key transition states. As a consequence, the intrinsic substrate-controlled regioselectivity of halogen dance chemistry can be modulated, leading to substantial rate acceleration.

Although the process still relies on strong base, this study provides the first clear example of catalyst-enabled acceleration of halogen dance reactivity. It thus represents a significant conceptual advance and suggests a viable path toward more general and efficient catalytic halogen translocation reactions.

Accordingly, even after 2020, the development of truly catalytic and highly selective halogen dance reactions with high selectivity had remained elusive. Very recently, however, advances toward this goal have begun to appear. In 2025, Liu

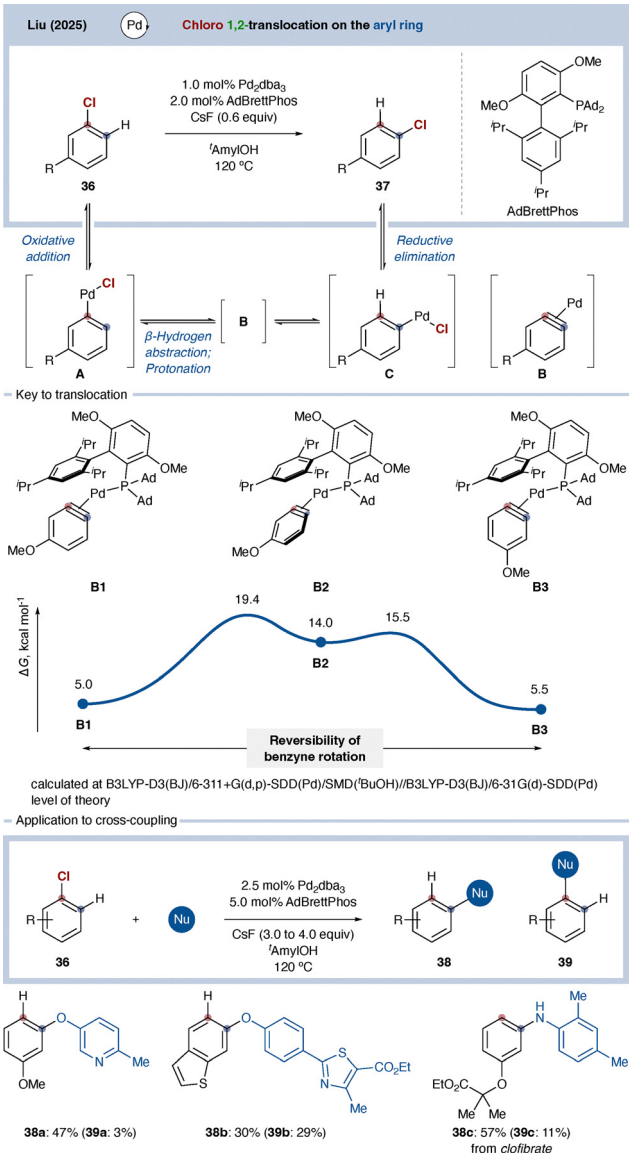

Scheme 15 Pd-catalyzed chloro 1,2-translocation and migratory aryl cross-coupling.

and co-workers reported a migratory cross-coupling reaction of aryl chlorides (Scheme 15).[73] They found that a Pd catalyst bearing the bulky AdBrettPhos ligand,[74] in combination with CsF as an additive, promoted partial migration of a *para*-positioned chloro group to the *meta* position. Mechanistically, oxidative addition of the aryl chloride **36** generates intermediate **A**, which undergoes β-hydride elimination to form a Pd–benzyne intermediate **B**.[75] This step is proposed to be reversible. Re-insertion of the palladium species into the benzyne moiety, followed by protonation, affords intermediate **C**. Subsequent reductive elimination from **C** preferentially furnishes the thermodynamically more stable *meta*-substituted product **37**, thereby regenerating the palladium catalyst. DFT calculations supported this proposal, indicating a minimal energy difference of only 0.5 kcal mol^{-1} between the *para*- and *meta*-substituted benzyne intermediates (**B1** and **B3**). The observed regioselectivity is likely governed by thermodynamic equilibration between the isomeric aryl halides under the reaction conditions.

Moreover, under Buchwald–Hartwig-type cross-coupling conditions, the *meta* isomer was found to react slightly faster than the corresponding the *para* isomer. This kinetic preference enabled selective formation of the *meta*-coupled product **38a–38c**. Although migratory cross-coupling reactions have previously been described for bromoarenes,[76] extension of this strategy to chloroarenes represents a significant and previously unexplored advance in catalytic translocation chemistry.

3.2. Ester group (ester dance reaction)

Beyond alkyl, aryl, halogen, acyl, and silyl groups, 1,2-translocation of other functional groups on the aromatic ring had remained unexplored, and catalytic implementations were entirely absent. In 2020, Yamaguchi and co-workers reported the ester dance reaction, enabling 1,2-transposition of an ester group on an aromatic framework (Scheme 16).[77] This transformation was discovered during investigations on the decarbonylation of aryl phenyl esters[78] where use of a Pd catalyst in combination with the dcypt (3,4-bis(dicyclohexylphosphino)thiophene) ligand led to unexpected ester migration.[79] For example, treatment of phenyl 1-naphthoate (**40a**) under the optimized conditions afforded the transposed product **41a** in 86% yield with high regioselectivity.

The scope of the reaction proved broad. Variation of substituents on the phenyl moiety of the ester was tolerated (**41b**), and heteroaromatic substrates were likewise compatible. In pyridine-derived ester **40c**, the ester group migrated selectively from the C4 to the C3 position (**41c**). Pyrene derivatives also underwent smooth translocation. Notably, phenyl ester **40d**, readily prepared from pyrene-1-carboxylic acid ($112/g, Sigma-Aldrich, May 2026), was converted into the corresponding pyrene-2-carboxylic acid phenyl ester **41d**. Subsequent hydrolysis provided the corresponding pyrene-2-carboxylic acid ($1001/g, Sigma-Aldrich, May 2026), highlighting the practical utility of ester dance for accessing otherwise difficult positional isomers from simple feedstock materials.

Mechanistically, oxidative addition of ester **40** to Pd/dcypt catalyst generates intermediate **A**, followed by concerted deprotonation to form a Pd–aryne-type intermediate **B**. Subsequent protonation, carbonylation, and reductive elimination deliver the transposed ester **41**. The reaction operates under thermodynamic control, as supported by calculated Gibbs free energies. For example, product **41a** was calculated to be 3.73 kcal mol^{-1} more stable than **40a**, consistent with the observed equilibrium distribution.

Importantly, the authors demonstrated that ester dance can be combined with a decarbonylative coupling to achieve formal *cine*-coupling outcomes.[80,81] In contrast to thermodynamically governed translocation step, the selectivity of the subsequent coupling step is determined by nucleophile reactivity. For instance, coupling of phenyl thiophene-3-carboxylate (**40e**) with thiazole **42a** furnished **43ea** preferentially. Although **40e** does not undergo ester dance under the reaction conditions due to near isoenergetic ester isomers, coupling proceeds *via* the more

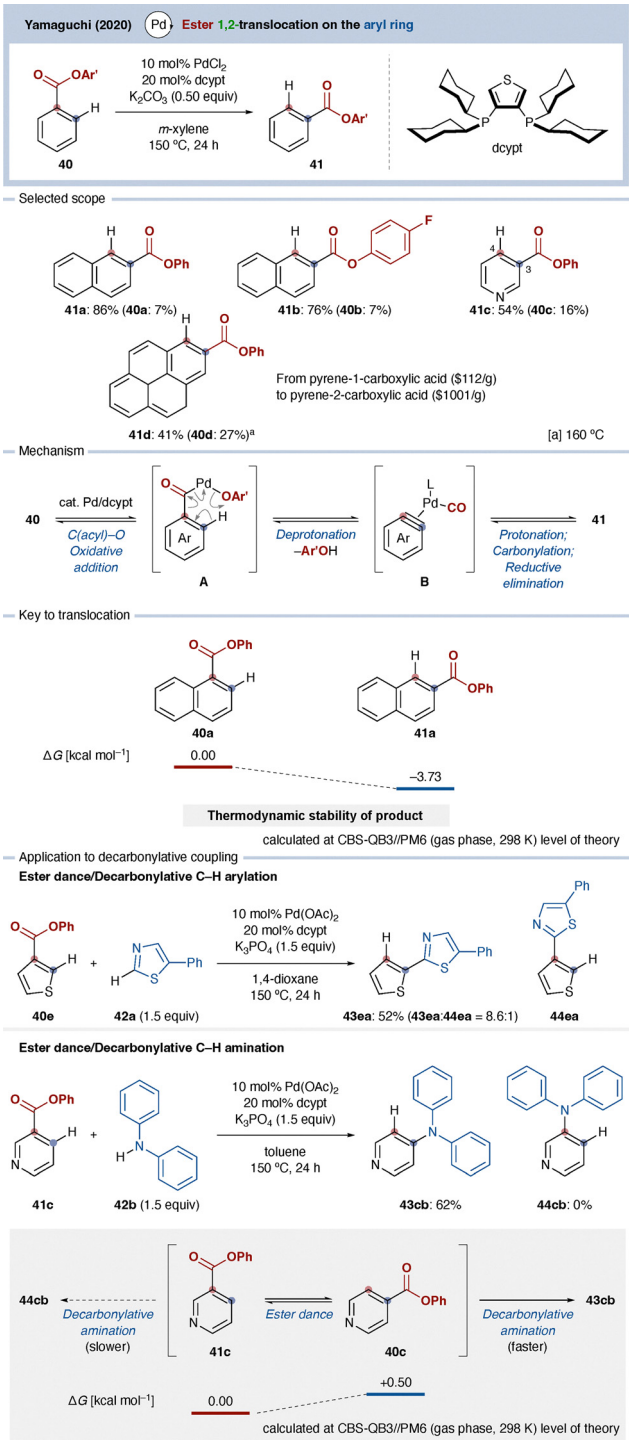

Scheme 16 Pd-catalyzed ester dance reaction.

reactive position effectively overriding thermodynamic preferences. Similarly, coupling of phenyl nicotinate (**41c**) with diphenylamine (**42b**) afforded the C4-arylated product **43cb**, selectively, despite the minimal (0.5 kcal mol^{-1}) thermodynamic bias between positional isomers (**40c** and **41c**).

These studies illustrate that integration of ester dance with downstream decarbonylative coupling enables access to substitution patterns unattainable by either process alone. This contrast between thermodynamically controlled translocation and kinetically controlled coupling selectivity underscores the mechanistic diversity possible within functional group translocation chemistry.

3.3. Silyl group

In 2021, Tobisu and co-workers reported a Ru-catalyzed 1,2- and 1,3-translocation of silyl groups on aromatic and heteroaromatic frameworks (Scheme 17).[82] Although thermal or strongly acid-promoted silyl migration had been documented previously,[83] this study constituted the first example of silyl group translocation enabled by transition metal catalysis.

When *ortho*-silylaniline derivative **45a** was heated in toluene at 180 °C in the presence of a $[RuCl_2(p\text{-cymene})]_2$, BINAP, and $Cu(OAc)_2$, efficient 1,3-migration occurred to afford the *para*-silylated product **46a** in high yield. The reaction exhibited broad substrate compatibility; even substrates bearing a triethylsilyl group ($SiEt_3$) underwent translocation, albeit in diminished yield, to give **46b**. Naphthylamine and pyridylamine derivatives also underwent 1,3-translocation to give products **46b–46d**. In contrast, substrates bearing silyl groups at the 2-position of indole or pyrrole preferentially underwent 1,2-migration. In these cases, the reactions preferentially underwent 1,2-migration under identical conditions, furnishing the

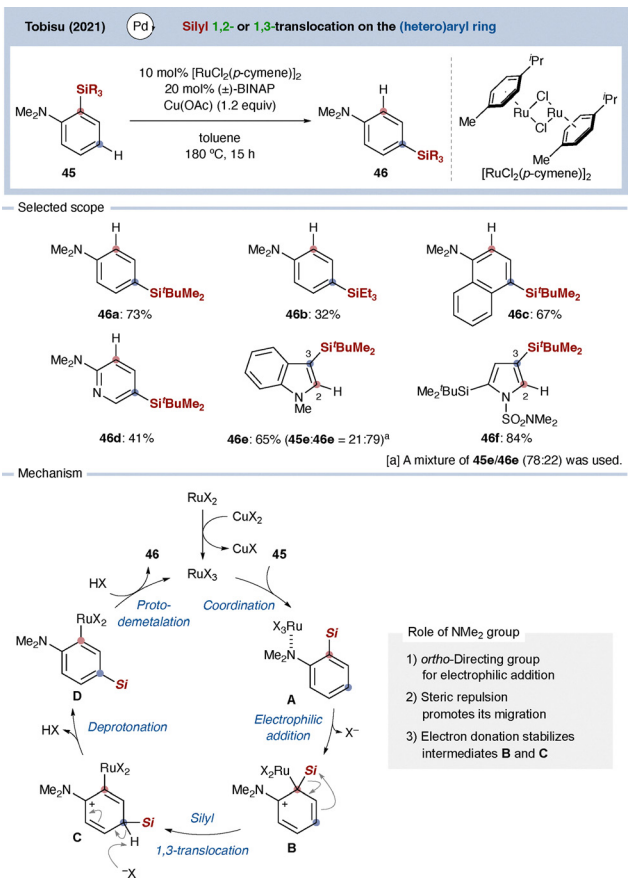

Scheme 17 Ru-catalyzed silyl translocation on aromatic and heteroaromatic frameworks.

corresponding 3-silylated indole **46e** and pyrrole **46f** (Notably, photoinduced 1,2-silyl migration in pyrroles has also been reported).[49b] These results indicate that the migration distance is highly dependent on the heteroaromatic scaffold, underscoring the distinctive reactivity patterns enabled by metal–catalyzed silyl translocation.

A plausible reaction mechanism was proposed. $Cu(OAc)_2$ oxidizes the Ru(II) precatalyst, to generate active Ru(III) species, which coordinates to the aniline nitrogen to form complex **A**. Electrophilic attack at the *ipso* carbon bearing the silyl group produces intermediate **B**. Subsequent migration of the silyl group, driven in part by relief of steric congestion, affords intermediate **C**. Rearomatization then furnishes intermediate **D**, and regeneration of the catalytically active Ru species occurs *via* protodemetalation with HX, delivering the transposed product **46**, and completing the catalytic cycle. Electron-donating substituents such as NMe_2, act as directing groups to facilitate the initial electrophilic activation step. Notably, the size of the silyl group proved critical: small groups such as trimethylsilyl (TMS) were ineffective, whereas bulkier substituents including *t*-butyldimethylsilyl (TBS) and triisopropylsilyl (TIPS) enabled efficient migration. Electron-rich aromatic systems were also found to promote the process, by stabilizing key cationic intermediates.

3.4. Aryl group

As discussed in Section 2, aryl migration reactions have been recognized for over a century. Related behavior has also been observed for heteroaromatic systems, where aryl migration from the C3 position to the C2 position of indoles, benzothiophenes, and related scaffolds was reported under strongly acidic or otherwise forcing conditions.[84] However, these early studies did not establish broad substrate scope, and, importantly, migration in the reverse direction (C2 to C3) had not been reported.

In 2022, Yamaguchi and co-workers reported an $AlCl_3$-mediated 1,2-aryl translocation reaction of aryl heteroarenes that established both broad substrate generality and bidirectional migration on heteroaromatic frameworks (Scheme 18).[85] A range of C3-aryl-substituted benzothiophenes **47**, indoles, and thiophenes underwent efficient C3-to-C2 migration to furnish products **48a–48c**. Notably, the previously unreported C2-to-C3 migration was realized in benzothiophene derivatives bearing electron-donating substituents at the C6 position (*e.g.* **47d** and **47e**). In these cases, $Zn(OTf)_2$ proved crucial as an effective additive to suppress undesired demethylation of methoxy groups under Lewis acidic conditions, thereby enabling productive aryl translocation.

A mechanistic pathway consistent with these observations was proposed. Under Lewis acidic conditions, electrophilic activation occurs preferentially at the more nucleophilic C3 position to generate acid adduct **A**, which evolves into Wheland intermediate **B**. Rearomatization, facilitated by lone-pair donation from heteroatom, and subsequent acid dissociation affords the C2-arylated product **48**. In contrast, when an electron-donating substituent is present at the C6 position,

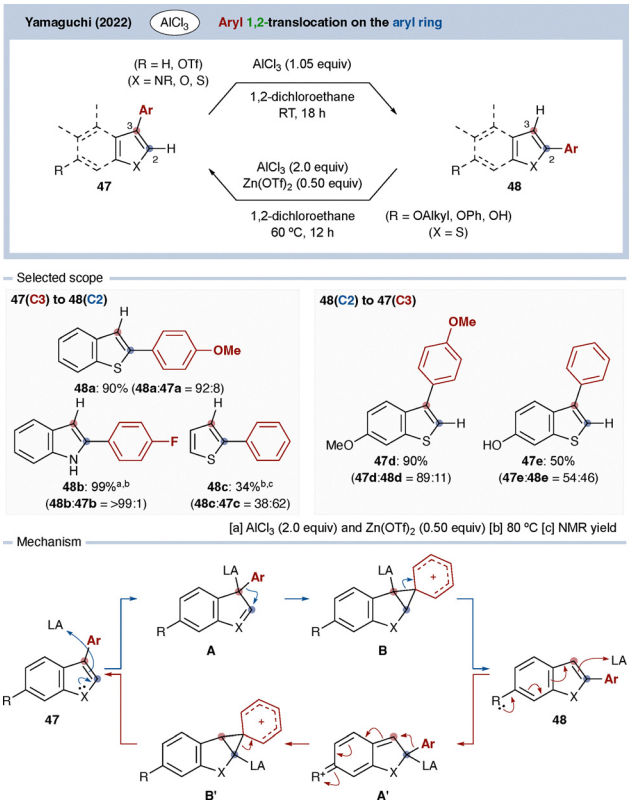

Scheme 18 Aryl dance reaction.

electronic activation of the C2 position enables formation of adduct **A′**. This intermediate proceeds through a related Wheland-type species **B′**, ultimately furnishing the C3-arylated product **47**. These results demonstrate that the directionality of aryl translocation on the heteroaromatic system can be electronically controlled with the migration pathway governed by differential stabilization of key cationic intermediates.

Very recently, Liu and co-workers reported an exceptionally distinctive example of 1,2-aryl translocation on an aromatic framework in the context of 1,2-azaborines (Scheme 19).[86] 1,2-Azaborines, in which one C–C bond of benzene is replaced by an isoelectronic B–N unit, are widely regarded as benzene analogues.[87] During investigation into their synthesis and functionalization, the authors discovered a photochemical strategy that enables formal 1,2-aryl migration, thereby providing flexible access to diverse substitution patterns. Upon blue-light irradiation in the presence of the photocatalyst 4CzIPN,[88] 5-arylated 1,2-azaborines **49**, underwent selective migration of the aryl group from the C5 to C4 position to afford **50**. Likewise, 3-aryl-5-substituted derivatives **51** furnished product **52**, in which the aryl groups initially located at the 3- and 5-positions relocated to the 5- and 4-positions, respectively.

The reaction exhibits broad tolerance toward both electron-rich and electron-deficient aryl substituents (**50a** and **50b**), and accommodate heteroaryl units such as pyrimidine (**50c**) as well as complex motifs including caffeine (**50d**). Notably, related azaborine-type substrates (**51**) also undergo analogous translocation processes. In these systems, migration can occur

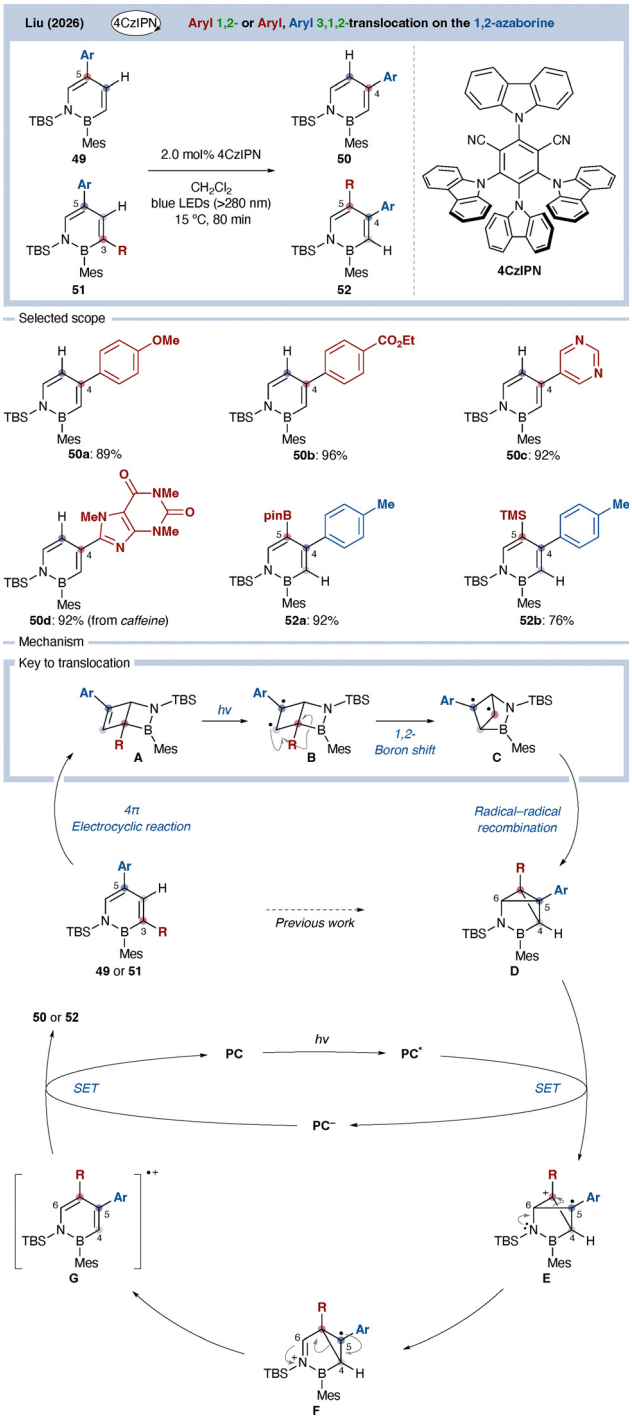

Scheme 19 1,2-Aryl translocation of 1,2-azaborines.

between an aryl group and a boryl substituent (**52a**), or between an aryl group and a trimethylsilyl (TMS) group (**52b**). Importantly, the process can be viewed not merely as aryl migration, but in certain cases as an exchange between an aryl group and hydrogen. or even between an aryl group and boron, underscoring the distinctive reactivity of the azaborine scaffold.

Mechanistically, irradiation first induces 4π-electrocyclization of **49** or **51** to generate a 1,2-BN-Dewar benzene intermediate **A**. Further photoexcitation promotes homolytic cleavage to form biradical **B**, followed by a 1,2-radical boron shift to give intermediate **C** and subsequent radical recombination to afford 1,2-BN-benzvalene **D**. These steps are consistent with the groups' earlier studies.[89] The crucial innovation arises under visible-light photoredox conditions; oxidation of **D** by 4CzIPN generates radical cation [BN-benzvalene]$^{\bullet+}$ **E**, rendering the central C5–C6 σ bond highly labile. Bond cleavage leads to a prefulvene-like intermediate **F**, which undergoes further bond reorganization to produce a rearranged radical cation **X**.

Finally, reduction by the photocatalyst (Ir(II) or PC^{-}) restores aromaticity and furnishes the translocated products **50** or **52**.

Although mechanistically unique, this study establishes a fundamentally new mode of 1,2-aryl translocation on an aromatic framework. Moreover, the authors demonstrated that product **52** (R = Me) can serve as a versatile intermediate for the synthesis of fully substituted 1,2-azaborines, highlighting the broader synthetic potential of this transformation. Very recently, Liu and co-workers further demonstrated that BN-benzvalene intermediates can undergo catalyst-controlled divergent rearomatization to furnish either C3- or C5-functionalized 1,2-azaborines, thereby expanding the concept of positional editing on BN-aromatic frameworks.[90]

Building on these recent advances in aryl translocation chemistry, Chiba and co-workers reported a photoredox-catalyzed 1,2-aryl translocation on pyridine frameworks (Scheme 20).[91] Under irradiation with 427 nm light, treatment of C4-arylpyridines **53** with the organic photocatalyst 3DPAFIPN[92] in the presence of potassium formate, Cs_2CO_3, and HFIP in DMSO promoted migration of the aryl group from the C4 position to the adjacent C5 position, affording translocated pyridines **54**. Under related conditions, 2,4-diarylpyridines **55** underwent selective C4-to-C3 aryl translocation to furnish pyridines **56**. Interestingly, addition of MeOH altered the reaction pathway, enabling C2-to-C3 translocation of the aryl group to give products **57**. The reaction showed moderate substrate generality. For the C4-to-C5 translocation manifold, amide-containing aryl groups and pyridine-containing aryl substituents were tolerated, affording products **54a** and **54b**. In the C4-to-C3 translocation, products such as **56a** and **56b** were obtained efficiently. In the C2-to-C3 migration pathway, the presence of a *para*-methoxyphenyl (PMP) group at the C4 position proved crucial for efficient translocation (**57a** and **57b**). On the other hand, because the reaction operates under relatively reducing conditions, functionalities such as ketones and other readily reducible groups were not compatible.

A plausible reaction mechanism of C4-to-C5 translocation was proposed as follows. First, photoexcited 3DPAFIPN together with formate-derived reductants promotes sequential single-electron reduction and protonation of pyridine **53** to generate intermediate **A**. Further reduction and protonation convert the aromatic pyridine ring into the corresponding 1,4-dihydropyridine intermediate **B**. The authors proposed that this process occurs through an ECEC (electrochemical–chemical–electrochemical–chemical) sequence. Subsequent single-electron oxidation of **B** generates an azacyclohexadienyl

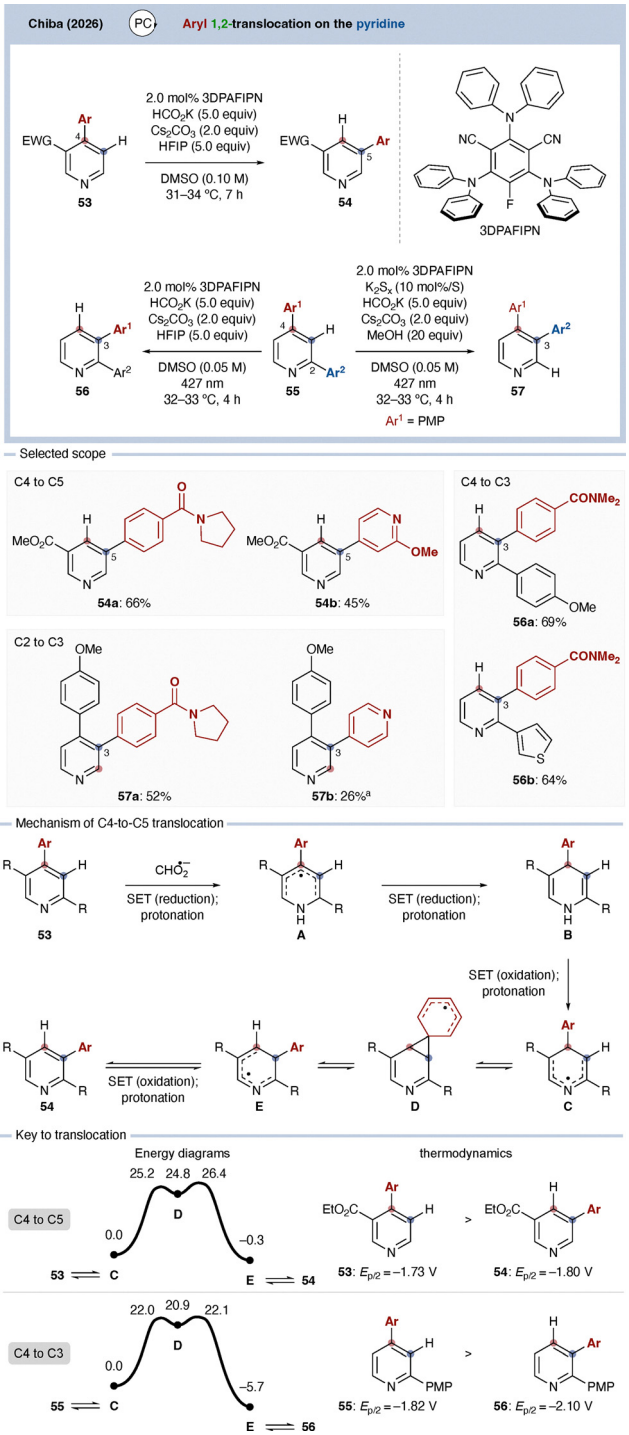

Scheme 20 Photoredox-catalyzed aryl translocation on pyridine frameworks.

radical intermediate **C**. In this species, the radical center is positioned adjacent to the aryl substituent, enabling intramolecular radical addition onto the aryl ring to form spiro radical intermediate **D**. Because this spiro intermediate is highly unstable, rearomatization accompanied by C–C bond reorganization proceeds readily, resulting in 1,2-translocation of the aryl group and formation of a new azacyclohexadienyl radical intermediate **E**. Subsequent single-electron transfer then furnishes the translocated pyridine product **54**. The key feature enabling this transformation is that temporary dearomatization generates an azacyclohexadienyl radical manifold capable of reversible aryl migration, while the overall selectivity is governed by the relative thermodynamic stability and redox properties of the resulting isomers. In the C4-to-C5 translocation pathway, the activation barrier for formation of spiro radical intermediate was calculated to be 25.2 kcal mol^{-1}, and the resulting C5 radical was found to be 0.3 kcal mol^{-1} more stable than the corresponding C4 radical. The reduction potentials of the starting C4-arylpyridine **53** and the C5-translocated product **54** were measured as $E_{p/2}$ = −1.73 V and −1.80 V *vs.* SCE, respectively. In the C4-to-C3 translocation pathway, formation of the corresponding spiro radical proceeds through a lower activation barrier of 22.0 kcal mol^{-1}, and the resulting **E** intermediate was calculated to be 5.7 kcal mol^{-1} more stable than **C**. Correspondingly, the reduction potentials of 2,4-diarylpyridine **55** and the translocated 2,3-diarylpyridine **56** were measured as $E_{p/2}$ = −1.82 V and −2.10 V *vs.* SCE, respectively. Thus, photoredox-induced temporary dearomatization creates a reversible radical translocation manifold that enables positional editing of aryl groups on pyridine frameworks.

3.5. Hydroxy group (Phenolic OH)

Alkyl group translocation reactions on phenolic aromatic systems had long been known under Friedel–Crafts conditions. Bolton and co-workers reported positional isomerization of *tert*-butylphenols, while Jacquesy and co-workers later disclosed intramolecular 1,2-bromine shift reactions of bromophenols under superacidic conditions.[93] In contrast, from the perspective of late-stage functionalization of complex molecules, *ortho*- and *para*-hydroxylation of aromatic rings can often be achieved through C–H functionalization strategies.[94] However, selective installation of a hydroxy group at the *meta* position has remained a longstanding synthetic challenge. To address this limitation, Lumb and co-workers reported in 2024 a formal 1,2-hydroxy translocation from the *para* to the *meta* position of phenols (Scheme 21).[95]

In this approach, *para*-substituted phenol **58** is first oxidized with 2-iodoxybenzoic acid (IBX) to generate the corresponding *ortho*-quinone **A**. Subsequent treatment with 2,4,6-triisopropylbenzenesulfonyl hydrazide (TPSH) enables selective diazotization, forming diazo intermediate **B**. A following Cu-mediated reduction of **B** completed the sequence, ultimately delivering the *meta*-phenol **59**. The bulky triisopropylbenzene unit of TPSH plays a dual role: it promotes α-elimination and suppresses undesired sulfonylation of intermediate **A**.

Regarding substrate scope (*e.g.* **59a–c**), efficient conversion requires initial oxidation to the *ortho*-quinone, and phenols bearing electron-donating substituents generally provide higher yields. Although this strategy proceeds through multiple discrete steps and therefore does not meet the strict definition of a single-step, catalytic 1,2-functional group translocation emphasized in this review, purification is required only at the

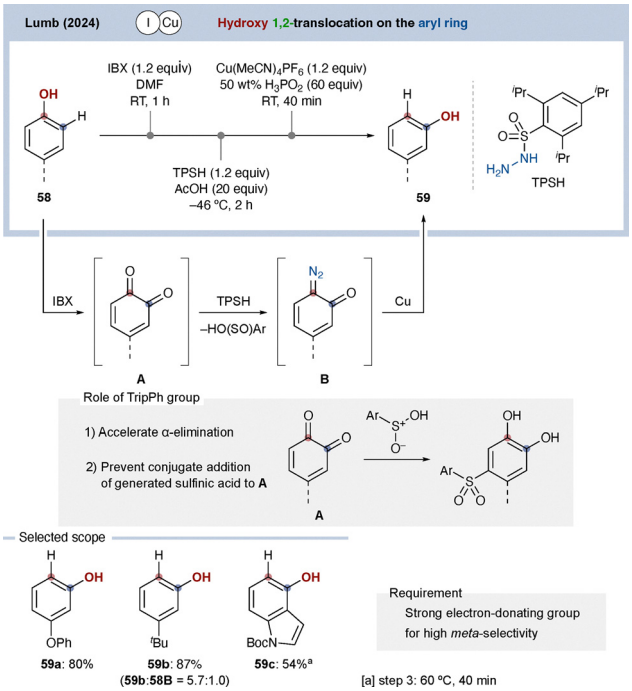

Scheme 21 Hydroxy group 1,2-translocation of phenols.

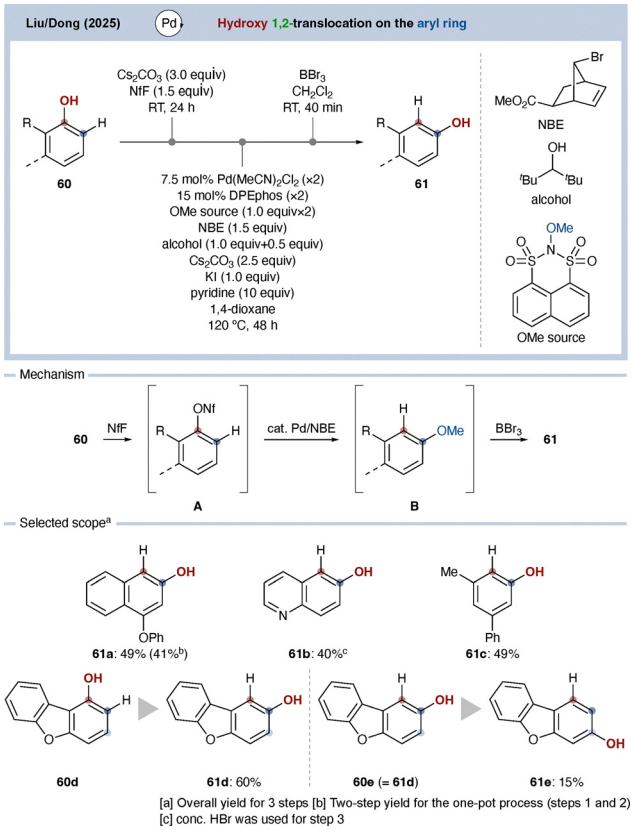

Scheme 22 Phenolic OH group 1,2-translocation by Pd/NBE cooperative catalysis.

final stage. Consequently, this method represents practical and conceptually noteworthy solution for positional relocation of hydroxy groups on aromatic rings, particularly in late-stage molecular editing.

Although the phenolic 1,2-hydroxy translocation reported by Lumb and co-workers provides an effective solution, it is subject to several limitations. Most notably, the method requires an electron-donating substituent at the *para* position of the starting phenol, and consequently the hydroxy migration is restricted to formal *para*-to-*meta* translocation. These structural constraints limit both the generality and positional flexibility of the strategy.

In 2025, Dong and co-workers disclosed a complementary approach that overcomes these restrictions (Scheme 22).[96] Although their protocol also proceeds through multiple steps, it enables hydroxy migration without requiring a *para*-substituent on the starting phenol. In this sequence, phenol **60** is first converted into the corresponding nonaflate (ONf) **A**, which undergoes a Pd-catalyzed norbornene-mediated Catellani reaction.[97] This transformation effects *ortho* methoxylation in conjunction with *ipso* hydrogenation. Subsequent demethylation of intermediate **B** furnishes the transposed phenol **61**. Under these conditions, *meta*-naphthol **61a** was obtained in moderate yield. Importantly, substrates lacking a *para* substituent were well tolerated, as illustrated by **61b**, and phenols bearing a phenyl substituent also underwent efficient translocation to afford **61c**. In the case of benzofuran-derived substrate **60d**, a single 1,2-hydroxy translocation delivered **61d**, while iterative application of the sequence enabled further positional relocation to give **61e**. Collectively, these results demonstrate that the Catellani manifold provides a versatile platform for controlled hydroxy translocation on aromatic frameworks.

3.6. Alkyl group

As discussed in Sections 2, 1,2- and 1,3-migration of alkyl groups has been known for many decades, typically under strongly acidic or thermal conditions. In 2025, Leonori and co-workers reported a conceptually distinct photochemical strategy that enables controlled 1,2- and 1,3-methyl migration to generate positional isomers of phenols (Scheme 23).[98] Using *meta*-cresol (**62a**) as a model substrate, treatment with $AlBr_3$ followed by irradiation at 310 nm afforded *para*-cresol (**63a**) in 68% yield. In contrast, switching the light source to 390 nm selectively delivered *ortho*-cresol (**64a**) in 64% yield. Thus, simple modulation of the irradiation wavelength reverses the positional selectivity of alkyl migration.

This wavelength-dependent selectivity can be rationalized by the proposed mechanism. Under acidic conditions, **62a** is converted into protonated arenium ions **A** and **A′**. Upon photoexcitation, these species undergo 4π electrocyclization to generate bicyclic cation intermediates **B** and **B′**. Intermediate **B** undergoes a 1,2-methylene shift to give **C**, followed by rearomatization through arenium ion **D** to furnish *para*-cresol (**63a**). In contrast, **B′** proceeds *via* an analogous pathway through **C′**, and arenium ion **D′** to afford *ortho*-cresol (**64a**). Although multiple arenium ions can be formed under the reaction conditions, each exhibits a distinct absorption maximum. Irradiation at 310 nm[99] selectively excites the C4-protonated arenium ion **A**, directing the reaction toward

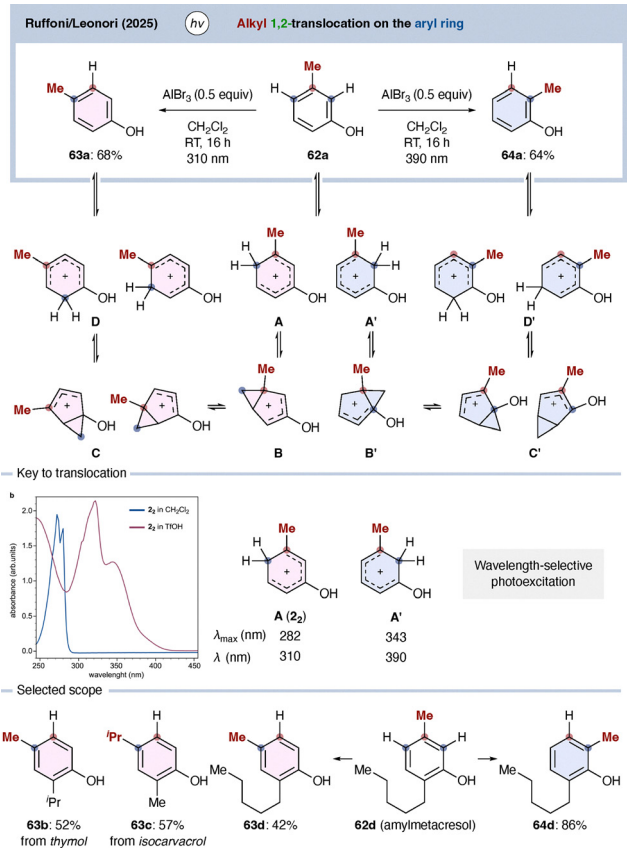

Scheme 23 1,2- or 1,3-Methylene shift of cresol.

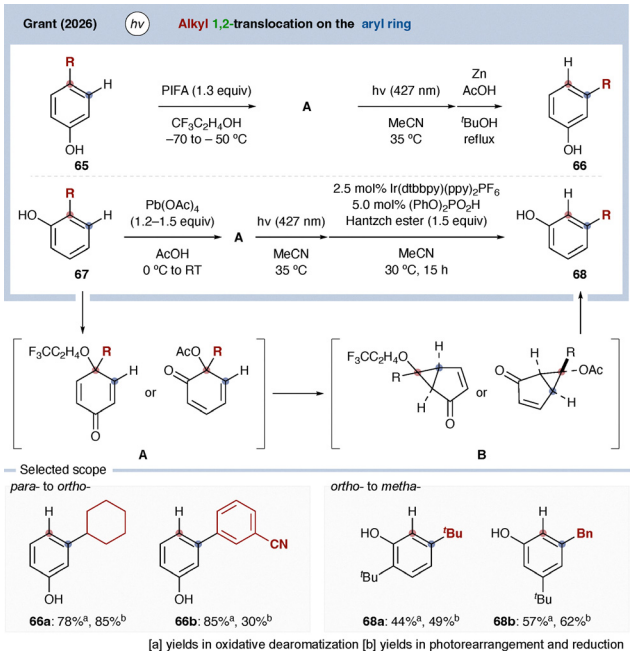

Scheme 24 Photochemical translocation of substituents on phenols *via* skeletal editing.

para-cresol (**63a**), whereas irradiation at 390 nm preferentially excites the C2-protonated arenium ion **A′**, leading to *ortho*-cresol (**64a**).

The generality of the wavelength-controlled strategy was demonstrated across several substrates. Products **63b** and **63c** from simple natural products were obtained with high positional selectivity, and in the case of amyl-*meta*-cresol (**62d**), irradiation at 310 nm furnished **63d** in 42% yield, while 390 nm irradiation provided **64d** in 86% yield.

The success of this approach relies on advances in LED technology, which enable precise wavelength selection, as well as on the ability to predict absorption properties of reactive intermediates computationally. Together, these features suggest that selective excitation of specific intermediates may emerge as a powerful design principle for controlling functional group translocation in aromatic systems.

Very recently, Grant and co-workers reported a conceptually distinct strategy for 1,2-translocation of substituents on phenolic aromatic systems (Scheme 24).[100] In this approach, phenols **65** were first oxidized with PIFA ([bis(trifluoroacetoxy)iodo]benzene) to generate dienone intermediate **A**. Subsequent photochemical rearrangement followed by treatment with Zn/AcOH furnished *meta*-substituted phenols **66** through formal *para*-to-*meta* translocation of the substituent. In the case of *ortho*-substituted phenols **67**, oxidation with lead tetraacetate generated the corresponding *ortho*-dienones **A**, which upon irradiation and subsequent photoredox-mediated rearomatization similarly afforded *meta*-substituted phenols **68**.

Mechanistically, photoexcitation of dienone **A** induces a di-π-methane rearrangement to generate bicyclo[3.1.0]hexenone intermediate **B**.[101] Under reductive conditions, these intermediates initially form cyclopropyl ketyl radicals. However, β-scission of these radicals was found to be relatively slow, allowing further two-electron reduction to occur. The resulting anionic intermediate then undergoes concerted rearomatization, selectively furnishing the *meta*-substituted products. Substrates bearing cyclopropyl or aryl substituents at the *para* position were compatible, giving the corresponding *meta*-substituted phenols **66a** and **66b**. Phenols bearing *ortho tert*-butyl or benzyl substituents also underwent efficient translocation to afford products **68a** and **68b** in moderate yields.

Collectively, Sections 3.5 and 3.6 highlight several fundamentally distinct modes of translocation chemistry on phenolic aromatic systems. Whereas the methods developed by Lumb and Dong involve peripheral editing through positional relocation of hydroxy groups, the photochemical translocation reported by Leonori proceeds through arenium-ion-mediated alkyl migration. In contrast, Grant's strategy operates through skeletal editing of the aromatic framework itself *via* photochemical valence rearrangement and rearomatization. These examples illustrate how superficially similar "translocation" reactions can proceed through fundamentally different mechanistic and conceptual manifolds.

3.7. Acyl group

As described in Sections 2, 1,2-acyl migration reactions are well established, but traditionally require forcing conditions, including high temperatures and strong Brønsted or Lewis acids.

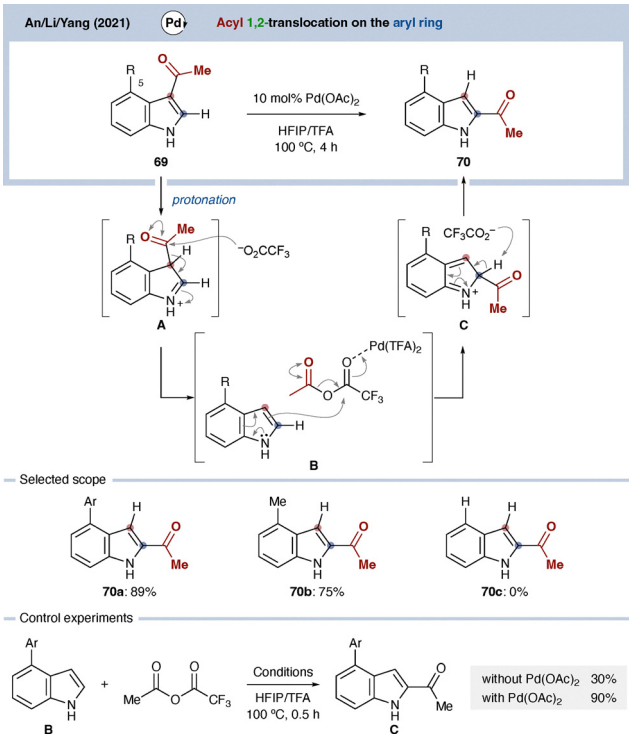

Scheme 25 Acyl 1,2-translocation of indoles.

In 2021, Yang and co-workers discovered that 1,2-acyl migration on indoles can be markedly promoted by the addition of a Pd catalyst (Scheme 25).[102] When C3-acylated indole **69** was heated at 100 °C in HFIP/TFA in the presence of catalytic $Pd(OAc)_2$, complete migration of the acyl group to the C2 position was observed, affording product **70** in high yield. Mechanistically, acid-mediated isomerization of **69** is proposed to generate intermediate **A**. Nucleophilic attack of trifluoroacetate at the acyl group then induces cleavage to give indole **B** and a mixed anhydride. The $Pd(TFA)_2$ species formed *in situ* subsequently activates the mixed anhydride, facilitating nucleophilic acylation of the indole to form intermediate **C**, which undergoes rearomatization to furnish the C2-acylated product **70**. Importantly, the reaction is dependent on substitution at the C5 position of the indole. Indoles bearing an aryl group at C5 afforded the corresponding C2-acylated products in high yield (*e.g.*, **70a**, 89%), and a methyl substituent was also tolerated (**70b**), In contrast, unsubstituted indoles failed to undergo acyl migration (**70c**), and no reaction occurred in the absence of $Pd(OAc)_2$.

Although the positional outcome remains confined to C3-to-C2 migration, the ability to promote acyl translocation under comparatively milder and catalyst-assisted conditions represents a meaningful conceptual advance beyond classical, purely acid driven rearrangements.

4. Translocation on $sp^3(sp^2)$ to sp^3

Before discussing recent catalytic and photochemical translocation reactions on sp3 carbon centers, it is worth noting that related radical-mediated acyl and cyano migrations were already explored by Beckwith and co-workers in the late 1980s.[103] Although these studies were originally viewed as radical rearrangements, they established the key addition/β-scission logic that underlies many modern radical-mediated translocation reactions. Recent advances in photoredox and HAT catalysis have enabled these concepts to evolve into more general and selective translocation processes.

4.1. Carbonyl group

Carbonyl groups are among the most versatile functional handles in synthetic organic chemistry. The ability to reposition a carbonyl group to a site amenable to subsequent functionalization would provide a powerful platform for modular molecular editing. In practice, however, formal 1,2-translocation of a carbonyl group typically requires multistep sequences,[104] often involving three to five discrete operations, which limits efficiency.

In 2021, Dong and co-workers reported a one-pot or two-step strategy for formal 1,2-carbonyl translocation (Scheme 26).[105] In this approach, carbonyl compound **71** is first converted into the corresponding enol triflate, either directly in a one-pot operation or as a discrete intermediate. A subsequent Pd-catalyzed Catellani-type reaction employing ligand **L1** transforms the enol triflate into an enamine, which upon hydrolysis furnishes the carbonyl group at the adjacent position, thereby achieving streamlined 1,2-carbonyl relocation to give **72**. For example, α-tetralone was converted to β-tetralone (**72a**) in 72% yield. The method is applicable to six-membered rings as well as five-membered cyclic ketones **72b** and bicyclic systems **72c**. As a synthetic application, the authors demonstrated access to compound **72d** bearing a γ-stereogenic center, a motif difficult to construct. Following enantioselective 1,4-addition of a Grignard reagent to furnish **71d**,[106] application of the carbonyl translocation sequence enabled efficient conversion to **72d**, demonstrating the utility of this strategy for complex molecule construction.

A plausible mechanism begins with oxidative addition of the C–O bond of the enol triflate **A** to Pd, generating intermediate **B**. Subsequent norbornene (NBE) insertion affords complex **C**, and formation of palladacycle **D** follows. Use of a specifically designed NBE derivative was critical to suppress formation of an undesired byproduct **X**.[107] Insertion of the amine source and β-carbon elimination regenerate NBE and deliver intermediate **F**. Decarboxylation generates a Pd–H species **G**, which undergoes reductive elimination to afford enamine **H**. Final hydrolysis of **H** furnishes product **72**, corresponding to formal carbonyl 1,2-migration. This study represents an elegant extension of Catellani-type chemistry to carbonyl editing, demonstrating how strategic relay process reorganization of carbonyl group within an sp^3 framework.

Building upon these studies, Dong and co-workers further expanded the concept of carbonyl editing to atom-swapping reactions. In 2026, they reported a transformation converting cyclic ketones into cyclic amines through a formal CO-to-N atom swap process.[108] Using the specially designed NAHA-G2

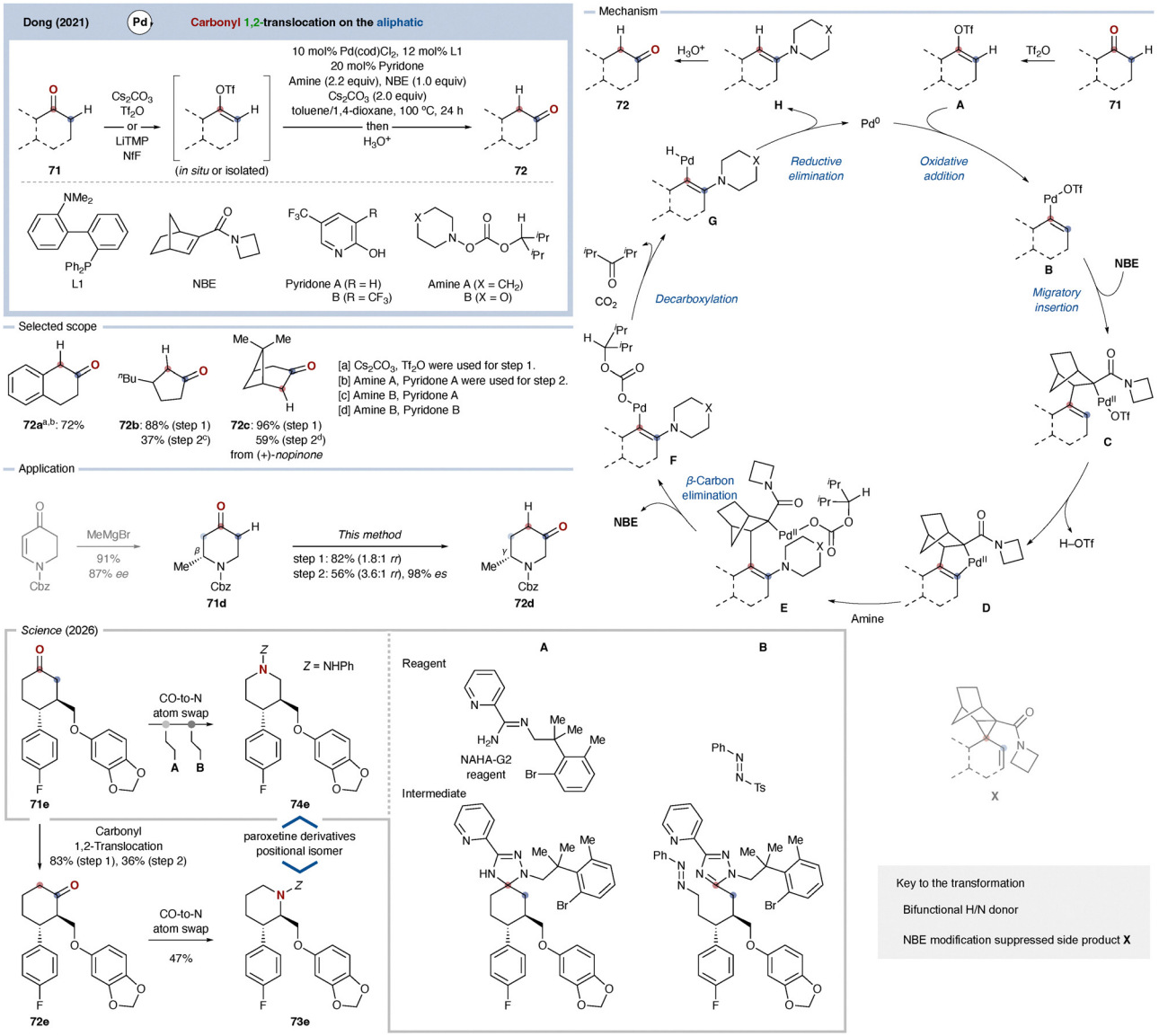

Scheme 26 Pd-catalyzed 1,2-carbonyl translocation and CO-to-N atom swap of cyclic ketones.

reagent, ketone substrates first form prearomatic intermediate **A**. Subsequent radical fragmentation induces sequential C–C bond cleavage to generate an alkyl radical, which adds to *p*-tosyldiazene (TsN_2Ph) **B** to form the first C–N bond. A second radical generation and C–C bond cleavage then occur, enabling formation of the second C–N bond at the opposite carbon terminus. Final cyclization and hydrogen-transfer processes furnish the corresponding piperidine skeleton.

Particularly interestingly, Dong and co-workers demonstrated that this atom-swap chemistry could be integrated with their previously developed carbonyl translocation strategy. Thus, cyclohexanone derivative **71e** was first converted into the transposed ketone **72e** through 1,2-carbonyl translocation, followed by CO-to-N atom swap to furnish amine **71e**. Although direct CO-to-N atom swap of **71e** also provided amine **73e**, the combined translocation/atom-swap sequence enabled selective access to the distinct positional isomer **74e**. These studies elegantly illustrate how functional group translocation and atom-swapping reactions can be merged to achieve programmable skeletal editing of cyclic molecules.

While the strategy developed by Dong and co-workers represents a powerful, kinetically controlled and irreversible approach to carbonyl translocation, a fundamentally different concept was reported in 2023 by Bhawal, Morandi, and co-workers. They disclosed a reversible, transition-metal-free and thermodynamically controlled 1,2-translocation of carbonyl groups (Scheme 27).[109]

This work was inspired by the classical Willgerodt–Kindler reaction,[110] in which the carbonyl group of a ketone is formally shifted to the adjacent carbon atom and converted into an amide. In the present study, cyclic ketones **75** were treated with catalytic pyrrolidine and elemental sulfur (S_8) in isopropyl alcohol with added water. Heating under these conditions enabled formal 1,2-migration of the carbonyl group, furnishing

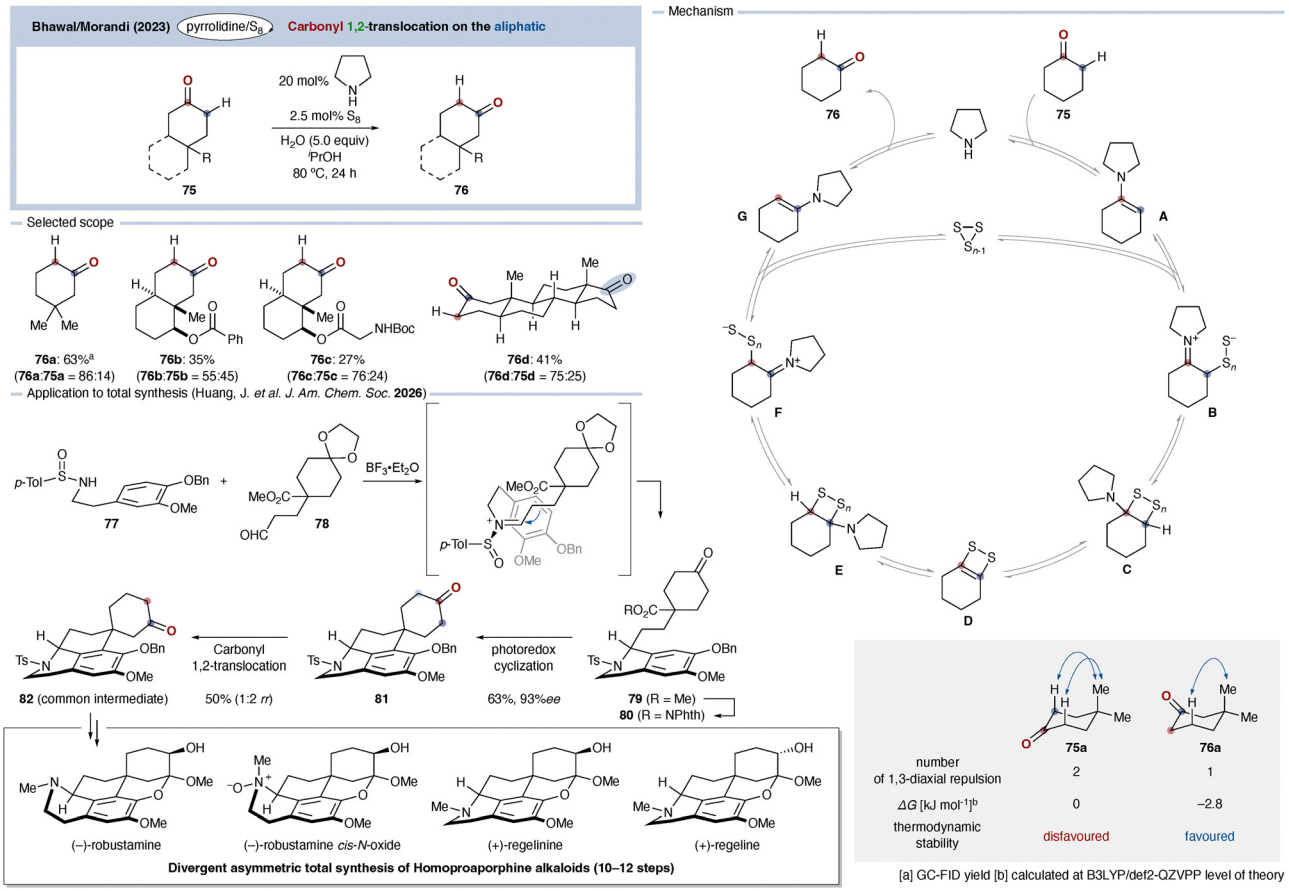

Scheme 27 Transition-metal-free, and thermodynamically controlled 1,2-translocation of carbonyl groups and its application to total synthesis.

rearranged cyclic ketones **76**. For example, a cyclohexanone derivative was converted to the corresponding 1,2-transposed ketone **76a** in 63% yield. Bicyclic substrates (**76b** and **76c**), as well as the tetracyclic steroid androstenedione, were also compatible, affording product **76d**. Notably, in substrates bearing two carbonyl groups, the reaction proceeds with high selectivity for one site. Because the transformation operates under thermodynamic control, mixtures of starting materials and further rearranged products arising from additional 1,3-migration can be observed, which may complicate isolation. Nevertheless, this equilibrium-driven process represents a compelling example of reinterpreting a classical transformation in the context of modern molecular editing.

Mechanistically, cyclohexanone **75** first forms enamine **A** upon reaction with pyrrolidine. Nucleophilic attack of this enamine on S_8 generates polysulfide anion **B**, which then intramolecularly attacks the corresponding iminium ion to form cyclic disulfide intermediate **C**. Although not explicitly proposed by the original authors, a plausible sequence involving reversible elimination and readdition of pyrrolidine can be considered to establish an equilibrium among intermediates **C**, **D**, and **E**. The thermodynamically more stable intermediate **E** preferentially reverts to iminium species **F**, followed by sulfide extrusion to regenerate enamine **G**. Hydrolysis of **G** then furnishes the 1,2-transposed cyclohexanone **76**. The driving force for this equilibrium lies in conformational effects within the cyclohexanone framework. Specifically, product **76a**, bearing only one 1,3-diaxial interaction, is calculated to be 2.8 kJ mol^{-1} more stable than isomer **75a**, which contains two such interactions. Consideration of these subtle steric effects enables rational prediction of the direction and outcome of the carbonyl migration.

Notably, in 2026, Huang and co-workers demonstrated an elegant application of this carbonyl 1,2-translocation strategy in the total synthesis of pentacyclic homoproaporphine alkaloids.[111] In their synthesis, the stereochemistry of the spiro center was introduced at a late stage through a desymmetrizing ketone transposition strategy. Specifically, condensation of chiral sulfinamide **77** with *meso* aldehyde **78** followed by cyclization afforded tetracyclic intermediate **79**. Conversion of the methyl ester **79** into the corresponding redox-active ester **80** and subsequent photoredox-catalyzed arylation furnished spirocyclic ketone **81**. Importantly, although the spiro center in **81** itself is not stereogenic, subsequent carbonyl 1,2-translocation converted **81** into desymmetrized ketone **82** possessing the desired stereochemical arrangement. During this process, undesired regioisomeric products arising from alternative carbonyl migration were also formed; however, resubjection of these isomers to the reaction conditions partially converted them into **82** under thermodynamic control. Using **82** as a

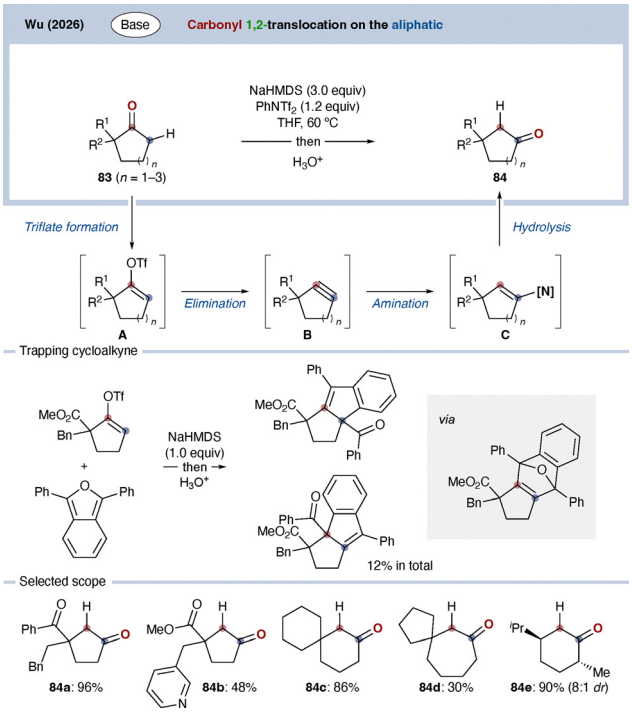

Scheme 28 Transition-metal-free strategy for formal 1,2-carbonyl translocation.

common intermediate, they accomplished the total synthesis of four pentacyclic homoproaporphine alkaloids in only 10–12 steps. This study nicely illustrates how late-stage conversion of a symmetrical ketone into a desymmetrized ketone through carbonyl translocation can streamline complex molecule synthesis, representing a particularly sophisticated application of modern molecular editing concepts in total synthesis.

Following these advances in 1,2-carbonyl translocation, Wu and co-workers reported in 2025 a notably simple, transition-metal-free strategy for formal 1,2-carbonyl translocation (Scheme 28).[112] In this approach, ketone **83** is treated with NaHMDS and Commins' reagent ($PhNTf_2$), and subsequent acidic workup furnishes the corresponding 1,2-migrated carbonyl compounds **84** in good yields.

Mechanistically, reaction of the ketone with one equivalent of NaHMDS and Commins' reagent generates enol triflate **A**. Upon warming to 60 °C, a second equivalent of NaHMDS promotes elimination to form a highly strained cycloalkyne intermediate **B**. Nucleophilic attack by $HMDS^-$ or the Ph_2N^- anion derived from Commins' reagent occurs preferentially from the less hindered face of the cycloalkyne, affording enamine intermediate **C**, which upon hydrolysis delivers the product corresponding to formal 1,2-carbonyl migration. The role of NaHMDS is crucial, as these nucleophiles efficiently trap the transient cycloalkyne, which would otherwise undergo oligomerization due to its high instability. Support for the intermediacy of **B** was obtained by conducting the reaction in the presence of diphenylisobenzofuran, leading to formation of a cycloaddition-derived product in low yield.

Although the reaction can proceed at room temperature, excessive heating diminished the yield. A related reaction was reported by Wang and co-workers in 2021;[113] however, differences in base selection, nucleophile identity, and the absence of enamine hydrolysis, mean that the reaction was not interpreted as carbonyl migration. The present study therefore represents a distinct contribution by explicitly framing the transformation as 1,2-carbonyl translocation.

Steric congestion at the α-position is a key determinant of selectivity. Cyclopentenone derivatives smoothly afforded **84a**, and substrates bearing coordinating groups such as pyridines were also tolerated (**84b**). Six-membered rings underwent the transformation efficiently (**84c**), whereas seven-membered rings gave lower yields (**84d**), consistent with the reliance on ring strain to drive formation and capture of the cycloalkyne intermediate. Notably, even when the α-position is not a quaternary carbon, sufficiently bulky substituents enable selective carbonyl migration, as exemplified by product **84e**.

Overall, this strain-driven, metal-free protocol represents a particularly practical example of carbonyl translocation, proceeding cleanly without recovery of starting material, and avoiding the use of precious catalysts. It highlights the power of transient high-energy intermediates as design elements in functional group translocation chemistry.

In 2026, Yamaguchi and co-workers reported a nickel-catalyzed formal 1,2-carbonyl translocation of tetralone derivatives (Scheme 29).[114] Treatment of α-tetralone derivative **85** with K_3PO_4 and pivalic anhydride (Piv_2O), followed by reaction with a Ni catalyst bearing the dcype ligand and *N*-methylaniline, enabled selective formation of β-tetralone derivatives **86**. Quenching the reaction mixture with silica gel led to hydrolysis of the intermediate enamine, affording β-tetralone products **86a–86c** in good yields and with high positional selectivity. Notably, this transformation is currently limited to tetralone frameworks and has not yet been generalized to other carbonyl systems.

Mechanistically, α-tetralone (**85a**) is first converted into the corresponding enol pivalate **A**. Oxidative addition of its C–O bond to Ni(0) generates complex **B**, which undergoes a characteristic 1,2-migration of the nickel center to form intermediate **C**. Subsequent ligand exchange with the amine nucleophile affords complex **D**, and reductive elimination yields enamine intermediate **E** with regeneration of the nickel catalyst. Hydrolysis of **E** during silica workup then delivers β-tetralone **86a**. The proposed 1,2-migration of the nickel complex is strongly supported by prior studies from the same group.[115] In earlier *cine*-substitution coupling reactions of tetralones using an analogous catalytic system, intermediate **B** was isolated and its conversion to **C** was confirmed by NMR analysis. Moreover, related substrates subjected to comparable conditions were shown to form intermediate **C** in similar yields. Conceptually, the present transformation builds directly on this *cine*-substitution platform, replacing the carbon nucleophile with an amine inspired by related work from Dong and co-workers,[105] while introducing nickel catalysis in place of palladium as a defining mechanistic distinction.

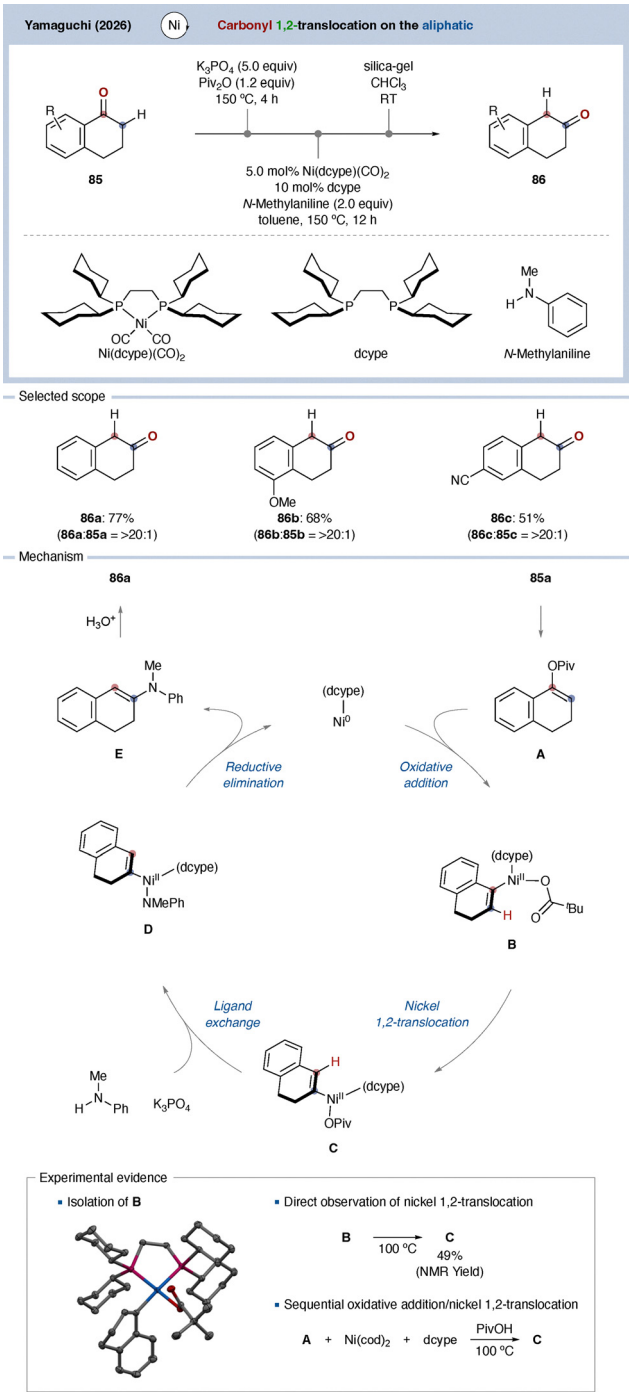

Scheme 29 Carbonyl 1,2-translocation of tetralones.

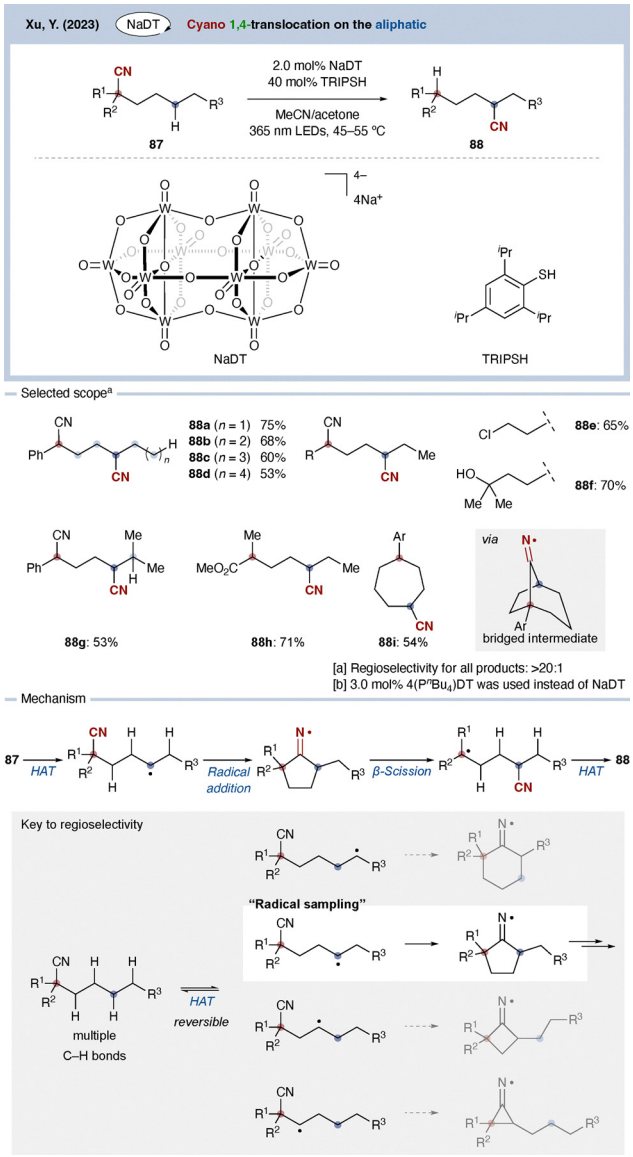

Scheme 30 1,4-Translocation of cyano groups on sp^3 carbon centers.

4.2. Cyano group

In 2023, Yan Xu and co-workers reported a 1,4-translocation of cyano groups on sp^3 carbon centers (Scheme 30).[116] Under irradiation with 365 nm LEDs, a tungsten photocatalyst (sodium decatungstate, NaDT)[117] in combination with a catalytic amount of aryl thiol (TRIPSH) enabled efficient 1,4-cyano migration. Benzylic dinitrile substrates underwent selective migration of one cyano group *via* a 1,4-shift, irrespective of the length of the intervening carbon chain (**88a–88d**). Importantly, a benzylic position is not required, as simple aliphatic dinitriles also participate smoothly. Functional groups such as halides and tertiary alcohols are well tolerated (**88e** and **88f**). Notably, even in substrates containing a tertiary carbon center, migration can proceed selectively at a secondary position (**88g**). Furthermore, cyano migration proceeds efficiently when one of the two cyano groups is replaced by an ester (**88h**). The reaction is applicable to both acyclic and cyclic substrates; in the latter case (**88i**), product formation is proposed to proceed *via* a bridged radical intermediate.

Mechanistic studies support a radical relay pathway. Upon irradiation with 365 nm light, photoexcited NaDT* abstracts a hydrogen atom from substrate **87**, generating a pool of carbon centered radicals through a largely unselective and reversible HAT process. TRIPSH functions as a hydrogen-atom donation catalyst, enabling radical equilibration (radical sampling) among different positions. Selectivity arises in the subsequent

intramolecular cyclization step. Radicals capable of forming a five-membered ring undergo rapid cyclization, which determines the migration site under kinetic control. Even in substrates bearing tertiary C–H bonds, migration proceeds *via* secondary radical pathways when cyclization is faster. The resulting cyclic radical undergoes β-scission to effect 1,4-cyano translocation, followed by hydrogen atom transfer to furnish the rearranged product **88**. In cyclic systems, the reaction proceeds *via* a bridged radical intermediate prior to fragmentation.

From a synthetic perspective, this transformation is particularly valuable because it enables selective functionalization of internal C–H bonds by first installing a cyano group at a terminal position and subsequently relocating it through a 1,4-shift. In this way, molecular architectures that are difficult to access by direct C–H functionalization can be efficiently constructed *via* cyano translocation.

4.3. Acyl and ester

As discussed in Section 2, acyl translocation on heteroaromatic rings has long been known; however, example of controlled 1,2-migration of acyl groups on sp^3 carbon centers remain rare[118] and are typically limited to specific rearrangement manifolds rather than deliberate translocation strategies. In 2025, Sarpong and co-workers disclosed an unusual example of sp^3 acyl 1,2-translocation in the highly specific context of dihydrobenzofuran frameworks (Scheme 31).[119] Encouraged by related precedents,[120] the authors hypothesized that photoirradiation might enable such migration through a sequence involving reductive activation and C–O bond cleavage.

Specifically, acid-activated ketones **89** were proposed to undergo single-electron reduction under photochemical conditions, triggering C–O bond cleavage concomitant with intramolecular arene attack to generate a spirocyclic intermediate **A**. Subsequent ring opening of the cyclopropane moiety by the counteranion of the acid affords intermediate **B**, which then undergoes an intramolecular S_N2-type displacement to deliver the product **90** arising from formal 1,2-acyl migration.

The reaction conditions are notably simple. Treatment of 2-acyl dihydrobenzofurans **89** with hydrochloric acid, followed by irradiation at 370 nm in $^{i}PrOH/H_2O$ and subsequent addition of triethylamine as a base (Conditions A), or alternatively with LiI in acetone/H_2O under 370 nm irradiation (Conditions B), furnishes 3-acyl dihydrobenzofurans **90**. Both light irradiation and protic solvents are essential: no reaction occurs in the absence of light, while decomposition predominates without a protic solvent. With respect to substrate scope, benzoyl (**90a**, and **90b**) and heteroaroyl (**90c**) groups are compatible. Dihydrobenzofuran substrates bearing electron-withdrawing substituents at the C5 position generally afford higher yields, presumably due to facilitated ring opening (**90d** and **90e**). Moreover, switching the irradiation wavelength to 310 nm enables single-electron reduction of ester (**90f**), carboxylic acid (**90g**), and amide (**90h**) functionalities as well. Although the substrate scope remains limited, this study represents a compelling example of "new reactivity from old ideas" and

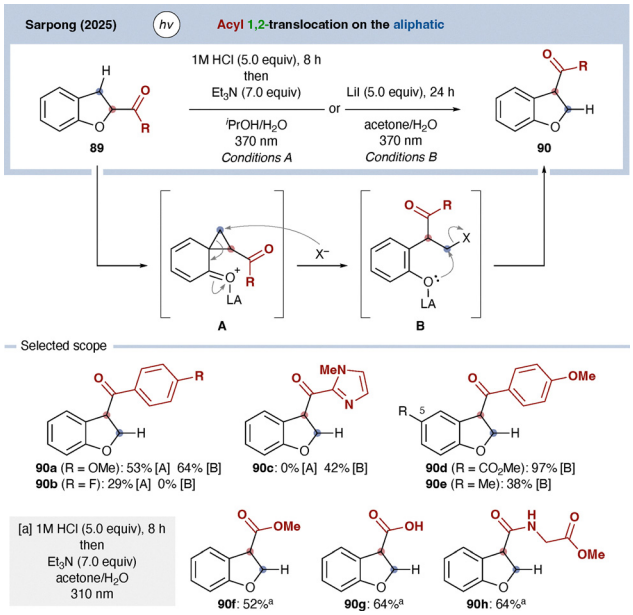

Scheme 31 sp^3 Acyl 1,2-translocation.

illustrates how renewed interest in functional group translocation has brought such transformations into sharper focus.

In 2025, Wendlandt and co-workers reported an alternative photocatalytic strategy to the 1,4-translocation of ketone functionalities in cyclic systems (Scheme 32).[121] The reaction conditions and overall mechanistic logic resemble those developed by Xu and co-workers,[116] for cyano migration, with ketones employed in place of nitrile-containing substrates.

Although the current scope is largely limited to seven-membered rings and the reaction typically affords mixtures of diastereomers—thereby reducing its intermediate synthetic practicality—the transformation tolerates a range of substituents at the ketone site, including fluoro (**92a**), acetate (**92b**), unsubstituted (**92c**), and ester-functionalized derivatives (**92d**). Mechanistically, photoinduced generation of an alkyl radical **A** from substrate 91 initiates the process. Favorable 5-*exo*-trig cyclization leads to intermediate **B**, which accounts for the observed 1,4-selectivity. Subsequent β-scission (**C**) and hydrogen-atom transfer (HAT) steps then furnish the ketone product 92.

One year later, Palani and co-workers reported an even more sophisticated aroyl translocation strategy on saturated carbon frameworks (Scheme 33).[122] The earlier study by Wendlandt and co-workers relied on formation of a kinetically favored bicyclic radical intermediate through radical cyclization, followed by radical fragmentation to achieve remote acyl migration. In contrast, Palani and co-workers introduced a conceptually distinct strategy in which the "cyclization phase" and the "cleavage phase" were decoupled. As a result, the migration process was no longer governed primarily by the stability of radical intermediates, enabling transannular 1,3-translocation that had previously been difficult to achieve.

Specifically, irradiation of ketone **93** in $^{t}BuOH$ at 370 nm followed by treatment with $Mn(OAc)_3$, 1,10-phen (1,10-phenanthroline), and

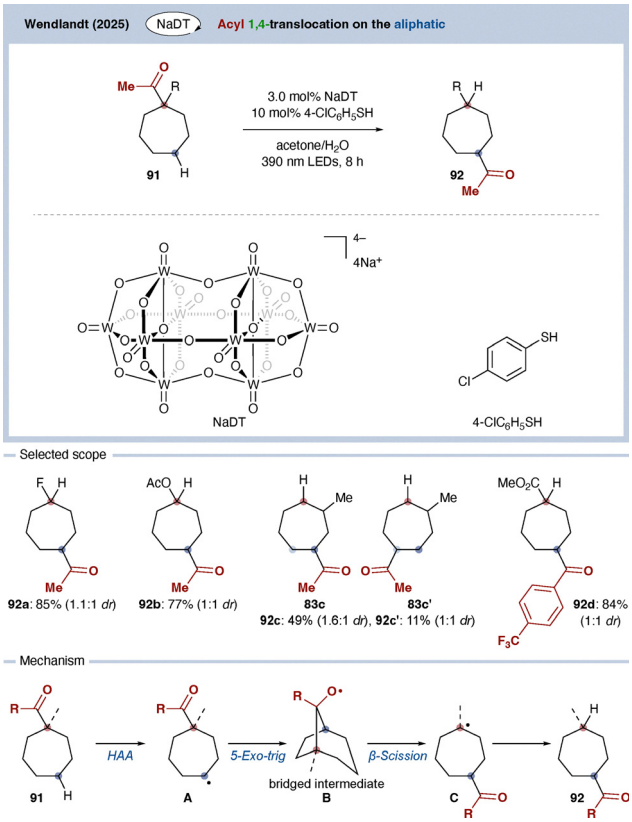

Scheme 32 The 1,4-translocation of Acyl functionalities on cyclic systems.

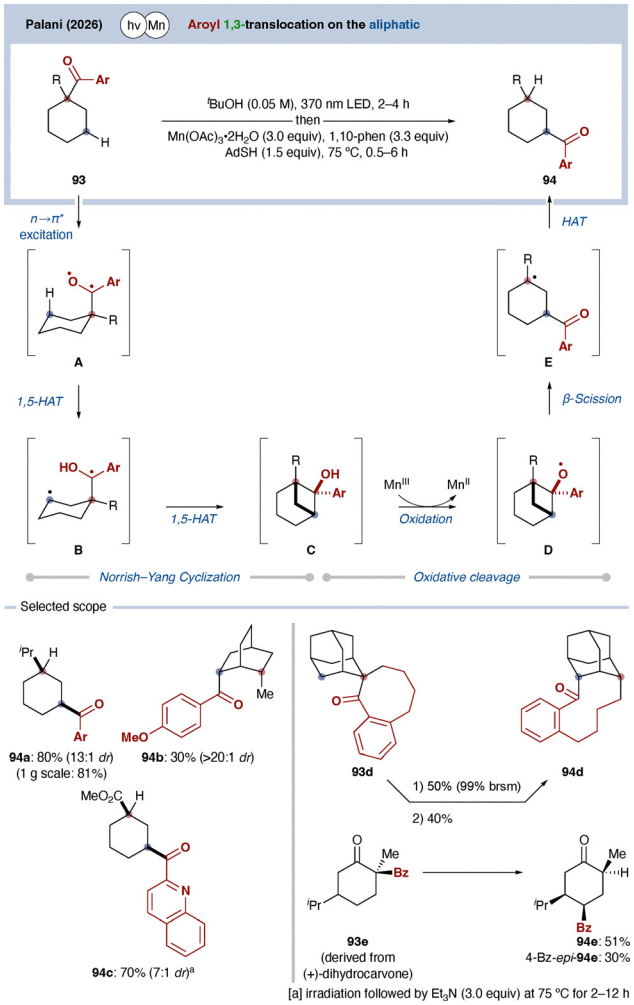

Scheme 33 Decoupled cyclization/cleavage strategy for transannular 1,3-aroyl translocation.

AdSH (adamantanethiol) afforded aroyl-translocated product **94** through formal 1,3-migration of the aroyl group. Mechanistically, photoexcitation of ketone **93** generates a triplet excited state **A**, and the resulting oxygen-centered radical undergoes Norrish–Yang-type 1,5-hydrogen atom transfer (1,5-HAT) from the γ-position. The resulting biradical intermediate **B** subsequently recombines to generate strained bicyclo[3.1.1] intermediate **C**. This sequence constitutes the cyclization phase of the reaction. In the subsequent cleavage phase, $Mn(OAc)_3$ promotes single-electron oxidation of the cyclobutanol moiety to generate alkoxy radical **D**. This radical undergoes β-scission to cleave the C–C bond, furnishing tertiary radical **E** in which the aroyl group has effectively migrated to a new position. Finally, hydrogen atom transfer from AdSH affords the 1,3-translocated ketone product **94**.

Thus, by decoupling cyclization and cleavage processes, the authors succeeded in enabling transannular 1,3-aroyl migration that had previously been difficult to access through conventional radical translocation strategies. The reaction was also demonstrated on gram scale, affording product **94a** with high diastereoselectivity. Bicyclic substrates similarly underwent efficient 1,3-translocation to furnish **94b**, and nitrogen-containing heteroaromatic aroyl groups were also compatible, as illustrated by **94c**. Furthermore, this strategy enabled unusual skeletal editing processes, including conversion of spirocyclic substrate **93d** into macrocyclic ketone **94d**. Migration of aroyl groups located at the α-position of ketones was also achieved, enabling transposition to the C4 position as shown in **94e**.

Although both the Wendlandt and Palani studies address carbonyl/aroyl translocation on saturated carbon frameworks, they differ fundamentally in conceptual design, mechanism, and accessible migration topology. In this sense, the work by Palani and co-workers can be regarded as a significant conceptual advance beyond the earlier Wendlandt strategy.

4.4. Boryl group

Organoboron compounds are versatile synthetic precursors that can be transformed into a wide range of functional groups. Consequently, numerous borylation methods have been developed, including borylation of olefins, halides, carbonyl compounds, and C–H bonds.

If readily accessible organoboron compounds could be converted into other organoboron isomers through boron migration, thereby transforming one or more C–H bonds into C–B bonds, this would provide a powerful entry to further

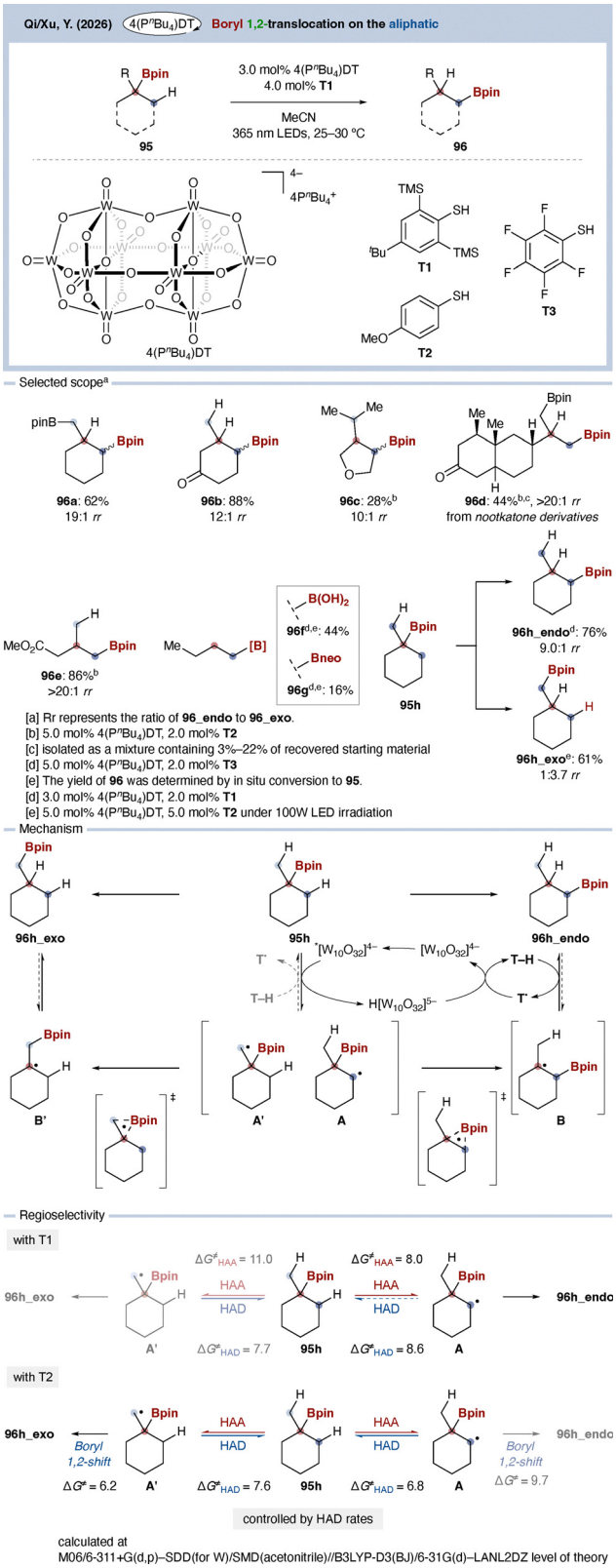

Scheme 34 Tungsten-photocatalyzed radical 1,2-boryl translocation of tertiary organoboron compounds.

functionalization. However, such transformations are inherently challenging. This challenge was addressed by Xu, Qi and co-workers (Scheme 34).[123] Drawing on their previous studies of 1,4-cyano migration,[116] they hypothesized that generation of alkyl radicals under tungsten photocatalysis might enable net boron migration. Indeed, using a tungsten photocatalyst, 4(P^{n}Bu$_4$)DT, in combination with a catalytic amount of a sterically hindered thiol under 365 nm LED irradiation, they observed 1,2-boron translocation.

Substrates bearing tertiary C–B bonds underwent 1,2-translocation to adjacent cyclic methylene positions, affording product **96a** in 62% yield. Although only modest diastereoselectivity was observed, with a ratio of 1.7 : 1, the regioselectivity was excellent and exceeded 20 : 1. Cyclohexanone derivatives (**96b**), tetrahydrofuran derivatives (**96c**), and bicyclic systems (**96d**) were also compatible, furnishing the corresponding 1,2-migrated products. Importantly, the transformation was not limited to cyclic systems, as acyclic substrates also underwent 1,2-migration efficiently (**96e**). Boronic acids such as B(OH)$_2$ and Bneo derivatives were likewise tolerated, although yields for these boronic acid derivatives were somewhat lower (**96f** and **96g**). Under optimized conditions, the *endo* isomer **96h** was obtained preferentially; however, under more intense irradiation conditions, selective methyl borylation led predominantly to the *exo* isomer (**96h_exo**).

Mechanistically, the reaction begins with generation of an alkyl radical from the organoboron substrate under tungsten photocatalysis. From **95h**, several radical intermediates can form, but only radicals **A** and **A'**, generated at adjacent carbon atoms, undergo 1,2-boron migration to give intermediates **B** and **B'**. Subsequent hydrogen atom transfer furnishes either **96h_endo** or **96h_exo**. Although a tertiary radical can in principle be regenerated from these products, steric congestion suppresses further boron translocation, rendering the process effectively irreversible. The observed regio- and stereoselectivity between the endo and *exo* products can be rationalized by the steric environment imposed by the thiol catalyst, which influences the hydrogen atom transfer step.

Although questions remain regarding the relative thermodynamic stability of the starting and translocated boron isomers, this study represents the first example of formal 1,2-translocation of an sp^3-bound boron substituent. As such, it constitutes an important conceptual advance in functional group translocation chemistry.

Almost simultaneously, Xi and co-workers reported a closely related 1,2-boryl taranslocation (Scheme 35).[124] As in Xu's study, tertiary boronic esters were employed as readily accessible starting materials. Treatment of these substrates **95** with catalytic ^{n}Bu$_4$NFeCl$_4$ and the disulfide (Trip$_2$S$_2$) under 390 nm LED irradiation afforded the 1,2-boryl-translocated products **96** preferentially. Mechanistically, the reaction is initiated by generation of a chlorine radical from the iron catalyst.[125] This chlorine radical abstracts a hydrogen atom from the substrate to form an alkyl radical, after which the process proceeds analogously to that proposed by Xu and co-workers, involving 1,2-boryl translocation followed by hydrogen atom transfer.

A range of substrates was tolerated. Seven-membered rings (**96i**), heterocyclic six-membered rings (**96j**), sulfones (**96k**), and

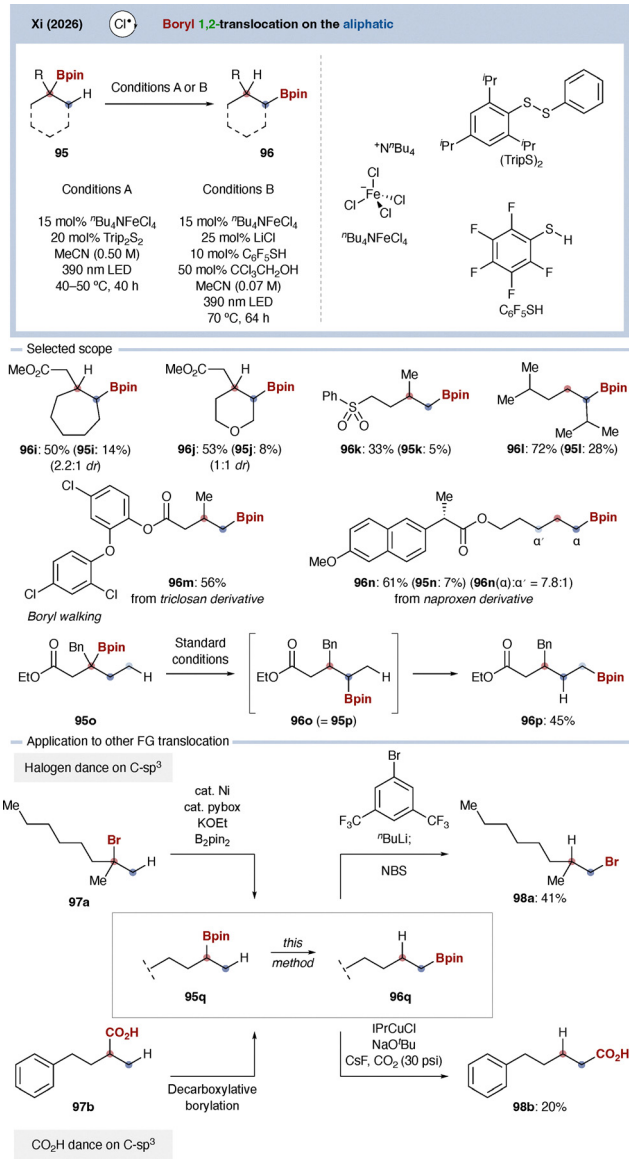

Scheme 35 Chlorine radical-mediated 1,2-boryl translocation.

other substrates bearing tertiary carbon centers (**96l**) all underwent efficient 1,2-boryl translocation. Organoboron compounds derived from complex, drug-like scaffolds were also compatible, furnishing products **96m** and **96n** in good yields. Moreover, when substrate **95o** was subjected to the standard conditions, product **96o** was formed, and a second 1,2-boryl shift could occur to give **96p**. As noted at the outset, tertiary boronic ester **95q** can be readily prepared from halides such as **97a** or from carboxylic acids such as **97b** using established methods.[126] Subsequent 1,2-boryl migration of **95s**, followed by treatment with NBS, regenerates the corresponding halide **98a**, whereas reaction with carbon dioxide furnishes the carboxylic acid **98b** although these transformations proceed *via* a boron intermediate, they formally constitute net halogen or carboxyl group translocation. This study therefore highlights how a boron relay strategy can be leveraged to achieve functional group translocation beyond boron itself.

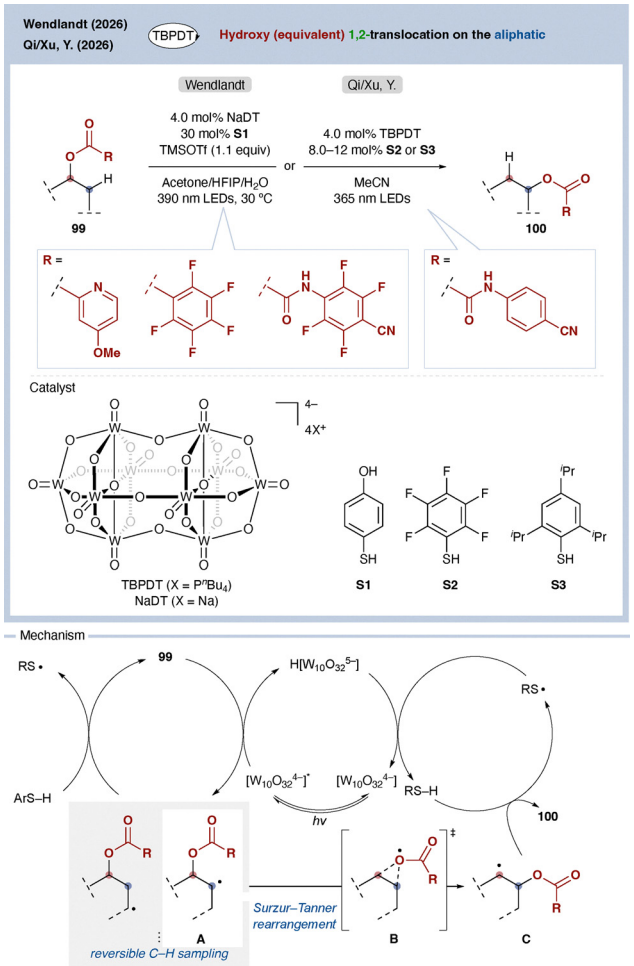

Scheme 36 Radical 1,2-acyloxy translocation *via* reversible C–H sampling.

4.5. Hydroxy group (equivalent)

Up to this point, cyanide (Scheme 30), acyl (Schemes 31–33), and boryl (Schemes 34 and 35) translocations mediated by tungsten/thiol catalytic systems under photoirradiation have been discussed. Around the same time, Xu and Wendlandt independently reported 1,2-translocation of acyloxy groups using closely related catalytic manifolds (Scheme 36).[127] In both cases, the reactions employ acyloxy groups, tungsten photocatalysts (NaDT or TBPDT), and thiol-based hydrogen atom donors, and the underlying mechanistic concepts are fundamentally similar.

As in the previously described systems, the photoexcited tungsten catalyst promotes reversible hydrogen atom abstraction (HAA) at multiple C–H bonds of **99**, thereby establishing a dynamic "C–H sampling" equilibrium among various carbon-centered radicals. Among these transient radical intermediates, only radical **A** generated at the β-position adjacent to the acyloxy group undergoes rapid Surzur–Tanner-type 1,2-acyloxy radical migration through highly charge-separated three-membered (or five-membered) transition states **B**. Subsequent hydrogen atom transfer from the thiol source to radical **C** furnishes the translocated products **100**.

In the Wendlandt system, addition of TMSOTf serves as a convenient triflic acid precursor for *in situ* protonation of the pyridyl ester auxiliary group. The resulting cationic pyridinium species promotes proximity-enhanced hydrogen atom abstraction through ion-pairing interactions with the decatungstate catalyst, thereby facilitating generation of the β-radical intermediate required for the subsequent Surzur–Tanner-type acyloxy migration. In contrast, both the Xu and Wendlandt systems employ electron-withdrawing oxamoyl auxiliaries, which facilitate rapid 1,2-acyloxy radical migration by stabilizing the highly charge-separated transition states associated with the Surzur–Tanner rearrangement.

Collectively, these studies demonstrate a fundamentally new design principle for positional editing reactions. Rather than relying on highly site-selective HAA processes, positional selectivity is achieved through reversible radical sampling followed by selective trapping through rapid translocation. The rapid expansion of this concept from cyanide, acyl, and boryl groups to acyloxy groups suggests that reversible radical translocation chemistry is emerging as a general strategy for late-stage positional editing on saturated carbon frameworks.

4.6. Translocation on sp^2 to sp^3

Thus far, we have described functional group translocations from an sp^3 carbon to an sp^3 carbon. Net translocations from an sp^3 carbon to an sp^2 carbon remain exceedingly rare, with only two examples reported to date. In both cases, the individual elementary steps formally involve sp^3-to-sp^3 processes, the overall outcome corresponds to formal functional group migration from an sp^3 carbon center to an sp^2 carbon.

The first example was reported in 2025 by Pan Xu and co-workers. Inspired by the 1,4-cyano translocation developed by Yan Xu and co-workers, they extended this concept to achieve cyano migration from sp^3 carbon to sp^2 carbon (Scheme 37).[128] Under blue LED irradiation, the use of 4CzIPN as a photoredox catalyst, together with catalytic amounts of quinuclidine derivative and 20 mol% of $(TripS)_2$, afforded the 1,4-translocated product **102**. In addition to benzylic dinitriles (**102a** and **102b**), substrates bearing simple aliphatic substituents (**102c**) or a combination of cyano and ester groups (**102d**) underwent efficient translocation. Even substrates with a shortened carbon chain delivered the corresponding 1,4-migrated product **102e**. Notably, complex molecules containing additional functional groups, including indomethacin derivatives, were also compatible (**102f**).

Mechanistically, photoexcitation of 4CzIPN in the presence of the amine additive initiates single-electron transfer to generate a radical ion pair consisting of an anion radical and a cation radical **A**. The nitrogen-centered radical then adds to the olefin, forming an alkyl radical intermediate **B**. As in the work by Yan Xu and co-workers, this radical undergoes a favorable 5-*exo*-dig cyclization to give intermediate **C**, followed by β-scission that effects 1,4-cyano translocation and generates cation radical **D**. Subsequent electron transfer from the reduced photocatalyst affords an anionic intermediate **E**, which undergoes proton transfer and elimination to furnish the final

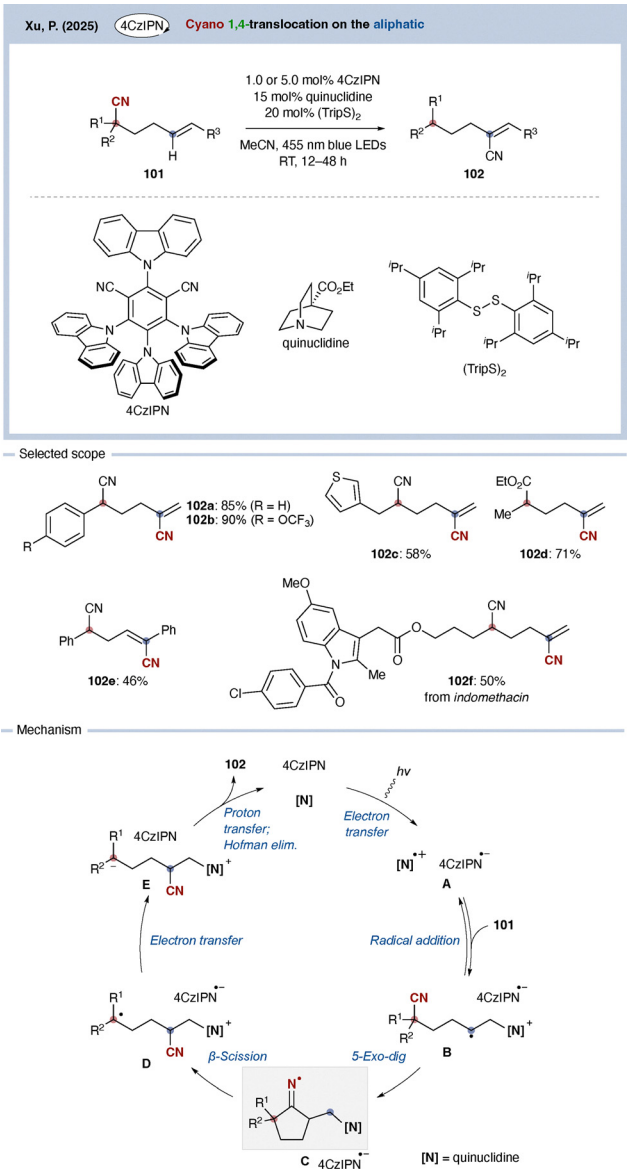

Scheme 37 Photoredox-catalyzed net sp^3-to-sp^2 1,4-cyano translocation.

product. Thus, although the key difference lies in the generation of alkyl radicals *via* amine radical addition, the overall translocation logic closely parallels that of the earlier Xu system.

Importantly, this study demonstrates that careful substrate design enables, for the first time, a 1,4-functional group translocation that is net from an sp^3 carbon to an sp^2 carbon. This finding significantly expands the conceptual framework and structural scope of functional group translocation chemistry.

Almost simultaneously with the report by Xu and co-workers, Zhen and Shu independently disclosed a closely related transformation (Scheme 38).[129] In their study, a sodium sulfonyl salt was employed as the additive in place of an amine. Remarkably, the substrate scope closely mirrors that reported by Xu and co-workers, and essentially identical substrates

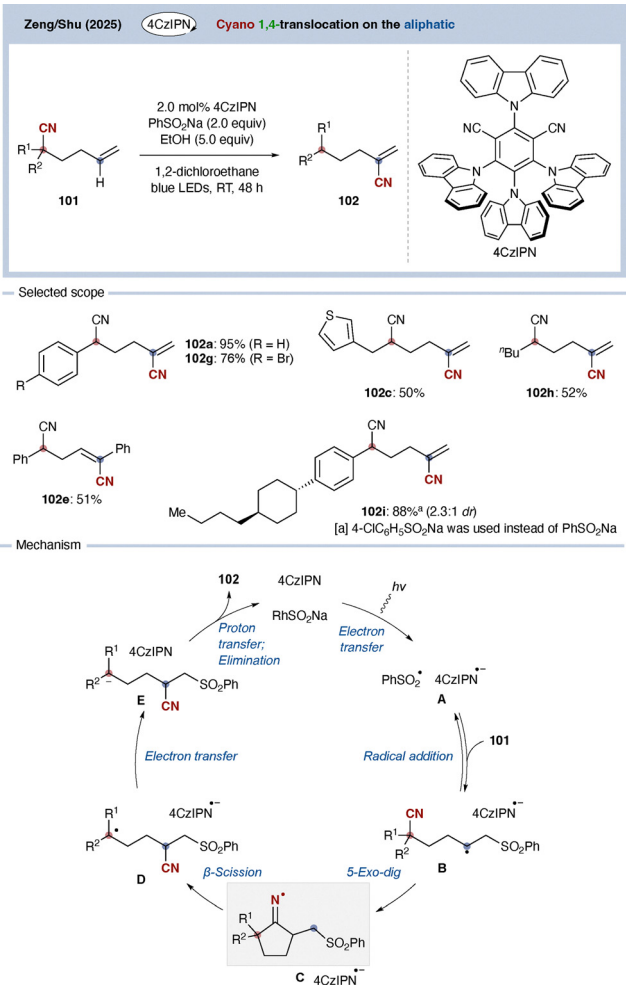

Scheme 38 Photoredox-catalyzed net sp^3-to-sp^2 1,4-cyano translocation.

undergo efficient 1,4-functional group transposition to afford the corresponding products **102a**, **102c**, **102e**, and **102g–102i**.

Mechanistically, the reaction proceeds through the same fundamental pathway as the Xu system, with the sole difference being the involvement of a sulfonyl radical instead of an aminyl radical. This parallel development further underscores the generality of radical relay strategies for achieving net sp^3-to-sp^2 functional group translocation.

5. Double functional group translocation

While the preceding sections addressed functional group translocations involving exchange with hydrogen, this section highlights emerging examples of double functional group translocation, in which two functional groups are interchanged.

5.1. Iodo/boryl exchange

In 2025, Chen and co-workers reported a double functional group translocation reaction in which an iodine atom on an

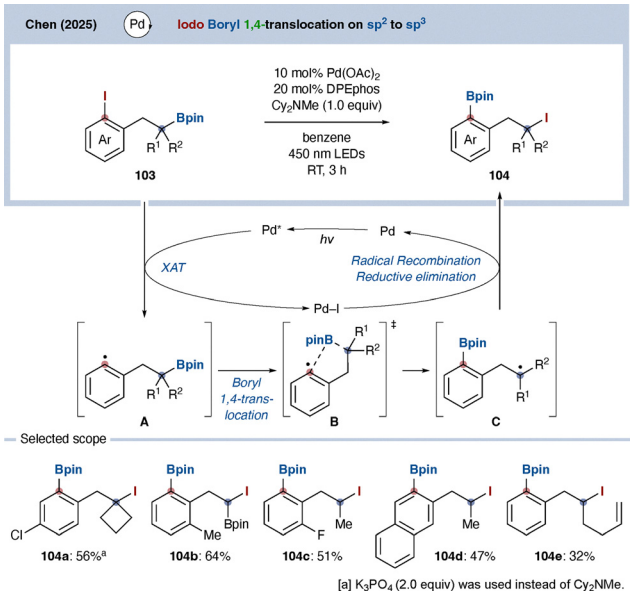

Scheme 39 Double functional group translocation reaction.

aromatic ring is exchanged with a boron substituent on an sp^3 carbon (Scheme 39).[130] Irradiation of iodinated boryl substrate **103** with 450 nm LEDs in the presence of $Pd(OAc)_2$/DPEPhos and potassium phosphate afforded the exchanged product **104**.

Mechanistic studies suggest the involvement of photoexcited palladium species. Upon light irradiation, the excited palladium complex engages the aryl iodide to generate an aryl radical **A**. This radical subsequently reacts with the boron substituent positioned at the 4-position, triggering a 1,4-migration of the boryl group *via* transiton state **B** to form alkyl radical intermediate **C**. The greater thermodynamic stability of alkyl radicals relative to aryl radicals likely serves as a driving force for this translocation process. The resulting alkyl radical then abstracts iodine from the palladium center, delivering product **104** and regenerating the palladium catalyst.

The substrate scope is currently limited to systems bearing an alkyl chain at the *ortho* position of an iodoarene and a Bpin group at the C4-position. Nevertheless, the transformation tolerates a range of additional functional groups, including chloro (**104a**), diboryl (**104b**), fluoro (**104c**), naphthyl (**104d**), and olefin-containing substrates (**104e**), affording the exchanged products in moderate yields. Although the immediate synthetic utility of this transformation is limited, it represents an intriguing example of intermolecular exchange between two reactive functional groups. Because this transformation involves functional groups located on sp^2 and sp^3 carbon centers, it is also discussed in Section 4.5.

5.2. Aryl/alkyl or amino group exchange

In 2024, the groups of Ruffoni and Leonori reported photochemical atom permutation and apparent functional group translocation reactions of thiazoles, isoxazoles, and other azoles, which they termed photochemical permutation (Scheme 40).[18] For example, irradiation of 1-phenylthiazole (**105**) with 310 nm LED light in the presence of triethylamine

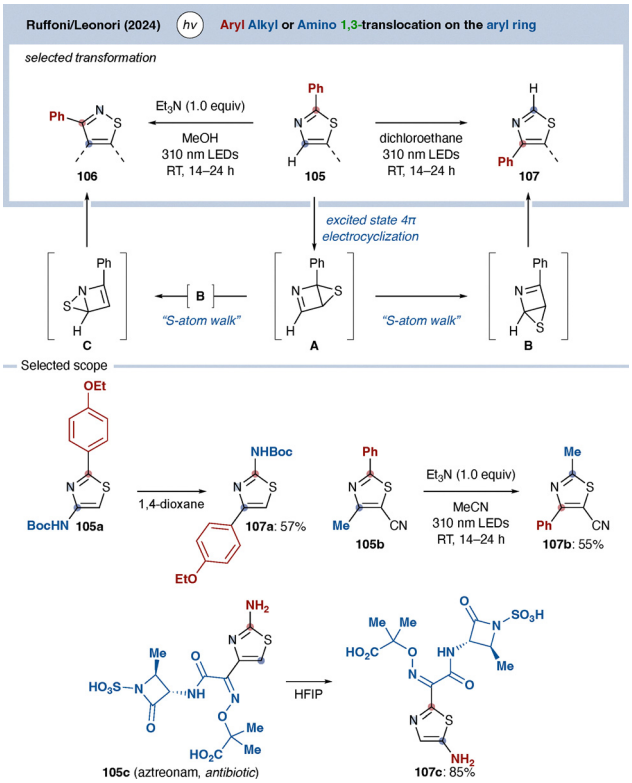

Scheme 40 Photochemical permutation of azoles enabling solvent-controlled apparent aryl translocation.

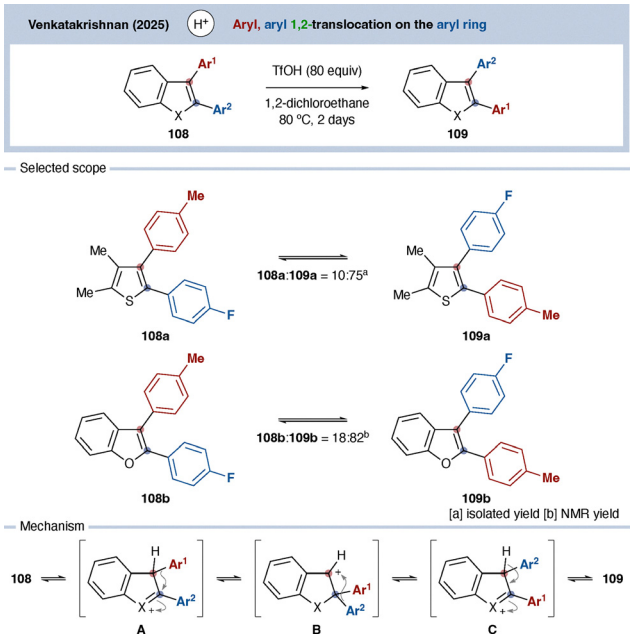

Scheme 41 TfOH-promoted thermodynamic aryl–aryl exchange in diaryl heteroarenes.

(Et_3N) and MeOH affords 2-phenylisothiazole (**106**). In contrast, irradiation at 310 nm in DCE results in a 1,3-aryl migration to give 4-phenylthiazole (**107**). In both cases, photoexcitation triggers a 4π electrocyclization to form intermediate **A**; subsequent sulfur atom migration ("S-atom walk") *via* **B** leads to **C** to give **106**, whereas arrest at **B** furnishes **107**. The divergence between these pathways is governed by the solvent and additives such as Et_3N, which modulate the reaction trajectory. Inpotantly, these transformations do not involve chassic stepwise functional group migration but rather proceeds through a sequence of pericyclic and rearrangement process that give the apperance of functional group translocation.

When thiazoles bearing two substituents are empolyed, the reaction appears as an exchange of substituents. For instance, irradiation of **105a** in 1,4-dioxane gives the exchanged product **107a** in 57% yield. Similarly, **105b** undergoes apparent exchange of methyl and phenyl groups to give **107b**. Even more complex substrate **105c** furnishes **107c** in HFIP.

Although azoles are known to undergo various translocation reactions,[49d] examples in which light, solvent, and simple additives alone enable such clean and switchable control are rare. Given the mild conditions and high selectivity, this photochemical permutation represents a synthetically valuable transformation.

5.3. Aryl/aryl exchange

Finally, we highlight a conceptually simple transformation in which two aryl groups are exchanged within a single molecule. In 2025, Venkatakrishnan and co-workers reported aryl migration reactions of diaryl(benzo)heteroles (Scheme 41).[131] These transformations rely on classical aryl rearrangements promoted by TfOH and proceed under thermodynamic control. Consequently, the selectivity is not perfect but reflects the relative stability of the isomeric products.

For example, prolonged treatment of a diaryl thiophene **108a** under these conditions affords the aryl-exchanged product **109a** together with recovered **108a** in a 75 : 10 ratio. Benzofuran derivatives are also amenable; diaryl benzofuran **108b** undergoes efficient aryl exchange to give **109b** with a product ratio of 18 : 82. Although the reaction conditions themselves are not novel, the clean intramolecular exchange of two aryl groups is noteworthy. From materials science perspective, such transformations are particularly attractive, as they enable access to alternative substitution patterns without the need for *de novo* synthesis of the molecular framework.

6. Miscellaneous

The following examples do not strictly fall within the definition of functional group translocation adopted in this review, particularly because some involve formal functional group interconversion corresponding to Group B discussed in Section 1. Nevertheless, they are included here because of their close conceptual relationship to recent translocation chemistry and because many of these studies explicitly build upon or cite the contemporary translocation literature discussed above. Importantly, the present review does not distinguish between intra- and intermolecular processes in its operational definition, nor does it require late-stage applicability as a defining criterion. Rather, the review aims to comprehensively summarize

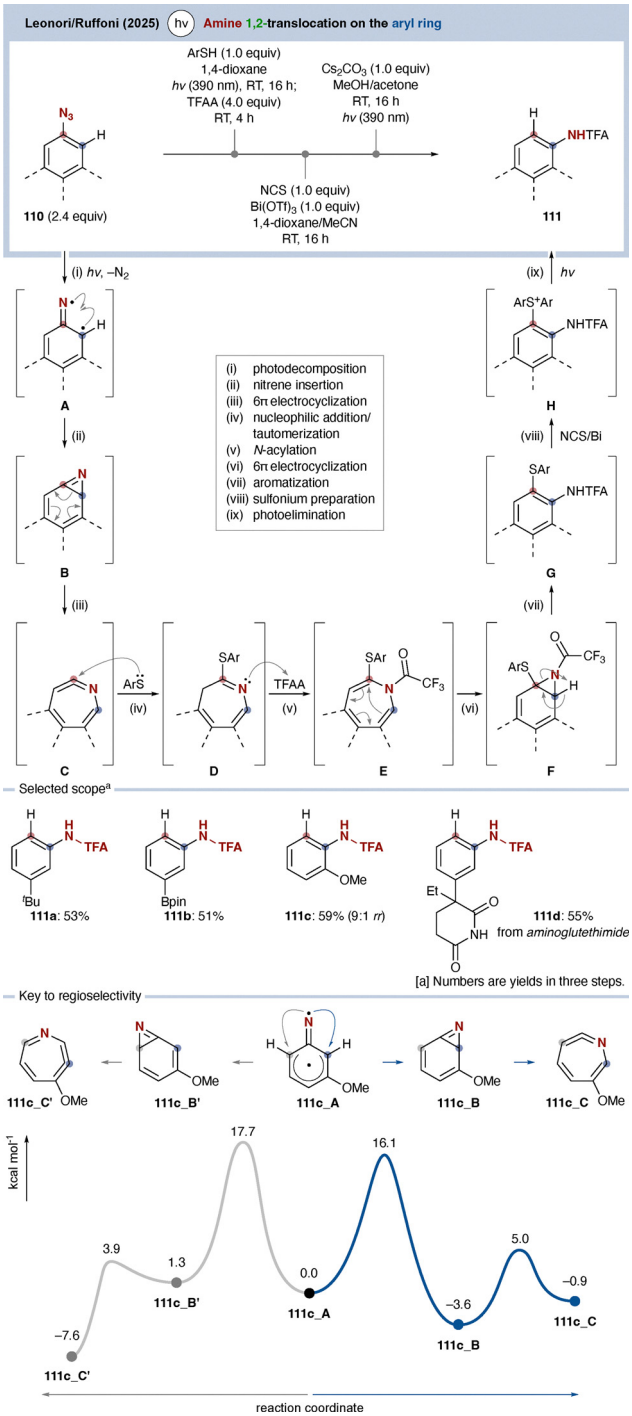

Scheme 42 Aromatic nitrogen *ortho*-isomerization.

reactions that formally achieve positional editing of functional groups within the conceptual framework outlined in this review. Owing to their substrate-specific nature or partial deviation from the strict translocation definition, the following studies are grouped together as miscellaneous examples.

6.1. Amine (equivalent)

This example does not strictly meet the definition of functional group translocation, as the functional group undergoes transformation following the migration event. Nevertheless, it is included here because it constitutes a formal 1,2-relocation of a nitrogen source within an aromatic framework.

In 2025, Leonori, Ruffoni and co-workers reported a strategy for the synthesis of anilines **110** *via* formal 1,2-migration of a nitrogen source from aryl azides **111** (Scheme 42).[132] The transformation proceeds through a three-step sequence. First, aryl azide **110** is irradiated with 390 nm in the presence of an aryl thiol and then addition of trifluoroacetic anhydride (TFAA). This is followed by treatment with *N*-chlorosuccinimide (NCS) and $Bi(OTf)_3$, and finally by addition of Cs_2CO_3 with a second irradiation at 390 nm. Each stage requires purification, rendering the process multistep in nature.

Mechanistically, photoexcitation of **110** generates a singlet nitrene **A**, which rearranges to an azirine **B** and subsequently undergoes 6π-electrocyclization to give ketimine **C**. Nucleophilic attack of the arylthiol affords azepine **D**, which upon activation with TFAA forms intermediate **E**. A second 6π-electrocyclization (**F**) followed by rearomatization furnishes *ortho*-aminothiophenol **G**. In the second stage, NCS and $Bi(OTf)_3$ converts the amine into an aminothiolium salt **H**, which undergoes C–S bond cleavage under basic conditions to deliver TFA-protected aniline **111**.

Despite the multistep character, the reaction tolerates diverse substituents, including *t*-butyl (**110a**), Bpin (**110b**), methoxy (**110c**), and imide (**110d**, derived from aminoglutethimide), affording the corresponding products **111a–111d** in moderate yields. Importantly, the transformation proceeds with high positional selectivity, consistently delivering the *ortho*-aminated products, reflecting a well-defined rearrangement manifold rather than a statistical redistribution of nitrogen functionality. Although the focus here is the formal 1,2-nitrogen relocation, the sulfonium intermediates formed in the sequence provide opportunities for further diversification.[133] Accordingly, this method offers a versatile platform for accessing structurally varied aniline derivatives through a formal nitrogen transposition manifold.

6.2. Cyanide group (intermolecular)

Very recently, Yamaguchi and co-workers reported a nickel-catalyzed aryl group interconversion between aromatic nitriles and aromatic esters (Scheme 43).[134] While nickel-catalyzed aryl interconversions had previously been developed by Morandi, Yamaguchi, and others,[135] combinations involving cyano groups and esters had not been explored. As an application of this chemistry, the authors demonstrated that a quinoline-based nitrile **112** undergo exchange with a series of aryl esters **113**, formally delivering products that correspond to 1,*n*-cyano translocation. For example, reaction of **112** with ester **113a** afforded product **114a**, which can be regarded as arising from a formal 1,2-cyano migration. Similarly, coupling with **113b–113e** furnished products **114b–114e**, corresponding to formal 1,3-, 1,4-, 1,5-, and 1,6-cyano migration, respectively. In each case, diaryl ether **115** was obtained as the complementary product of the exchange process.

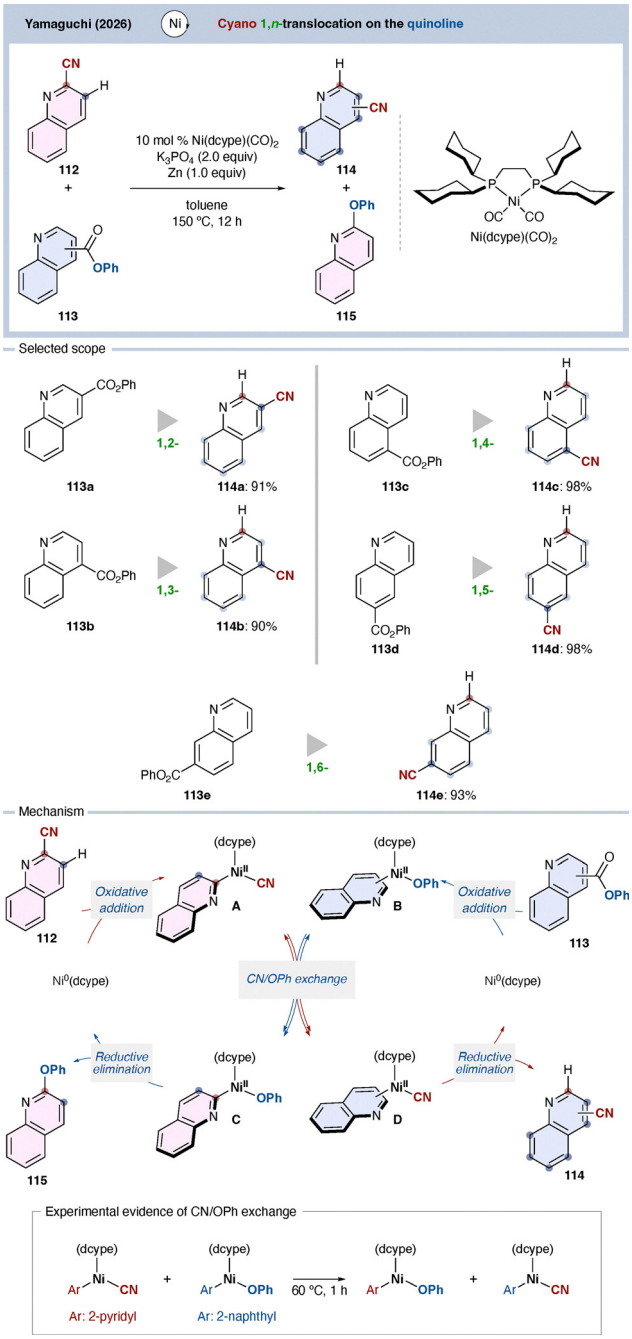

Scheme 43 Formal 1,*n*-cyano translocation by Ni catalysis.

Mechanistically, oxidative addition of the C–CN bond of nitrile **112** and the acyl C–O bond of ester **113** to the nickel catalyst, Ni(dcype)$(CO)_2$ (dcype = 1,2-bis(dicyclohexylphosphino)-ethane),[136] generates complexes **A** and **B**. Subsequent exchange of the anionic ligands, namely $^{-}$CN and $^{-}$OPh, furnishes complexes **C** and **D**, from which reductive elimination provides the diaryl ether **115** and quinoline products **114** bearing the cyano group at different positions. Although the cyano group does not migrate intramolecularly within a single molecule, NMR experiments confirmed the occurrence of ligand exchange at the metal center, supporting the proposed mechanism. This transformation

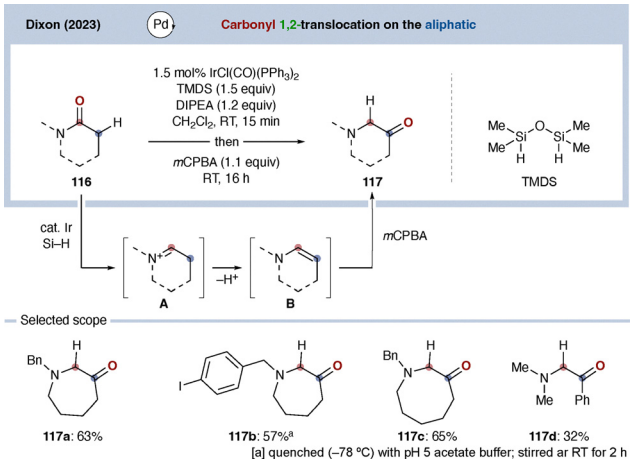

Scheme 44 Carbonyl 1,2-translocation from amides to ketones.

therefore represents a formal, rather than literal, cyano translocation. By exploiting intermolecular aryl exchange on a common scaffold, the strategy cleverly creates the net appearance of positional cyano migration. Conceptually, this work highlights how functional group interconversion chemistry can be leveraged to achieve positional diversification that mimics a translocation process, thereby expanding the design space of functional group editing.

6.3. Carbonyl (amide)

In a related but conceptually distinct example that formally combines functional group interconversion and positional editing, Dixon and co-workers reported in 2023 a method for formal 1,2-translocation of an amide-derived carbonyl group by integrating reduction, isomerization, and oxidation in a single

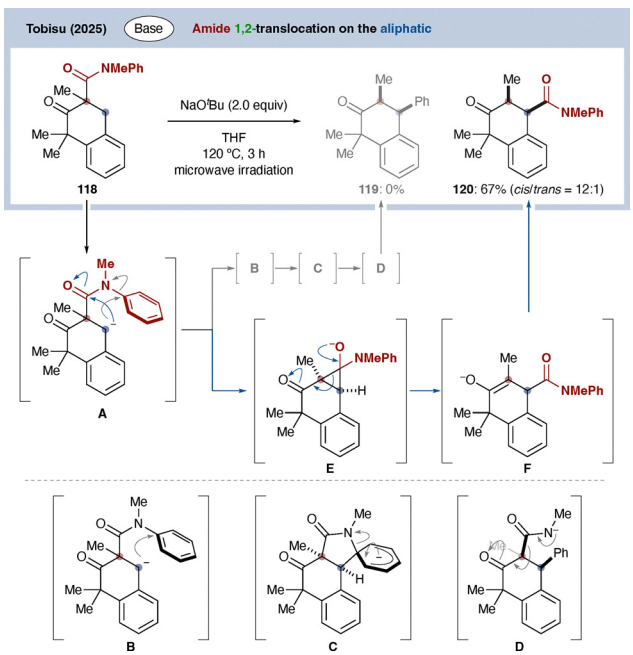

Scheme 45 Base-promoted 1,2-amide translocation.

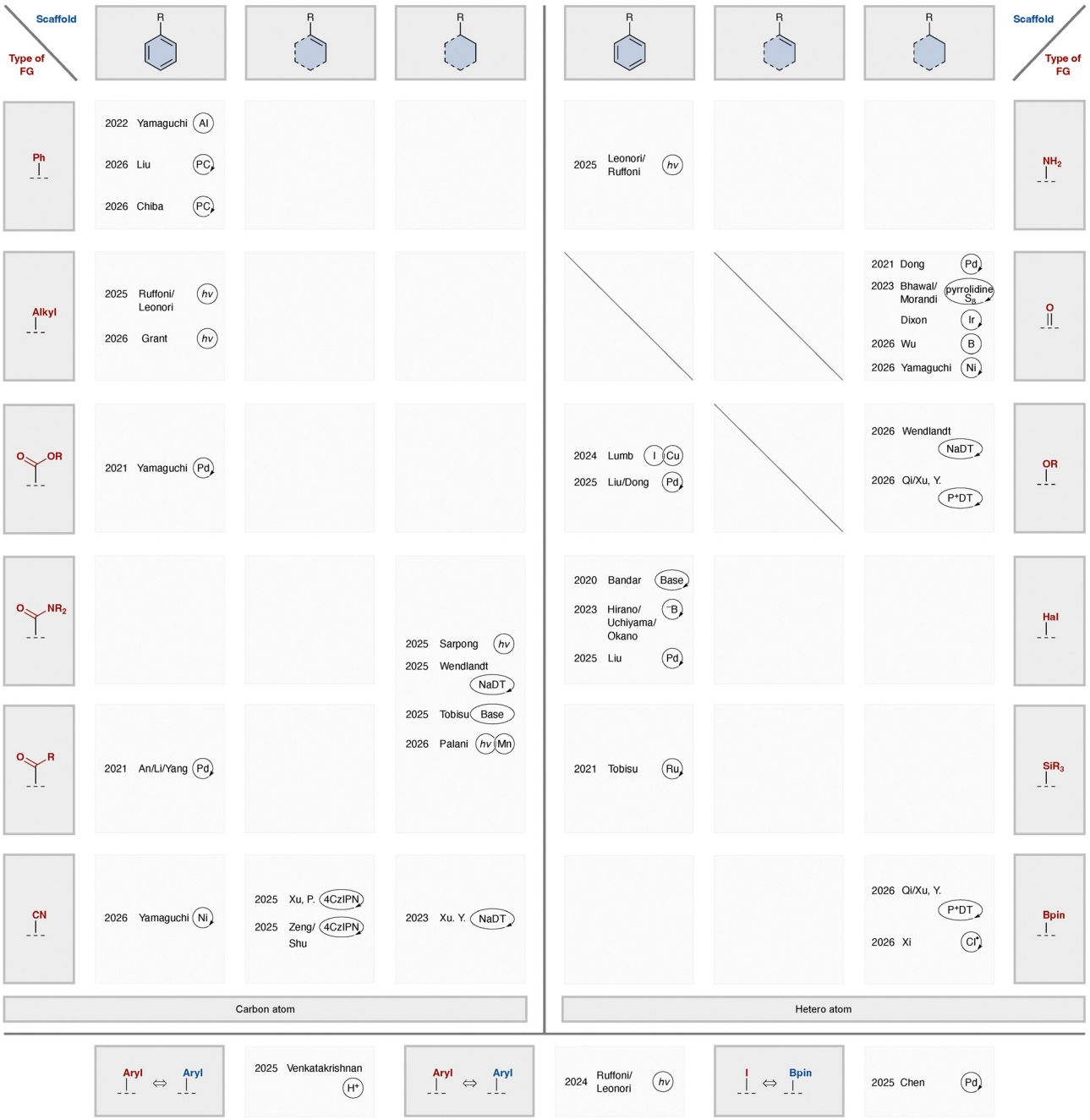

Fig. 6 Overview of functional group translocation reactions.

reaction sequence (Scheme 44).[137] Their approach builds on the group's established expertise in reductive amide activation using Vaska's complex to generate iminium intermediate **A**,[138] which undergoes nucleophilic addition. Subsequent deprotonation furnishes enamine **B**, and *in situ* oxidation with *m*-CPBA delivers ketone **117**, corresponding to formal 1,2-migration of the carbonyl functionality.

Although the functional group identity changes from an amide to a ketone during the sequence, the positional shift of the carbonyl unit clearly constitutes a formal 1,2-carbonyl translocation and is therefore included in this review. The method is applicable to several substrate classes: eight-membered lactams afforded the corresponding ketones (*e.g.* **117a**) and aryl iodide substituents, often incompatible with transition-metal-catalyzed processes, were well tolerated (**117b**). Additional eight-membered lactams underwent efficient conversion (**117c**), and even acyclic amides furnished the desired ketones **117d**, albeit in more modest yields.

While currently limited to amide substrates, this work provides an elegant demonstration of carbonyl relocation in a one-pot sequence through orchestrated redox manipulation and skeletal isomerization, thereby broadening the conceptual framework of carbonyl translocation chemistry.

6.4. Amide

In 2025, Tobisu and co-workers reported a formal 1,2-translocation of an amide group that was identified as a side reaction during studies aimed at the synthesis of compound **119** (Scheme 45).[139] Upon treatment of amide **118** with NaO^{t}Bu, deprotonation occurs at the benzylic position to generate an anionic intermediate **A**. This species undergoes intramolecular nucleophilic attack at the *ipso* carbon of the aromatic C–N bond *via* transition structure **B**, forming a Meisenheimer-type intermediate **C**. Subsequent C–N bond cleavage results in deamidation to generate intermediate **D**, ultimately affording ketone **119**. Mechanistically, this sequence closely resembles a Truce–Smiles rearrangement.

Interestingly, the reaction outcome depends strongly on the ring size of the starting ketone. With five-membered ring substrates, the above pathway predominates.[140] In contrast, for six-membered ring systems, nucleophilic attack preferentially occurs at the amide carbonyl group from intermediate **A**, generating tetrahedral intermediate **E**. This alternative pathway leads to a retro-Claisen-type fragmentation to give intermediate **F**, which upon protonation of **F** furnishes compound **120** (*cis*/*trans* = 12 : 1). Although this amide 1,2-translocation was not the primary focus of the original study, it represents an intriguing transformation that could prove valuable if its scope and generality can be further developed.

7. Conclusions and outlook

In this review, we have surveyed recent advances in functional group translocation, defined in a strict sense as transformations that preserve the molecular formula, the identity of the functional group, and the carbon framework, while altering only its position. By organizing the field according to scaffold type, functional group identity, and migration distance, we sought to provide a unified framework for a rapidly expanding yet conceptually diverse research area.

Over the past several years, functional group translocation has evolved from isolated and often harsh transformations into a catalytically enabled molecular editing strategy. Transition metal catalysis, photoredox activation, and radical relay processes have significantly broadened the accessible reaction space. Migrating groups now include halogens, aryl and alkyl substituents, acyl and ester units, cyano and boryl groups, together with a variety of heteroatom-containing functionalities such as amino, sulfonyl, and alkoxy groups. Translocations have been demonstrated across (hetero)aromatic frameworks, sp^2–sp^3 systems, and fully aliphatic sp^3–sp^3 manifolds, and select cases even in double functional group exchange processes.

To provide a systematic overview, we compiled a summary table correlating scaffold type and migrating functional group (Fig. 6). This overview reveals that, despite impressive progress, the landscape remains highly uneven. Aromatic systems are comparatively well explored, whereas fully aliphatic systems remain underdeveloped. Short-range 1,2-migrations dominate the field, while predictable long-range (1,*n*) translocations are still rare. Certain functional groups, such as cyano and boryl units, have recently emerged as versatile handles, yet many other functional group classes remain largely unexplored in a translocation context. These gaps highlight substantial opportunities for future development.

Several key challenges define the outlook of the field. First, achieving predictable site-selectivity in molecules containing multiple similar bonds remains intrinsically difficult. Second, controlling migration distance and directionality, particularly when thermodynamic differences between isomers are small, requires deeper mechanistic understanding. Third, reversibility and product inhibition, often rooted in subtle energy landscapes, must be addressed to ensure synthetic practicality. Finally, expanding translocation chemistry to complex, densely functionalized molecules will be essential for broader adoption in medicinal chemistry and materials science.

Looking ahead, the maturation of functional group translocation will likely depend on the development of general design principles that transcend individual reaction classes. Integration with C–H functionalization, skeletal editing, and late-stage diversification strategies may ultimately enable the controlled repositioning of functional groups within complex molecular architectures. If such principles can be established, functional group translocation has the potential to become a foundational tool for positional molecular design rather than a collection of isolated transformations. The field remains far from saturated. Its most compelling advances may still lie ahead.

Conflicts of interest

There are no conflicts to declare.

Data availability

No primary research results, software or code have been included and no new data were generated or analysed as part of this review.

Acknowledgements

This work was supported by JSPS KAKENHI Grant Number JP21H05213 (Digi-TOS), and JP25K01775 (to J. Y.). This work was partly supported by JST CREST Grant Number JPMJCR24T3 (to J. Y.). We thank the reviewers for their thoughtful and constructive comments, which greatly improved the clarity and scope of this review.

References

1 (*a*) M. Ishikawa, Y. Hiraiwa, D. Kubota, M. Tsushima, T. Watanabe, S. Murakami, S. Ouchi and K. Ajito, *Bioorg. Med. Chem.*, 2006, **14**, 2131–2150; (*b*) P. Zhang, J. Hao, J. Liu, Q. Lu, H. Sheng, L. Zhang and H. Sun, *J. Nat. Prod.*, 2009, **72**, 1414–1418.

2 (*a*) L. M. Barton, J. T. Edwards, E. C. Johnson, E. J. Bukowski, R. C. Sausa, E. F. C. Byrd, J. A. Orlicki, J. J. Sabatini and P. S. Baran, *J. Am. Chem. Soc.*, 2019, **141**, 12531–12535; (*b*) S. Takahashi, S. Nagai, M. Asami and S. Ito, *Mater. Adv.*, 2020, **1**, 708–719; (*c*) A. Ekbote, S. M. Mobin and R. Misra, *J. Mater. Chem. C*, 2020, **8**, 3589–3602; (*d*) B. Roy, I. Maisuls, J. Zhang, F. C. Niemeyer, F. Rizzo, C. Wölper, C. G. Daniliuc, B. Z. Tang, C. A. Strassert and J. Voskuhl, *Angew. Chem., Int. Ed.*, 2022, **61**, e202111805; (*e*) G. Fei, S. Li, Y. Liu, J. B. Carney, T. Chen, Y. Li, X. Gao, J. Chen, P. Chen, Y. Yue, K. Bao, B. Tang and G. Chen, *Chem. Commun.*, 2023, **60**, 10–25.

3 A. J. Tague, P. Putsathit, T. V. Riley, P. A. Keller and S. G. Pyne, *ACS Med. Chem. Lett.*, 2021, **12**, 413–419.

4 (*a*) C. G. Wermuth, J.-J. Bourguignon, R. Hoffmann, R. Boigegrain, R. Brodin, J.-P. Kan and P. Soubrié, *Bioorg. Med. Chem. Lett.*, 1992, **2**, 833–838; (*b*) *Analogue-based Drug Discovery*, ed J. Fischer and C. R. Ganellin, Wiley: VCH, Weinheim, Germany, 2006.

5 D. S. La, F. G. Salituro, G. M. Botella, A. M. Griffin, Z. Bai, M. A. Ackley, J. Dai, J. J. Doherty, B. L. Harrison, E. C. Hoffmann, T. M. Kazdoba, M. C. Lewis, M. C. Quirk and A. J. Robichaud, *J. Med. Chem.*, 2019, **62**, 7526–7542.

6 F. Chen, Y. Wang, S. Song, K. Wang and Q. Zhang, *J. Phys. Chem. C*, 2023, **127**, 8887–8893.

7 G. Fan and D. Yan, *Sci. Rep.*, 2014, **4**, 4933.

8 J. E. Anthony, J. S. Brooks, D. L. Eaton and S. R. Parkin, *J. Am. Chem. Soc.*, 2001, **123**, 9482–9483.

9 (*a*) M. Romain, S. Thiery, A. Shirinskaya, C. Declairieux, D. Tondelier, B. Geffroy, O. Jeannin, J. Rault-Berthelot, R. Métivier and C. Poriel, *Angew. Chem., Int. Ed.*, 2015, **54**, 1176–1180; (*b*) C. Poriel and J. Rault-Berthelot, *Acc. Chem. Res.*, 2018, **51**, 1818–1830; (*c*) C. Poriel and J. Rault-Berthelot, *Chem. Soc. Rev.*, 2023, **52**, 6754–6805.

10 (*a*) N. Funken, Y. Zhang and A. Gansäuer, *Chem. – Eur. J.*, 2017, **23**, 19–32; (*b*) L. Ping, D. S. Chung, J. Bouffard and S. Lee, *Chem. Soc. Rev.*, 2017, **46**, 4299–4328; (*c*) C. Nájera, I. P. Beletskaya and M. Yus, *Chem. Soc. Rev.*, 2019, **48**, 4515–4618.

11 Selected examples: (*a*) E. S. Isbrandt, D. E. Chapple, N. T. P. Tu, V. Dimakos, A. M. M. Beardall, P. D. Boyle, C. N. Rowley, J. M. Blacquiere and S. G. Newman, *J. Am. Chem. Soc.*, 2024, **146**, 5650–5660; (*b*) G. Marcos-Ayuso, D. Quesada, M. Y. Cobos-Abad, C. Lendínez, S. Fernández-Moyano, P. Mauleon and R. G. Arrayás, *ACS Catal.*, 2025, **15**, 20230–20242.

12 Selected reviews and acccounts: (*a*) C. Aubert, L. Fensterbank, P. Garcia, M. Malacria and A. Simonneau, *Chem. Rev.*, 2011, **111**, 1954–1993; (*b*) W. Li, W. Xu, J. Xie, S. Yu and C. Zhu, *Chem. Soc. Rev.*, 2017, **47**, 654–667; (*c*) X.-M. Zhang, Y.-Q. Tu, F.-M. Zhang, Z.-H. Chen and S.-H. Wang, *Chem. Soc. Rev.*, 2017, **46**, 2272–2305; (*d*) X. Dong, H. Wang, H. Liu and F. Wang, *Org. Chem. Front.*, 2020, **7**, 3530–3556; (*e*) X. Wu and C. Zhu, *Acc. Chem. Res.*, 2020, **53**, 1620–1636; (*f*) X. Wu, Z. Ma, T. Feng and C. Zhu, *Chem. Soc. Rev.*, 2021, **50**, 11577–11613; (*g*) A. R. Allen, E. A. Noten and C. R. J. Stephenson, *Chem. Rev.*, 2022, **122**, 2695–2751; (*h*) Y. Zhang, J. Chen and H. Huang, *Angew. Chem., Int. Ed.*, 2022, **61**, e202205671; (*i*) F. Chen, Z. Cao and C. Zhu, *Chem. Commun.*, 2024, **60**, 14912–14923; (*j*) R. Kumar, *Chem. – Asian J.*, 2024, **19**, e202400053; (*k*) Z. Shi, C.-Y. Wen, L.-X. Yang, J. Li and X. Sun, *Org. Chem. Front.*, 2025, **12**, 2499–2524.

13 (*a*) D. Kaiser, A. Noble, V. Fasano and V. K. Aggarwal, *J. Am. Chem. Soc.*, 2019, **141**, 14104–14109; (*b*) J. Chen, S. Liu, S. Su, R. Fan, R. Zhang, W. Meng and J. Tan, *Sci. Adv.*, 2023, **9**, eadi1370; (*c*) Y. Lee, Y. S. Nam, S. Y. Kim, J. E. Ki and H. G. Lee, *Chem. Sci.*, 2023, **14**, 7688–7698; (*d*) S. Wang, X. Luo, Y. Wang, Z. Liu, Y. Yu, X. Wang, D. Ren, P. Wang, Y.-H. Chen, X. Qi, H. Yi and A. Lei, *Nat. Chem.*, 2024, **16**, 1621–1629; (*e*) U. Mukherjee, J. A. Shah, D. G. Musaev and M.-Y. Ngai, *J. Am. Chem. Soc.*, 2024, **146**, 21271–21279; (*f*) K. Gu, M. T. Hall, Z. D. Tucker, G. M. Durling and B. L. Ashfeld, *Nat. Commun.*, 2025, **16**, 97; (*g*) Y. Lin, Y. Guo, S. Mu, G. Lin, W. Kong, X. Lei, J. Xu and Q. Song, *Org. Lett.*, 2025, **27**, 9825–9830; (*h*) K.-L. Tao, X. Wang, H. Liu, W.-Q. Chen, Y. Sun, Y.-Q. Zhang, Y.-X. Li, Z.-Y. Wang, Y. Ye, H. Xu, L. Lan and H.-X. Dai, *Nat. Synth.*, 2025, **4**, 209–218; (*i*) C. Guo, J. Zhang, Y. Ge, Z. Qiu and Z. Xie, *Angew. Chem., Int. Ed.*, 2025, **64**, e202416987; (*j*) L. Ding, M. Wang, Y. Liu, H. Lu, Y. Zhao and Z. Shi, *Angew. Chem., Int. Ed.*, 2025, **64**, e202413557; (*k*) X.-R. Shu, J.-Q. Liu, M.-Q. Yang, M.-Y. Tian, D.-Q. Yang, Y.-B. Zhang, C. Deng, J. Yu, W.-T. Wei and Y. Zhou, *Org. Lett.*, 2026, **28**, 546–552.

14 Selected reviews: (*a*) C. Dugave and L. Demange, *Chem. Rev.*, 2003, **103**, 2475–2532; (*b*) T. Nevesely, M. Wienhold, J. J. Molloy and R. Gilmour, *Chem. Rev.*, 2022, **122**, 2650–2694; (*c*) P.-Z. Wang, W.-J. Xiao and J.-R. Chen, *Nat. Rev. Chem.*, 2023, **7**, 35–50.

15 Selected examples:C. Cruz, J. Galicia, S. Bowers, J. Hua and E. A. Romero, *J. Am. Chem. Soc.*, 2026, **148**, 801–808.

16 Selected reviews and acccounts: (*a*) M. Korb and H. Lang, *Chem. Soc. Rev.*, 2019, **48**, 2829–2882; (*b*) C. Lefebvre, L. Fortier and N. Hoffmann, *Eur. J. Org. Chem.*, 2020, 1393–1404; (*c*) S. F. Kim, C. Amber, G. L. Bartholomew and R. Sarpong, *Acc. Chem. Res.*, 2025, **58**, 1786–1800; (*d*) D. Das, A. Mukherjee and S. Rej, *Green Chem.*, 2026, **28**, 4409–4448.

17 Selected examples(*a*) H. Tiefenthaler, W. Dörscheln, H. Göth and H. Schmid, *Tetrahedron Lett.*, 1964, **5**, 2999–3001; (*b*) E. F. Ullman and B. Singh, *J. Am. Chem. Soc.*, 1966, **88**, 1844–1845; (*c*) P. Beak, J. L. Miesel and W. R. Messer, *Tetrahedron Lett.*, 1967, **8**, 5315–5318; (*d*) H. Tiefenthaler, W. Dörscheln, H. Göth and H. Schmid, *Helv. Chim. Acta*, 1967, **50**, 2244–2258; (*e*) C. Bracken and M. Baumann, *J. Org. Chem.*, 2020, **85**, 2607–2617; (*f*) M. Yamashita, A. Suzuki, T. Yoshino, K. Higashida, M. Kojima and S. Matsunaga, *Chem. – Asian J.*, 2025, **20**, e00448; (*g*) A. Liu and Y. Yang, *J. Am. Chem. Soc.*, 2025, **147**, 43604–43611; (*h*) T. dos Santos, C. S. Buettner, D. B. Yildiz, M. Mamone, A. Ruffoni and

D. Leonori, *Angew. Chem., Int. Ed.*, 2025, **64**, e202423804; (*i*) G. L. Bartholomew, S. F. Kim, Y. Oyamada, F. Sbordone, J. A. Carroll, J. E. Jurczyk, C. S. Yeung, C. Barner-Kowollik and R. Sarpong, *Angew. Chem., Int. Ed.*, 2025, **64**, e202423803.

18 Y. Xu, L. Poletti, E. M. Arpa, B. Roure, A. Ruffoni and D. Leonori, *Nat. Commun.*, 2026, **17**, 2141.

19 Selected reviews: (*a*) I. Nakamura and M. Terada, *Tetrahedron Lett.*, 2019, **60**, 689–698; (*b*) J. L. Jat and G. Kumar, *Adv. Synth. Catal.*, 2019, **361**, 4426–4441; (*c*) B. N. Bhawal and B. Morandi, *Angew. Chem., Int. Ed.*, 2019, **58**, 10074–10103.

20 Selected examples: (*a*) S. Wang, X. Cao and Y. Li, *Angew. Chem., Int. Ed.*, 2017, **56**, 13809–13813; (*b*) I. Nakamura, T. Jo, Y. Ishida, H. Tashiro and M. Terada, *Org. Lett.*, 2017, **19**, 3059–3062; (*c*) C.-X. Ye, X. Shen, S. Chen and E. Meggers, *Nat. Chem.*, 2022, **14**, 566–573; (*d*) L.-P. Zhao, H. Liu, B. K. Mai, Y. Zhang, L. Cheng, P. Liu and Y. Yang, *Nat. Chem. Biol.*, 2025, **21**, 1773–1782; (*e*) K. Lin, L. Zhao, S. Wang, H. Liu, Y. Zhang, B. K. Mai, P. Liu and Y. Yang, *Angew. Chem., Int. Ed.*, 2025, e24718; (*f*) T. Yuan, M. Zhang, L. Cheng, X. Zheng, S. Jiang, X. Huang and H. Xiao, *J. Am. Chem. Soc.*, 2025, **147**, 44041–44047; (*g*) H. Na, M. Kim, L. Shen and J. H. Jeong, *J. Heterocycl. Chem.*, 2025, **62**, 1834–1839; (*h*) J.-C. Shi, M. Zhang, Y.-F. Yin, C. Yang, X. Peng and G.-W. Wang, *CCS Chem.*, 2026, DOI: 10.31635/ccschem.026.202506968.

21 T. Fujiwara, T. Inokuma and K. Yamada, *Org. Lett.*, 2026, **28**, 136–140.

22 Selected examples: (*a*) M. Franck-Neumann and C. Dietrich-Buchecker, *Tetrahedron Lett.*, 1976, **17**, 2069–2072; (*b*) Y. He, Y. Chen, H. Du, L. A. Schmid and C. J. Lovely, *Tetrahedron Lett.*, 2004, **45**, 5529–5532; (*c*) D. Armesto, M. J. Ortiz, A. R. Agarrabeitia and N. El-Boulifi, *Angew. Chem., Int. Ed.*, 2005, **44**, 7739–7741; (*d*) R. Goikhman, T. L. Jacques and D. Sames, *J. Am. Chem. Soc.*, 2009, **131**, 3042–3048; (*e*) R. K. Shiroodi, M. Soltani and V. Gevorgyan, *J. Am. Chem. Soc.*, 2014, **136**, 9882–9885; (*f*) P. R. Athawale, V. M. Zade, G. R. Krishna and D. S. Reddy, *Org. Lett.*, 2021, **23**, 6642–6647; (*g*) S. Shibata, K. Amano, T. Kojima and K. Mori, *Chem. Commun.*, 2023, **59**, 9976–9979; (*h*) F. Li, Y. Luo, X. Zhu, Y. Ye, Q. Yuan and W. Zhang, *Chem. – Eur. J.*, 2023, **29**, e202300027; (*i*) H. Bi, J. Chu, X.-L. Zhao and S. R. Wang, *Org. Lett.*, 2024, **26**, 1437–1441; (*j*) H.-L. Lan, W. Liu, W. Liu, J. Peng, Y. Bai and X. Shao, *Org. Chem. Front.*, 2024, **12**, 1167–1176; (*k*) G. Zhao, A. Khosravi, S. Sharma, D. G. Musaev and M.-Y. Ngai, *J. Am. Chem. Soc.*, 2024, **146**, 31391–31399; (*l*) X. Zheng, F. Huang, X. Li, K. Zhuo, D. Chen, M. Luo and H. Xia, *Chem. Sci.*, 2024, **15**, 8443–8450.

23 Selected reviews: (*a*) D. Lübken, B. Siekmeyer and M. Kalesse, *Eur. J. Org. Chem.*, 2022, e202200701; (*b*) P.-Z. Wang, W.-J. Xiao and J.-R. Chen, *Nat. Rev. Chem.*, 2023, **7**, 35–50.

24 (*a*) M. Hassam, A. Taher, G. E. Arnott, I. R. Green and W. A. L. van Otterlo, *Chem. Rev.*, 2015, **115**, 5462–5569; (*b*) X. Liu, B. Li and Q. Liu, *Synthesis*, 2019, 1293–1310; (*c*) S. Zhang and M. Findlater, *Synthesis*, 2021, 2787–2797.

25 Y. He, K. A. Unnikrishnan, W. Yin, R. Kuniyil, H. Du and W. Guo, *Green Chem.*, 2025, **27**, 6741–6746.

26 Selected examples: (*a*) A. L. Keen, M. Doster and S. A. Johnson, *J. Am. Chem. Soc.*, 2007, **129**, 810–819; (*b*) C. Odena, E. Gomez-Bengoa and R. Martin, *J. Am. Chem. Soc.*, 2024, **146**, 112–117.

27 H. Jung, J. Choi, D. Kim, J. H. Lee, H. Ihee, D. Kim and S. Chang, *Angew. Chem., Int. Ed.*, 2024, **63**, e202408123.

28 Selected review: (*a*) A. Parikh, H. Parikh and K. Parikh, in *Name Reactions in Organic Synthesis*, Cambridge University Press, 2006, pp. 579–582; (*b*) I. Fernández, F. P. Cossío and M. A. Sierra, *Chem. Rev.*, 2009, **109**, 6687–6711.

29 (*a*) R. Abrams, M. H. Jesani, A. Browning and J. Clayden, *Angew. Chem., Int. Ed.*, 2021, **60**, 11272–11277; (*b*) M. E. Matter, L. Čamdžić and E. E. Stache, *Angew. Chem., Int. Ed.*, 2023, **62**, e202308648.

30 (*a*) K. Inoue and K. Okano, *ChemCatChem*, 2024, **16**, e202400408; (*b*) S. N. Gat, P. P. Pattanaik and R. Dandela, *Org. Chem. Front.*, 2025, **12**, 4151–4180; (*c*) J.-L. Zhu and M.-L. Chen, *Molecules*, 2025, **30**, 2959.

31 (*a*) T.-C. Tsai, S.-B. Liu and I. Wang, *Appl. Catal., A*, 1999, **181**, 355–398; (*b*) C. Perego and P. Ingallina, *Green Chem.*, 2004, **6**, 274–279; (*c*) C. Perego and P. Pollesel, in *Advances in Aromatics Processing Using Zeolite Catalysts*, ed S. Ernst, Elsevier, 2010, pp. 97–149.

32 (*a*) *J. Chem. Soc.*, 1877, **32**, 725–791; (*b*) D. V. Nightingale, *Chem. Rev.*, 1939, **25**, 329–376.

33 R. Anschütz, *Justus Liebigs Ann. Chem.*, 1886, **235**, 150–229.

34 E. Fischer and T. Schmidt, *Ber. Dtsch. Chem. Ges.*, 1888, **21**, 1811–1812.

35 G. Baddeley and J. Kenner, *J. Chem. Soc.*, 1935, 303–309.

36 Z. Wang, in *Comprehensive Organic Name Reactions and Reagents*, John Wiley&Sons, Hoboken, 2012, pp. 128–131.

37 (*a*) D. V. Nightingale, *Chem. Rev.*, 1939, **25**, 329–376; (*b*) D. Nightingale and L. I. Smith, *J. Am. Chem. Soc.*, 1939, **61**, 101–104; (*c*) D. Nightingale and L. I. Smith, *J. Am. Chem. Soc.*, 1939, **61**, 101–104; (*d*) D. Nightingale and F. Wadsworth, *J. Am. Chem. Soc.*, 1941, **63**, 3514–3517.

38 (*a*) D. A. McCaulay and A. P. Lien, *J. Am. Chem. Soc.*, 1952, **74**, 6246–6250; (*b*) G. A. Olah and M. W. Meyer, *J. Org. Chem.*, 1962, **27**, 3464–3469; (*c*) R. H. Allen, *J. Am. Chem. Soc.*, 1960, **82**, 4856–4858.

39 (*a*) S. C. Sherman, A. V. Iretskii, M. G. White, C. Gumienny, L. M. Tolbert and D. A. Schiraldi, *J. Org. Chem.*, 2002, **67**, 2034–2041; (*b*) S. L. Skraba-Joiner, J. W. Brulet, M. K. Song and R. P. Johnson, *J. Org. Chem.*, 2017, **82**, 13076–13083; (*c*) P. Bourbon, K. Vitse, A. Martin-Mingot, H. Geindre, F. Guégan, B. Michelet and S. Thibaudeau, *Nat. Commun.*, 2024, **15**, 7435; (*d*) I. S. Mekeda, R. Yu Balakhonov and V. Z. Shirinian, *Org. Biomol. Chem.*, 2024, **22**, 7715–7724.

40 G. R. Clemo and J. C. Seaton, *J. Chem. Soc.*, 1954, 2582–2584.

41 H. Hartmann and J. Liebscher, *Molecules*, 2024, **29**, 3151.

42 (*a*) K. Nakashima, S. Hanamura, A. Imamura, Y. Matsushima, S. Hirashima and T. Miura, *Asian J. Org.*

Chem., 2022, **11**, e202200403; (*b*) K. Nakashima, Y. Kudo, Y. Matsushima, S. Hirashima and T. Miura, *Chem. Pharm. Bull.*, 2024, **72**, 336–339.
43 C. F. H. Allen and F. P. Pingert, *J. Am. Chem. Soc.*, 1942, **64**, 1365–1371.
44 A. Ajaz, E. C. McLaughlin, S. L. Skraba, R. Thamatam and R. P. Johnson, *J. Org. Chem.*, 2012, **77**, 9487–9495.
45 N. Ponugoti and V. Parthasarathy, *Chem. – Eur. J.*, 2022, **28**, e202103530.
46 Selected examples: (*a*) A. Necula, A. Racoveanu-Schiketanz, M. D. Gheorghiu and L. T. Scott, *J. Org. Chem.*, 1995, **60**, 3448–3451; (*b*) M. B. Goldfinger, K. B. Crawford and T. M. Swager, *J. Am. Chem. Soc.*, 1997, **119**, 4578–4593; (*c*) T. J. Sisto, L. N. Zakharov, B. M. White and R. Jasti, *Chem. Sci.*, 2016, **7**, 3681–3688; (*d*) M. Krzeszewski, K. Sahara, Y. M. Poronik, T. Kubo and D. T. Gryko, *Org. Lett.*, 2018, **20**, 1517–1520; (*e*) M. He and T. M. Swager, *J. Am. Chem. Soc.*, 2020, **142**, 17876–17880.
47 H. Wynberg and H. van Driel, *J. Am. Chem. Soc.*, 1965, **87**, 3998–4000.
48 (*a*) H. Wynberg, R. M. Kellogg, H. van Driel and G. E. Beekhuis, *J. Am. Chem. Soc.*, 1966, **88**, 5047–5048; (*b*) H. Wynberg and H. van Driel, *Chem. Commun.*, 1966, 203–204; (*c*) H. Wynberg, H. V. Driel, R. M. Kellogg and J. Buter, *J. Am. Chem. Soc.*, 1967, **89**, 3487–3494; (*d*) R. M. Kellogg and H. Wynberg, *J. Am. Chem. Soc.*, 1967, **89**, 3495–3498; (*e*) H. Wynberg, G. E. Beekhuis, H. V. Driel and R. M. Kellogg, *J. Am. Chem. Soc.*, 1967, **89**, 3498–3500; (*f*) H. Wynberg, R. M. Kellogg, H. V. Driel and G. E. Beekhuis, *J. Am. Chem. Soc.*, 1967, **89**, 3501–3505; (*g*) H. Hiraoka and R. Srinivasan, *J. Am. Chem. Soc.*, 1968, **90**, 2720–2721; (*h*) H. Hiraoka, *J. Phys. Chem.*, 1970, **74**, 574–581; (*i*) H. Hiraoka, *J. Chem. Soc. D: Chem. Commun.*, 1970, 1306; (*j*) H. Wynberg, *Acc. Chem. Res.*, 1971, **4**, 65–73.
49 (*a*) Y. Kanaoka and K. San-nohe, *Tetrahedron Lett.*, 1980, **21**, 3893–3896; (*b*) T. J. Barton and G. P. Hussmann, *J. Org. Chem.*, 1985, **50**, 5881–5882; (*c*) S.-H. Park, H.-J. Ha, C.-T. Lim, D.-K. Lim, K.-H. Lee and Y.-T. Park, *Bull. Korean Chem. Soc.*, 2005, **26**, 1190–1196; (*d*) J. W. Pavlik, P. Tongcharoensirikul, N. P. Bird, A. C. Day and J. A. Barltrop, *J. Am. Chem. Soc.*, 1994, **116**, 2292–2300.
50 Selected reviews, see: (*a*) W. A. Rendall, M. Torres, E. N. Lown and O. P. Strausz, *Rev. Chem. Intermed.*, 1986, **6**, 335–364; (*b*) M. D'Auria, A. Guarnaccio, R. Racioppi, S. Stoia and L. Emanuele, in *Photochemistry of Heterocycles*, ed M. D'Auria, A. Guarnaccio, R. Racioppi, S. Stoia and L. Emanuele, Elsevier, 2023, pp. 91–160.
51 (*a*) A. W. Burgstahler and P.-L. Chien, *J. Am. Chem. Soc.*, 1964, **86**, 2940–2941; (*b*) K. E. Wilzbach and L. Kaplan, *J. Am. Chem. Soc.*, 1964, **86**, 2307–2308(Reported concurrently; low isolated yields.).
52 (*a*) L. Kaplan, K. E. Wilzbach, W. G. Brown and S. S. Yang, *J. Am. Chem. Soc.*, 1965, **87**, 675–676; (*b*) K. E. Wilzbach and L. Kaplan, *J. Am. Chem. Soc.*, 1965, **87**, 4004–4006.
53 (*a*) E. E. van Tamelen and S. P. Pappas, *J. Am. Chem. Soc.*, 1962, **84**, 3789–3791; (*b*) E. E. van Tamelen and S. P. Pappas, *J. Am. Chem. Soc.*, 1963, **85**, 3297–3298; (*c*) E. E. van Tamelen, S. P. Pappas and K. L. Kirk, *J. Am. Chem. Soc.*, 1971, **93**, 6092–6101.
54 (*a*) M. Hayashi, *J. Chem. Soc.*, 1927, 2516–2527; (*b*) M. S. Newman and K. G. Ihrman, *J. Am. Chem. Soc.*, 1958, **80**, 3652–3656; (*c*) Z. Wang, in *Comprehensive Organic Name Reactions and Reagents*, John Wiley&Sons, Hoboken, 2012, pp. 1347–1349.
55 P. H. Gore, *Chem. Rev.*, 1955, **55**, 229–281.
56 (*a*) G. A. Olah, *Friedel–Crafts Chemistry*, John Wiley&Sons Inc., New York, 1973, p 102; (*b*) I. Agranat, Y. S. Shih and Y. Bentor, *J. Am. Chem. Soc.*, 1974, **96**, 1259–1260; (*c*) I. Agranat, T. Mala'bi, Y. N. Oded and H. D. Kraus, *Struct. Chem.*, 2020, **31**, 47–60.
57 (*a*) V. A. Budylin, A. N. Kost, E. D. Matveeva and V. I. Minkin, *Chem. Heterocycl. Compd.*, 1972, **8**, 63–67; (*b*) V. A. Budylin, E. D. Matveeva and A. N. Kost, *Chem. Heterocycl. Compd.*, 1980, **16**, 933–935.
58 I. Agranat, Y. S. Shih and Y. Bentor, *J. Am. Chem. Soc.*, 1974, **96**, 1259–1260.
59 (*a*) I. Agranat, Y. Bentor and Y.-S. Shih, *J. Am. Chem. Soc.*, 1977, **99**, 7068–7070; (*b*) L. Levy, S. Pogodin, S. Cohen and I. Agranat, *Lett. Org. Chem.*, 2007, **4**, 314–318; (*c*) A. Okamoto and N. Yonezawa, *Chem. Lett.*, 2009, **38**, 914–915.
60 (*a*) M. Schnürch, M. Spina, A. F. Khan, M. D. Mihovilovic and P. Stanetty, *Chem. Soc. Rev.*, 2007, **36**, 1046–1057; (*b*) N. de Souza and M. Vinicius, *Curr. Org. Chem.*, 2007, **11**, 637–646; (*c*) M. Schnürch, in *Halogenated Heterocycles*, ed J. Iskra, Springer, Berlin, Heidelberg, 2011, pp. 185–218; (*d*) W. Erb and F. Mongin, *Tetrahedron*, 2016, **72**, 4973–4988.
61 A. Vaitiekunas and F. F. Nord, *Nature*, 1951, **168**, 875–876.
62 (*a*) J.-C. Jacquesy and M.-P. Jouannetaud, *Tetrahedron Lett.*, 1982, **23**, 1673–1676; (*b*) J. F. Bunnett and D. J. McLennan, *J. Am. Chem. Soc.*, 1968, **90**, 2190–2192.
63 J. F. Bunnett and G. Scorrano, *J. Am. Chem. Soc.*, 1971, **93**, 1190–1198.
64 M. Mallet, G. Branger, F. Marsais and G. Quéguiner, *J. Organomet. Chem.*, 1990, **382**, 319–332.
65 B. Wu, W. Szymański, M. M. Heberling, B. L. Feringa and D. B. Janssen, *Trends Biotechnol.*, 2011, **29**, 352–362.
66 (*a*) J. Halpern, *Science*, 1985, **227**, 869–875; (*b*) T. Toraya, *J. Synth. Org. Chem., Jpn.*, 2009, **39**, 1039–1052.
67 Y. Murakami, Y. Hisaeda and T. Ohno, *Bioorg. Chem.*, 1990, **18**, 49–62.
68 J. S. Tou and A. A. Schleppnik, *J. Org. Chem.*, 1983, **48**, 753–755.
69 (*a*) T. Sammakia, E. L. Stangeland and M. C. Whitcomb, *Org. Lett.*, 2002, **4**, 2385–2388; (*b*) E. L. Stangeland and T. Sammakia, *J. Org. Chem.*, 2004, **69**, 2381–2385; (*c*) K. Morii, Y. Yasuda, D. Morikawa, A. Mori and K. Okano, *J. Org. Chem.*, 2021, **86**, 13388–13401.
70 T. R. Puleo and J. S. Bandar, *Chem. Sci.*, 2020, **11**, 10517–10522.
71 R. Schwesinger and H. Schlemper, *Angew. Chem., Int. Ed. Engl.*, 1987, **26**, 1167–1169.

72 K. Inoue, K. Hirano, S. Fujioka, M. Uchiyama, A. Mori and K. Okano, *ACS Catal.*, 2023, **13**, 3788–3793.
73 Y. Sekiguchi, P. Onnuch, Y. Li and R. Y. Liu, *J. Am. Chem. Soc.*, 2025, **147**, 1224–1230.
74 H. G. Lee, P. J. Milner and S. L. Buchwald, *Org. Lett.*, 2013, **15**, 5602–5605.
75 P. J. Milner, T. Kinzel, Y. Zhang and S. L. Buchwald, *J. Am. Chem. Soc.*, 2014, **136**, 15757–15766.
76 N. Tsukada, T. Abe and Y. Inoue, *Helv. Chim. Acta*, 2013, **96**, 1093–1102.
77 K. Matsushita, R. Takise, K. Muto and J. Yamaguchi, *Sci. Adv.*, 2020, **6**, eaba7614.
78 (*a*) R. Takise, R. Isshiki, K. Muto, K. Itami and J. Yamaguchi, *J. Am. Chem. Soc.*, 2017, **139**, 3340–3343; (*b*) M. Kubo and J. Yamaguchi, *Acc. Chem. Res.*, 2024, **57**, 1747–1760.
79 R. Takise, K. Muto, J. Yamaguchi and K. Itami, *Angew. Chem., Int. Ed.*, 2014, **53**, 6791–6794.
80 M. Kubo, N. Inayama, E. Ota and J. Yamaguchi, *Org. Lett.*, 2022, **24**, 3855–3860.
81 Selected reviews on decarbonylative coupling; (*a*) N. Rodríguez and L. J. Goossen, *Chem. Soc. Rev.*, 2011, **40**, 5030–5048; (*b*) R. Takise, K. Muto and J. Yamaguchi, *Chem. Soc. Rev.*, 2017, **46**, 5864–5888; (*c*) H. Lu, T.-Y. Yu, P.-F. Xu and H. Wei, *Chem. Rev.*, 2021, **121**, 365–411.
82 W. Ishiga, M. Ohta, T. Kodama and M. Tobisu, *Org. Lett.*, 2021, **23**, 6714–6718.
83 (*a*) D. Seyferth and D. L. White, *J. Am. Chem. Soc.*, 1972, **94**, 3132–3138; (*b*) D. Seyferth and S. C. Vick, *J. Organomet. Chem.*, 1977, **141**, 173–187; (*c*) U. Sjöstrand, F. Cozzi and K. Mislow, *J. Organomet. Chem.*, 1979, **179**, 323–329; (*d*) R. Sooriyakumaran and P. Boudjouk, *Organometallics*, 1982, **1**, 218–219.
84 (*a*) C. D. Jones, M. G. Jevnikar, A. J. Pike, M. K. Peters, L. J. Black, A. R. Thompson, J. F. Falcone and J. A. Clemens, *J. Med. Chem.*, 1984, **27**, 1057–1066; (*b*) S. Kim, J. Yang and F. DiNinno, *Tetrahedron Lett.*, 1999, **40**, 2909–2912; (*c*) M. Nakazaki, *Bull. Chem. Soc. Jpn.*, 2006, **33**, 461–465.
85 H. Nakahara and J. Yamaguchi, *Org. Lett.*, 2022, **24**, 8083–8087.
86 T. Ozaki, S. Diamandis, N. Rybansky, X. Yang, F. Bai, B. Li, J. Huang and S.-Y. Liu, *J. Am. Chem. Soc.*, 2026, **148**, 3820–3829.
87 P. G. Campbell, A. J. V. Marwitz and S. Liu, *Angew. Chem., Int. Ed.*, 2012, **51**, 6074–6092.
88 J. Luo and J. Zhang, *ACS Catal.*, 2016, **6**, 873–877; Correction: J. Luo and J. Zhang, ACS Catal., 2020, **10**, 14302–14303.
89 T. Ozaki, S. K. Bentley, N. Rybansky, B. Li and S.-Y. Liu, *J. Am. Chem. Soc.*, 2024, **146**, 24748–24753.
90 T. Ozaki, Y. Dai, B. Li, K. Miqueu and S.-Y. Liu, *J. Am. Chem. Soc.*, 2026, **148**, 11205–11214.
91 E. Y. K. Tan, T.-Y. Peng, T. Wakabayashi and S. Chiba, *Nat. Synth.*, 2026, DOI: 10.1038/s44160-026-01023-6.
92 S. Yadav, P. P. Singh, Y. Murti, P. Purohit, P. K. Singh and V. Srivastava, *Tetrahedron*, 2024, **163**, 134138.
93 (*a*) A. P. Bolton, M. A. Lanewala and P. E. Pickert, *J. Org. Chem.*, 1968, **33**, 3415–3418; (*b*) J.-C. Jacquesy and M.-P. Jouannetaud, *Tetrahedron Lett.*, 1982, **23**, 1673–1676.
94 (*a*) C. Yuan, Y. Liang, T. Hernandez, A. Berriochoa, K. N. Houk and D. Siegel, *Nature*, 2013, **499**, 192–196; (*b*) R. Sang, S. E. Korkis, W. Su, F. Ye, P. S. Engl, F. Berger and T. Ritter, *Angew. Chem., Int. Ed.*, 2019, **58**, 16161–16166; (*c*) Z. Li, Z. Wang, N. Chekshin, S. Qian, J. X. Qiao, P. T. Cheng, K.-S. Yeung, W. R. Ewing and J.-Q. Yu, *Science*, 2021, **372**, 1452–1457.
95 S. Edelmann and J.-P. Lumb, *Nat. Chem.*, 2024, **16**, 1193–1199.
96 Q. Zhu, J. M. Taylor, X. Liu and G. Dong, *J. Am. Chem. Soc.*, 2025, **147**, 43098–43104.
97 X. Liu, Y. Fu, Z. Chen, P. Liu and G. Dong, *Nat. Chem.*, 2023, **15**, 1391–1399.
98 M. Alonso, G. Lonardi, E. M. Arpa, B. Roure, A. Ruffoni and D. Leonori, *Nat. Commun.*, 2025, **16**, 7502.
99 R. F. Childs and B. E. George, *Can. J. Chem.*, 1988, **66**, 1343–1349.
100 S. Malik, S. N. Ullal, J. D. Hart, M. Sodoor, P. A. Hume and P. S. Grant, *J. Am. Chem. Soc.*, 2026, **148**, 12217–12226.
101 H. E. Zimmerman and D. Armesto, *Chem. Rev.*, 1996, **96**, 3065–3112.
102 Y. Cheng, S. Yu, Y. He, G. An, G. Li and Z. Yang, *Chem. Sci.*, 2021, **12**, 3216–3225.
103 (*a*) A. L. J. Beckwith, D. M. O'Shea, S. Gerba and S. W. Westwood, *J. Chem. Soc., Chem. Commun.*, 1987, 666–667; (*b*) A. L. J. Beckwith, D. M. O'Shea and S. W. Westwood, *J. Am. Chem. Soc.*, 1988, **110**, 2565–2575.
104 D. G. Morris, *Chem. Soc. Rev.*, 1982, **11**, 397–434.
105 Z. Wu, X. Xu, J. Wang and G. Dong, *Science*, 2021, **374**, 734–740.
106 Y. Guo and S. R. Harutyunyan, *Angew. Chem., Int. Ed.*, 2019, **58**, 12950–12954.
107 J. Wang, Z. Dong, C. Yang and G. Dong, *Nat. Chem.*, 2019, **11**, 1106–1112.
108 Z. Zhang, Z. Liang, R. Ye and G. Dong, *Science*, 2026, **392**, 536–542.
109 Y. Brägger, O. Green, B. N. Bhawal and B. Morandi, *J. Am. Chem. Soc.*, 2023, **145**, 19496–19502.
110 (*a*) C. Willgerodt, *Ber. Dtsch. Chem. Ges.*, 1887, **20**, 2467–2470; (*b*) K. Kindler, *Justus Liebigs Ann. Chem.*, 1923, **431**, 187–230; (*c*) D. L. Priebbenow and C. Bolm, *Chem. Soc. Rev.*, 2013, **42**, 7870–7880.
111 L. Pu, Z. Wang, J. Xia, Z. Chen, M. Xiao, L. Zhu and J. Huang, *J. Am. Chem. Soc.*, 2026, **148**, 16576–16582.
112 K. Ji, Y. Liao, S. Deng and Z. Wu, *Nat. Synth.*, 2026, DOI: 10.1038/s44160-026-01059-8.
113 S. Cho, E. J. McLaren and Q. Wang, *Angew. Chem., Int. Ed.*, 2021, **60**, 26332–26336.
114 E. Moriya, K. Muto and J. Yamaguchi, *Chem. – Asian J.*, 2026, **21**, e00991.
115 E. Moriya, K. Muto and J. Yamaguchi, *ACS Catal.*, 2024, **14**, 10412–10417.
116 K. Chen, Q. Zeng, L. Xie, Z. Xue, J. Wang and Y. Xu, *Nature*, 2023, **620**, 1007–1012.

117 (*a*) B. S. Jaynes and C. L. Hill, *J. Am. Chem. Soc.*, 1993, **115**, 12212–12213; (*b*) V. D. Waele, O. Poizat, M. Fagnoni, A. Bagno and D. Ravelli, *ACS Catal.*, 2016, **6**, 7174–7182; (*c*) D. Ravelli, M. Fagnoni, T. Fukuyama, T. Nishikawa and I. Ryu, *ACS Catal.*, 2018, **8**, 701–713; (*d*) G. Laudadio, Y. Deng, K. van der Waals, D. Ravelli, M. Nuño, M. Fagnoni, D. Guthrie, Y. Sun and T. Noël, *Science*, 2020, **369**, 92–96.

118 C. P. Lenges and M. Brookhart, *Angew. Chem., Int. Ed.*, 1999, **38**, 3533–3537.

119 R. T. Steele, M. Fujiu and R. Sarpong, *Science*, 2025, **388**, 631–638.

120 (*a*) E. von Schmid, Gy Fráter, H.-J. Hansen and H. Schmid, *Helvetica Chim. Acta*, 1972, **55**, 1625–1674; (*b*) Y. Kanaoka and K. San-nohe, *Tetrahedron Lett.*, 1980, **21**, 3893–3896; (*c*) A. G. Schultz, D. M. Graves, N. J. Green, R. R. Jacobson and D. M. Nowak, *J. Am. Chem. Soc.*, 1994, **116**, 10450–10462.

121 W. Han, T. Hwang, C. Lian, S. Kolb, M. Yamane, V. Palani and A. E. Wendlandt, *J. Am. Chem. Soc.*, 2025, **147**, 32077–32084.

122 L. H. Ramu, D. Narasimman, J. Ghosh and V. Palani, *ChemRxiv*, preprint, 2026, DOI: 10.26434/chemrxiv.15003306/v1.

123 L. Xie, P. Luo, T. Lu, W. Zheng, Y. Su, J. Wang, X. Qi and Y. Xu, *Chem*, 2026, 102961.

124 W. Zhang, S. Mao, M. Peng and Y. Xi, *Nat. Synth.*, 2026, DOI: 10.1038/s44160-026-01018-3.

125 (*a*) F. Juliá, *ChemCatChem*, 2022, **14**, e202200916; (*b*) F. Glaser, A. Aydogan, B. Elias and L. Troian-Gautier, *Coord. Chem. Rev.*, 2024, **500**, 215522.

126 C. Li, J. Wang, L. M. Barton, S. Yu, M. Tian, D. S. Peters, M. Kumar, A. W. Yu, K. A. Johnson, A. K. Chatterjee, M. Yan and P. S. Baran, *Science*, 2017, **356**, eaam7355.

127 (*a*) Q. Xu, Y. Nie, J.-J. Haaksma, R. Zhang, N. Holmberg-Douglas, F. van der Mei, P. M. Scola, C. Williams, J. A. Johnson and A. E. Wendlandt, *Nature*, 2026, **652**, 660–666; (*b*) Y. Su, D. Wang, K. Chen and Y. Xu, *Natl. Sci. Rev.*, 2026, nwag260.

128 L. Li, T. Yu, K. Du and P. Xu, *Nat. Commun.*, 2025, **16**, 7251.

129 B. Shi, X. Li, Z. Zhu, Z. Li, Y. Zhao, M. Wang, J. Zeng and C. Shu, *CCS Chem.*, 2025, **7**, 2987–2995.

130 M. Xu, C. Wu and M. Chen, *J. Am. Chem. Soc.*, 2025, **147**, 40058–40063.

131 N. Ponugoti, J. Chhatria, S. Kunnikuruvan and P. Venkatakrishnan, *J. Org. Chem.*, 2025, **90**, 10206–10217.

132 G. Lenardon, X. Yzeiri, G. L. Berre, D. B. Yildiz, D. Leonori and A. Ruffoni, *Chem. Sci.*, 2025, **16**, 21416–21422.

133 F. Berger, M. B. Plutschack, J. Riegger, W. Yu, S. Speicher, M. Ho, N. Frank and T. Ritter, *Nature*, 2019, **567**, 223–228.

134 H. Tanaka, E. Moriya, Y. Onozawa and J. Yamaguchi, *JACS Au*, 2026, **6**, 1269–1279.

135 (*a*) T. Delcaillau, P. Boehm and B. Morandi, *J. Am. Chem. Soc.*, 2021, **143**, 3723–3728; (*b*) R. Isshiki, M. B. Kurosawa, K. Muto and J. Yamaguchi, *J. Am. Chem. Soc.*, 2021, **143**, 10333–10340; (*c*) P. Boehm, P. Müller, P. Finkelstein, M. A. Rivero-Crespo, M.-O. Ebert, N. Trapp and B. Morandi, *J. Am. Chem. Soc.*, 2022, **144**, 13096–13108; (*d*) B. Mouhsine, M. Norlöff, J. Ghouilem, A. Sallustrau, F. Taran and D. Audisio, *J. Am. Chem. Soc.*, 2024, **146**, 8343–8351.

136 K. Amaike, K. Muto, J. Yamaguchi and K. Itami, *J. Am. Chem. Soc.*, 2012, **134**, 13573–13576.

137 B. D. A. Shennan, S. Sánchez-Alonso, G. Rossini and D. J. Dixon, *J. Am. Chem. Soc.*, 2023, **145**, 21745–21751.

138 Selected examples, see:(*a*) D. Matheau-Raven and D. J. Dixon, *Angew. Chem., Int. Ed.*, 2021, **60**, 19725–19729; (*b*) K. Yamazaki, P. Gabriel, G. D. Carmine, J. Pedroni, M. Farizyan, T. A. Hamlin and D. J. Dixon, *ACS Catal.*, 2021, **11**, 7489–7497.

139 M. Morimoto, R. Shimazumi, V. K. Rawat, H. Fujimoto and M. Tobisu, *J. Org. Chem.*, 2025, **90**, 9313–9318.

140 R. Shimazumi, M. Morimoto and M. Tobisu, *Org. Lett.*, 2024, **26**, 5587–5591.

